5-2018

Rapid and Sensitive Detection of Escherichia coli O157:H7 Using a QCM Sensor based on Aptamers Selected by Whole-Bacterium SELEX and a Multivalent Aptamer System

Xiaofan Yu
University of Arkansas, Fayetteville

Citation

Rapid and Sensitive Detection of *Escherichia coli* O157:H7 Using a QCM Sensor based on Aptamers Selected by Whole-Bacterium SELEX and a Multivalent Aptamer System

A dissertation submitted in partial fulfilment
of the requirements for the degree of
Doctor of Philosophy in Cell and Molecular Biology

by

Xiaofan Yu
Southeast University
Bachelor of Clinical Medicine, 2011
Southeast University
Master of Clinical Medicine, 2013

May 2018
University of Arkansas

This dissertation is approved for recommendation to the Graduate Council.

_____
Yanbin Li, Ph.D.
Dissertation Director

_____   _____
Young Min Kwon, Ph.D.   Mack Ivey, Ph.D.
Committee Member   Committee Member

_____
Jiangchao Zhao, Ph.D.
Committee Member

Abstract

Escherichia coli O157:H7 is one of the top five pathogens contributing to foodborne diseases, causing an estimated 2,138 cases of hospitalization in the US each year. The extremely low infectious dose demands for more rapid and sensitive methods to detect *E. coli* O157:H7. The objective of this study is to select aptamers specifically binding to *E. coli* O157:H7 using whole-bacterium SELEX (Systematic Evolution of Ligands by Exponential Enrichment) and to create a multivalent aptamer system by rolling circle amplification (RCA) with the selected aptamer sequence for sensitive detection of *E. coli* O157:H7 using a quartz crystal microbalance (QCM) sensor. Briefly, A total of 19 rounds of selection against live *E. coli* O157:H7 and 6 rounds of counter selection were performed for SELEX. One sequence S1 that appeared 16 (out of 20) times was characterized and a dissociation constant (K_d) of 10.30 nM was obtained. Using phi29 DNA polymerase, RCA reaction was performed, which produced a long ssDNA strand composed of thousands of repetitive aptamer sequences, termed as a multivalent aptamer system, on the electrode. The QCM sensor based on a multivalent aptamer system was able to quantitatively detect *E. coli* O157:H7. The limit of detection (LOD) of the QCM sensor was determined to be 34 CFU/ml, respectively, with the whole detection procedure in less than 40 min. The QCM sensor also showed high specificity for *E. coli* O157:H7 when it was cross-tested with five non-target bacteria. The QCM aptasensor in this study provided a common platform for detection of different foodborne pathogens.

Keywords: Whole-bacterium SELEX; aptamer; *E. coli* O157:H7; QCM; RCA

Acknowledgements

I would like to thank my advisor, Dr. Yanbin Li, for his guidance and leading during my graduate studies. His constant forgiveness of my mistakes and failures encouraged me to go on in research without losing heart. He inspired me to develop new ideas and helped me learn to stand upon the shoulders of giants. From each discussion with him, I could not only get instant help but also learned how to face the problem directly without trying to make a detour. His advices of independent research, help seeking, time management, and risk assessment will benefit me a lot in my whole research career.

I also thank my advisory committee members, Dr. Young Min Kwon, Dr. Mack Ivey, and Dr. Jiangchao Zhao. I appreciate their helpful suggestions and continuous care for me during each step of my research and study. I'm grateful for the instruction of Dr. Douglas Rhoads, the program director of Cell and Molecular Biology, in my accomplishment of degree requirement, and for his help in my obtainment of research assistantship.

I'm thankful for the great help from the research group: Dr. Ronghui Wang for her critical suggestions on all the problems I met in research and her guidance on both biology and engineering related experiments; Lisa Cooney Kelso for her laboratory assistance and training; Sardar Abdullah for his advice on molecular biological tests; Fang Chen and Lijun Wang for their help with PCR tests; Meng Xu and Zach Callaway for helping with electrochemical tests; Qinqin Hu for her suggestion on QCM experiments. I also thank the rest of the group members who spent time with me and gave a hand to me both in work and daily life. I appreciate the help of Adil Al-Ogaili with RCA test design and provision of some RCA reagents and the helping

hand of Bo Ma with the preparation of atomic force microscopy samples and the imaging of the samples.

I want to say thank you to Department of Biological and Agricultural Engineering, Department of Poultry Science and Molecular Biology Program for supporting my graduate studies and research. I also thank Graduate School and International Education for guiding me through graduate education and providing me travel grants for attending international conferences.

Finally, I want to give thanks to my Mom for her unconditional love and her changeless support in whatever I do. Her encouragement and comfort helped me go through all difficulties in my pursuing of my PhD degree. I also thank my uncle for his meticulous care as of a father and his reliable advices on my decision-making. My achievement is not from my own effects but from the whole family's support.

Table of Contents

List of Tables

List of Figures

Introduction

Foodborne illness is a serious public health problem. CDC (2011) estimated that each year roughly 1 in 6 Americans (or 48 million people) gets sick, 128,000 are hospitalized, and 3,000 die of foodborne diseases. Great financial loss has been caused by foodborne illness in terms of pain, suffering, reduced productivity, and medical costs. Among all the foodborne pathogens, *Escherichia coli* O157:H7 as the fifth leading cause of domestically acquired foodborne illness resulting in hospitalization, is related to 73,000 illnesses in the United States each year, and also a major cause of hemolytic uremic syndrome develops in children (CDC). To control outbreaks and disease progression in individuals infected, it is critical to rapidly identify the pathogen by methods with high sensitivity and selectivity, in which a recognition element that can specifically bind to the target is essentially required.

Traditional methods for the detection of *E. coli* O157:H7, including culture, ELISA and PCR, are time-consuming, labor-intensive, or trained personnel-requiring. A biosensor is an analytical device, composed of a bio-recognition element and a transducer. QCM is an acoustic (mass-based) piezoelectric biosensor. The decrease in resonant frequency of the quartz is linearly proportional to adsorbed mass on the quartz surface based on the piezoelectric effect. QCM sensors possess the advantages of simplicity, cost effectiveness, label-free detection, and real-time monitoring, and are able to detect mass change down to nanogram level (Marrazza, 2014). Many QCM immunosensors and DNA/RNA biosensors have been studied for the detection of *E. coli* O157:H7, but no QCM aptasensor has been developed to detect *E. coli* O157:H7. The only two QCM aptasensors for the detection of foodborne pathogens were reported by Ozalp et al. (2015) and Wang et al. (2017).

Aptamers are single-stranded DNA (ssDNA) or RNA oligonucleotides that are capable of specifically binding to selected targets, including whole cells, proteins, peptides and small molecules, through their folding into unique three-dimensional structures. Aptamers are usually selected from large random nucleic acid libraries by Systematic Evolution of Ligands by Exponential Enrichment (SELEX), which involves three major steps - selection of oligonucleotides binding to the target, partitioning of bound aptamers from unbound oligonucleotides, and amplification of bound aptamers (Gopinath et al., 2007). Several advantages of aptamers over antibodies are: (i) aptamers can be quickly generated against a wider spectrum of targets; (ii) they can be chemically synthesized with low cost and easily modified, (iii) they are thermostable and can usually be reversibly denatured and have much longer shelf life, (iv) they are non-immunogenic and has better penetration into tissue, cell membrane or nuclear pore (Hyeon et al., 2012; Joshi et al., 2009; Keefe et al., 2010). Aptamers have been studied for the detection of pathogens or chemicals in food, environment and clinical samples (Bai et al,. 2012; Yildirim et al., 2012; Turek et al., 2013). But so far, only one RNA aptamer specifically targeting *E. coli* O157:H7 has been reported (Lee et al., 2012). Although RNA aptamers have superior binding affinity compared with DNA aptamers, they are less stable, harder to produce, and cost more if modified to be RNase-resistant.

RCA is an isothermal amplification method, which is initiated by a primer hybridized to a small circular template in the presence of some mesophilic polymerase (e.g. phi29 DNA polymerase) (Mayboroda et al., 2018). The RCPs are tens of thousands of nucleotide long, containing tandem repetitive sequences complimentary to the circular template. RCA has been widely used in biosensors for signal amplification due to its high efficiency of amplification, no requirement for thermal cycling instrument, no significant damage to biological molecules or

2

environment, and easy modification of RCPs with fluorescence or nanoparticles labeled short complimentary DNA strands (Zhao et al., 2008). So far, only two biosensors based on multivalent aptamer system by RCA are reported, which were designed to capture and deliver drugs into leukemia cells (Zhao et al., 2012; Zhang et al., 2013).

In this study, we described the selection of DNA aptamers against *E. coli* O157:H7 with high affinity and specificity using whole bacterium-SELEX and the construction of a novel multivalent aptamer system based on RCA, which comprises repetitive aptamer sequences against *E. coli* O157:H7. Based on the selected aptamers and the created multivalent aptamer system, a QCM aptasensor was developed for sensitive, specific, rapid, and label-free detection of *E. coli* O157:H7.

Chapter 1 Literature Review

1.1 Aptamer and SELEX

Aptamers are a class of small single-stranded DNA or RNA oligonucleotides that are capable of binding to selected targets, including whole cells, proteins, peptides and small molecules with high specificity and affinity, through their folding into unique three-dimensional (3D) structures. Aptamers are usually selected from large random nucleic acid libraries by Systematic Evolution of Ligands by EXponential enrichment (SELEX), which involves four major steps - binding of oligonucleotides to the target, partitioning of bound aptamers from unbound oligonucleotides, amplification of bound aptamers, and regeneration of single-stranded aptamer molecules (Gopinath et al., 2007).

The SELEX was first developed by Larry Gold and Craig Tuerk in 1990, aiming to elucidate the interaction between the bacteriophage T4 (gp43) and the ribosome binding site of the mRNA. In this process, two RNA sequences were selected from an initial RNA pool of estimated 65, 536 different species, which had a random region of 8 nt after four SELEX cycles. The results not only proposed the possibility of in vitro selection of nucleic acids to be used in protein recognition, but also helped answer some questions on the natural evolution (Tuerk and Gold, 1990). In the same year, Ellington and Szostak independently designed the same process to select RNA molecules bound to different organic dyes. They termed these individual RNA sequences "aptamers" according to the Lain "aptus" (to fit) and found out that 10^2-10^5 different sequences could be selected from a RNA pool with complexity of around 10^{13} sequences to bind to the target after six selection cycles. They also determined the specificity of aptamers by measuring their binding affinity to the other different dyes (Ellington and Szostak, 1990). With

rapid development of SELEX techniques for over two decades, the first aptamer-based drug, Pegaptanib Sodium (trade name Macugen), was approved by the US Food and Drug Administration (FDA) in December 2004, and by Europe, Brazil, Canada and Australia 1-2 years later. Pegaptanib specifically targets vascular endothelial growth factor (VEGF), and used to treat the vision loss associated with aberrant angiogenesis of Age-Related Macular Degeneration (AMD) by intravitreal injection of 0.3 mg per eye once every 6 weeks. Due to its shortage of not binding to all isoforms of human VEGF, the market of Macugen was later shared by Lucentis, which is a monoclonal antibody fragment (Fab)-based drug approved by FDA in 2006 (Keef et al., 2010)

Similar to antibodies, aptamers bind to targets via van der Waals forces, hydrogen bonding, electrostatic and stacking interaction. However, aptamers have some advantages over antibodies: 1) they can be chemically synthesized with low cost and easily modified, 2) aptamers can be quickly generated against a wider spectrum of targets 3) they are thermostable and can usually be reversibly denatured and have much longer shelf life, and 4) they are non-immunogenic and has better penetration into tissue, cell membrane or nuclear pore (Hyeon et al., 2012; Joshi et al., 2009; Keefe et al., 2010; Sun et al., 2014; Ray et al., 2012).

Table 1.1 Comparison between antibodies and aptamers

Antibodies	Aptamers
Production 1. Production of polyclonals demands a live animal 2. Production of monoclonals requires training for the high technology and is laborious 3. Polyclonals have batch-to batch variability, monoclonals have low or no batch-to batch variability once a hybridoma is made 4. Time scale is long for hybridomas 5. Monoclonals are expensive to produce 6. Viral or bacterial contamination can affect antibody quality	**Production** 1. Most aptamers are developed in vitro and produced chemically without the use of a live animal 2. No variability between batches 3. Automated SELEX decreased the developing time to within one week and greatly reduced labor intensity 4. Cost effective 5. Not subject to viral or bacterial contamination
Targets Must provoke a strong immune response.	**Targets** A wide range of targets, such as ions, toxin, peptides, proteins, bacteria, cells, and even tissues
Storage Susceptible to irreversible denaturation at high temperature, resulting in a limited shelf life	**Storage** Thermally stable, can usually be reversibly denatured, resulting in a long shelf life
Affinity and Specificity 1. K_d values of high affinity antibodies are usually in nanomolar (10^9) to picomolar (10^{12}) range. 2. Polyclonals are non-specific, monoclonals are highly specific	**Affinity and Specificity** 1. K_d values of high affinity aptamers are usually in nanomolar (10^9) to picomolar (10^{12}) range 2. Specificity could be improved by negative- or counter- selection
***In vivo* application** 1. Large size (12-15 nm) limits bioavailability or prevents access to many biological compartments 2. Large size prevents filtration 3. Not susceptible to nuclease degradation 4. Often immunogenic (antibodies produced from animals could be eliminated from human immune system)	***In vivo* application** 1. Small size (3-5 nm) allows more efficient and faster entry into biological compartments *in vivo* 2. Small size makes them susceptible to renal filtration and they therefore have a shorter half-life. Addition of conjugation partners can increase circulating half-time 3. Susceptible to nuclease degradation. Chemical modifications can enhance nuclease resistance 4. Non-immunogenic

1.1.1 The process of SELEX

The process of SELEX is usually repeated for 5-15 times (cycles or rounds) until aptamers acquire high binding affinity and specificity for the target. The aptamer pool with the highest affinity is chosen for cloning, sequencing and further characterization.

1.1.1.1 Initial library of random sequences

In a typical SELEX process, an initial oligonucleotide library composed of random sequences is usually required to start the selection of aptamers. The library generally comprises a complexity of individual molecules ranging from 10^{13} to 10^{15} (~20 pmol to 2 nmol) to make sure the selected aptamers will have high affinity. The oligonucleotide that constitutes the library could be RNA or single-stranded (ss) DNA. RNA differs from ssDNA in the presence of a ribose 2'- hydroxyl group and the lack of a methyl group on the uracil ring. As a result, RNA and ssDNA having the same sequence might not have the same binding affinity to one target due to their different conformation (Ellington and Szostak, 1992). In addition, the 2'-OH group on one hand allows RNA to fold into more varied secondary and tertiary dimensional structures, resulting in higher binding affinity than ssDNA, on the other hand, causes RNA to be more susceptible to nuclease hydrolysis. So far, a lot of efforts have been made to increase RNA stability through chemical modifications including the replacement of 2'-OH group with 2'-fluoro, 2'-amino, or 2'-O-methoxy motifs, and the alternation of the oxygen atom to the non-bridging sulfur atom in the phosphodiester backbone (Sun et al., 2014). The length of the random sequence is typically 15-45 nucleotides (nt) in size, flanked by two primer binding sites 20-25 nt in length for aptamer amplification so as to enrich aptamer pools.

1.1.1.2 Binding and partitioning

The first step in each cycle of SELEX is the binding of the targets with the initial library or subsequent aptamer pools, which need to be denatured beforehand by heating at 95°C for 5 min and cooling on ice for 10 -15 min to avoid the unwanted hybridization between diverse oligonucleotide sequences. Then the binding step usually takes 30 min to 1 h at 25°C or room temperature for the sufficient interaction between targets and oligonucleotides. The binding could also be carried out at 4°C instead to avoid the internalization of DNA sequences, which might result in production of non-specific or low-affinity aptamers (Li et al., 2014). That is because at 37°C the receptor-binding aptamers are more easily lost due to possible endocytosis during the selection process (Sefah et al., 2010). After the binding of aptamers to targets, a partitioning step is followed to separate bound aptamers from unbound oligonucleotides. In the conventional method for partitioning, purified target molecules were immobilized to a solid support such as a column. Then the aptamer pools were applied to affinity columns in high-salt buffer and columns were washed buffer to remove non-binding oligonucleotides (Ellington and Szostak, 1992). Current methods include centrifugation, filtration, magnetic separation and capillary electrophoresis (CE) (Hamula et al., 2008; Bing et al., 2010). Directly after partitioning, bound aptamers are normally eluted from the targets by heating at 95°C for 10 min as to be used as template in the next amplification step for enrichment.

1.1.1.3 Amplification

The amplification of a random ssDNA library by polymerase chain reaction (PCR) is a key step in each round of SELEX, however, its subjection to artificial by-products formed by primer-product or product-product hybridization may prohibit the enrichment of target-

recognizing aptamers. He et al. (2013) found that the amount of by-products increased with the increase of template amount and thermal cycle number. Tolle et al. (2014) reported the formation of two different forms of longer by-products, termed ladder- and non-ladder-type, and proposed a molecular mechanism through which these by-products were built. In the cloned and sequenced by-products from 8th round SELEX library, they found one set of sequences possessing two copies of the forward primer linked by stretches of random region and another set of sequences having continuous multiple full-length reverse primer binding sites fused without gap. Their explanation was that the random region on one sequence, which was complimentary to the reverse primer binding site of another strand could serve as a primer and led to the elongation of this strand. If there was no gap between hybridization site and the primer binding site, this mechanism could lead to increasingly longer by-products. If the hybridization site was in the middle of the random region, further extensions was avoided. They tried skipping of the elongation step and the use of single strand binding protein (SSB), but both couldn't eliminate the by-products. And they thought proper primer design could be a possible solution.

1.1.1.4 Regeneration

As input for the incubation with the target cells in the next cycle, ssDNA is regenerated from PCR products (dsDNA) though several methods, including denaturing urea-polyacrylamide gel electrophoresis (PAGE), asymmetric PCR, magnetic separation (using streptavidin-coated beads to capture antisense strands labelled with biotin) and lambda exonuclease digestion. For denaturing PAGE, one primer containing a spacer as terminator and an extension of 20 adenine nucleotides (polyA) is used in PCR to produce strands with different lengths, which could be separated by electrophoresis. Then the desired strand in the right band could be extracted from the gel. By adding uneven amounts of forward and reverse primers in asymmetric PCR, ssDNA

could be produced with the higher concentration of primers, but still needs to be separated and eluted from the small amount of dsDNA generated with both primers through PAGE and gel extraction. Therefore, both methods are tedious and time-consuming. For the magnetic separation of two strands of dsDNA, the antisense strand is biotinylated by using a biotinylated primer in PCR and then is immobilized onto streptavidin-coated magnetic beads. After alkaline treatment, the dsDNA dissociates and the antisense strands could be removed through magnetic separation. If 5'-phosphate group is used to label one primer in PCR, the phosphorylated strands of dsDNA could be removed by digestion with lambda exonuclease which selectively digests the 5'-phosphorylated strand of dsDNA (Avci-Adali et al., 2009)

A new method developed by He et al. is called single-primer-limited amplification (SPLA) that can generate ssDNA free from by-products. Briefly, minus-stranded DNA (msDNA) of an ssDNA library was first amplified with reverse primer of 5-fold molar quantity of the template, followed by the amplification of plus-stranded DNA (psDNA) of the msDNA with forward primer of 10-fold molar quantity of the template and recovery of psDNA by gel excision. By the optimization of template amount and thermal cycle, they successfully amplified target ssDNA without detectable by-products and produced psDNA 16.1 times as much as that by asymmetric PCR. (He et al., 2013)

1.1.1.5 Selection pressure

To enhance the binding affinity of aptamers as SELEX proceeds, selection pressure could be gradually increased from cycle to cycle by means of decreasing the amount of ssDNA pool, the incubation time, or the target cell number, and increasing the times and duration of washing steps. While the selectivity of aptamers could be raised through the insertion of negative or

counter selections into the positive selections. Developed in 1992 and 1994, respectively, negative and counter selections are used to eliminate aptamers that non-specifically bound to environmental substances, solid supports and molecules close related to the targets in SELEX process and these two terms are now used interchangeably (Ellington & Szostak, 1992; Torres-Chavolla & Alocilja, 2009). The "negative" or "counter" substances or molecules introduced in negative and counter selections vary considerably according to different targets and diverse methods used in SELEX. Bing et al. employed streptavidin sepharsoe beads as solid supports in SELEX and used the beads as the counter-targets as well in the counter selections (Bing et al., 2010). Li et al. took metastatic CRC LoVo cells as the target cells, and used non-metastatic HCT-8 cells as the negative cells (Li et al., 2014). Counter selection are performed either after all rounds of SELEX (Moon et al., 2013; Dwivedi et al., 2010) or before each round of SELEX. To further improve selection pressure, the number of counter selection could be increased before each cycle of SELEX (Li et al., 2014).

1.1.1.6 Characterization and truncation of aptamers

During SELEX process, the enriched aptamer pools from different cycles are subject to binding affinity screening via flow cytometry, capillary electrophoresis (CE) or quartz crystal microbalance (QCM). With regard to flow cytometry, the aptamer pools were first fluorescently labeled through PCR amplification with 5′-FAM modified sense primers. Following incubation of aptamer pools with targets, the mixture was injected and prone to fluorescence detection. Large number of target cells with fluorescence or higher fluorescence intensity indicated higher binding affinity of aptamer pools. As SELEX is going on, the binding affinity of aptamer pools is usually increasing cycle by cycle. However, in the last few cycles of SELEX, deselection sometimes happens – the decline of the binding affinity of aptamer pools, probably due to the

loss of high affinity aptamers during partitioning and elution or the decrease of the aptamer pool complexity (Li et al., 2014; Hamula et al., 2008). After all SELEX cycles are completed, the aptamer pool with the highest affinity is selected to be cloned and sequenced.

Based on the sequence information, the secondary structures of aptamer candidates and their free energies accordingly could be predicated using software, such as Oligo Analyser and DNA Mfold, which are available on the Internet. Afterwards, the distinction and repetition of predicted secondary structures will help distribute obtained sequences into several families or categories, such as tight hairpins, branched hairpins, and few or no hairpins (Hamula et al., 2008). Meanwhile, by comparing the similarities of structures in each family, the binding motifs of aptamers could also be determined given that sequences with the same secondary structure should bind to the same target. Upon the determination of the motifs of aptamers that directly interact with the targets or are responsible for folding into the structure that facilitates targets binding, the unnecessary nucleotides in the whole sequences of aptamers may undergo truncation, resulting in shorter aptamers, which have larger yield and lower cost in synthesis, higher structural stability, less susceptibility to random degradation, and advanced tissue penetration compared with long sequences (Shangguan et al., 2007; Bing et al., 2010). For example, Li et al. (2014) truncated the sequences of aptamers to a length of approximately 50 nt without influencing their binding domains. However, motifs of aptamers cannot always be decided based on secondary structure difference. Bing et al. grouped 17 of these 28 sequences into 3 families based on the primary sequence homology, nonetheless, they identified a consensus bulge-hairpin structure segment (around 29 mer) existing in all 28 sequenced aptamers. To elucidate the critical nucleotides for the streptavidin binding, mutated sequences derived from the suspected binding motif were evaluated via competition assay. In addition, by

extending the terminal stem or truncating part of the sequence or replacing certain nucleotides, they identified the segment that is essential for maintaining the binding affinity (Bing et al., 2010).

The final step following the synthesis of aptamer sequences with or without truncation is the measurements of their equilibrium dissociation constants (K_d). By using a concentration range of aptamers, for example, 0-120 nM, in the incubation with targets for the same period of time, the binding characteristics of aptamers are evaluated via fluorescence instruments, such as flow cytometry, under the same condition. Making use of software, such as GraphPad Prism and Sigma Plot, a nonlinear regression curve can be generated for the calculation for the value of K_d using the equation $Y = B_{max} \times X/(K_d + X)$ (Bing et al., 2010).

1.1.2 Whole-cell SELEX

1.1.2.1 Comparison between conventional and whole-cell SELEX

Conventional SELEX have been applied for the selection of aptamers for a wide range of targets from small molecules going through protein complexes purified from cells, including ATP, toxins, antibiotics, cytokines, proteases, kinases, cell-surface receptors, antibodies, carbohydrate, lipopolysaccharide (LPS), peptidoglycan, viruses and membranes of human blood cells (Ferreira et al., 2014). The advantage of using purified molecules as targets is that high-affinity aptamers can be obtained within fewer cycles of SELEX, however, some problems also exist, such as the binding sites of cell-surface molecules could be different from their isolated forms (Hamula et al., 2011) and some proteins (e.g. cell surface transmembrane proteins) couldn't even be purified due to the loss of some fragments essential for the formation of native conformations during purification process (Cerchia et al., 2005).

In 1999, Homann et al. (1999) performed the first whole-cell SELEX to select RNA aptamers for live African trypanosomes. They used a starting pool of 10^{16} RNA molecules with an estimated complexity of 2×10^{15} unique sequences to incubate with trypanosomes at a cell density of $1\text{-}2 \times 10^6$ cells/ml for 60 min. After 12 rounds of SELEX, they acquired high affinity aptamers with K_d of 60 ± 17 nM. Since then, the whole-cell SELEX has been extended to the selection of aptamers for diverse target cells: bacteria (Duan et al., 2013), spores (Bruno et al., 2012), cancer cells (Xu et al., 2015), somatic cells (Kim et al., 2014), embryonic stem cells (ESCs) (Iwagawa et al., 2012), virus infected cells (Tang et al., 2009), parasites infected cells (Birch et al., 2015) and so on.

The advantages of whole-cell SELEX over conventional SELEX are: 1) Complex purification and target-partitioning are avoided; 2) Molecules are targeted in their native conformations on the cell surface; 3) Pathogens or cancer cell lines are targeted or differentiated without previous knowledge of the characteristics of the antigenic determinants or molecular biomarkers present in target cells; 4) Unknown or new targets or biomarkers can be discovered on the surface of the cell; and 5) Multiple aptamers for both multi-functional and multi-target applications could be obtained via a single whole-cell SELEX, exhibiting improved selection efficiency. Li et al. (2014) performed Cell-SELEX to target CRC LoVo cells and generated a panel of seven aptamers that can specifically bind metastatic potential cancer cell lines and recognize distinct targets without any mutual interference. Utilizing the Cell-SELEX strategy, Shangguan et al. (2006) also generated a group of leukaemia cell-specific aptamers, which targeted multiple molecules, including membrane proteins, carbohydrates and lipids.

The drawbacks have been observed for the use of whole-cell SELEX are as follows: 1) Gram negative bacteria with a negatively-charged outer membrane would resist the binding of

14

nucleic acid molecules; 2) Capsules enveloping the surface of bacteria may cover up target proteins or molecules; 3) The fast growing speed make cell surface molecules vary greatly among cultures and colonies (Hamula et al., 2011); and 4) The nonspecific adsorption of single-stranded nucleic acids to dead cells causing severe contamination to the enriched aptamer. One way to overcome this problem is through the recovery of bound aptamers by chelating divalent cations. Divalent cations are necessary for the formation of high-order RNA structures, thus their elimination (by adding EDTA, etc.) would contribute to the dissociation most of the bound aptamers, but wouldn't affect the non-specific adsorption of the nucleic to dead cells (Tang et al., 2009; Ohuchi et al., 2006)

Table 1.2 Examples of bacterial targets of aptamers selected using whole-cell SELEX

Target	Aptamer type	Random sequence	SELEX Rounds	K_d (nM)	Reference
Escherichia coli	ssDNA	N_{45}	10	12.4	Kim et al., 2013
Escherichia coli O157:H7	RNA	N_{60}	6	110	Lee et al., 2012
Escherichia coli K88	ssDNA	N_{35}	13	15±4	Peng et al., 2014
Escherichia coli NSM59	ssDNA	N_{24}	5	110	Savory et al., 2014
Salmonella spp.	ssDNA	N_{40}	12	7	Kolovskaya et al., 2013
Salmonella Typhimurium	ssDNA	N_{40}	9	6.33±0.58	Duan et al., 2013
Salmonella Typhimurium	ssDNA	N_{40}	8	$1.73\pm0.54\times10^3$	Dwivedi et al., 2013
Salmonella Paratyphi A	ssDNA	N_{40}	13	47±3	Yang et al., 2013
Listeria spp.	ssDNA	N_{40}	6	74.4±52.69	Suh et al., 2014
Listeria monocytogenes	ssDNA	N_{35}	8	48.74±3.11	Duan et al., 2013
Listeria monocytogenes	ssDNA	N_{40}	10	$2.01\pm0.12\times10^{-3}$	Lee et al., 2015
Staphylococcus aureus	ssDNA	N_{40}	17	94.61±18.82	Turek et al., 2013
Campylobacter jejuni	ssDNA	N_{40}	10	292.8±53.1	Dwivedi et al., 2010
Lactobacillus acidophilus	ssDNA	N_{40}	8	13±3	Hamula et al., 2008
Shigella dysenteriae	ssDNA	N_{40}	8	23.47±2.48	Duan et al., 2013
Streptococcus pyogenes	ssDNA	N_{40}	20	4	Hamula et al., 2011
Vibrio parahemolyticus	ssDNA	N_{40}	9	16.88±1.92	Duan et al., 2012

1.1.2.2 Investigation of the binding sites on target cells

Since the target molecules in whole-cell SELEX are unknown during the selection process, some researchers endeavored to discover the possible binding sites of aptamers on target cells through cell surface protein digestion or fluorescence detection. Hamula et al. (2008) carried out capillary electrophoresis with laser-induced fluorescence (CE-LIF) to investigate the possible binding site on the surface of target *L. acidophilus* cells by incubating the S-layer

protein extracted from the cell surface with the aptamers selected through whole cell-SELEX and detecting the fluorescence of cells. S-layer is a common surface structure surrounding the cell wall, which has been found in many bacteria as well as archaea. It consists of a monomolecular assemblies composed of identical protein subunits, which are called S-layer proteins. Seeing an accelerating peak of formation of aptamer-protein complex with the increasing concentration of S-layer protein, they confirmed that S-protein is a likely target of the aptamer. Li et al. (2014) verified the aptamers' binding sites by incubating target LoVo cells with 0.05% trypsin or 0.1 mg/mL proteinase K at 37°C for 3 min or 10 min, respectively. After enzyme treatment, the binding of FITC-labeled aptamers with the treated cells was investigated using flow cytometry. The aptamers that showed decreased fluorescence intensity were identified to be targeting cell membrane protein, while the aptamers that displayed no change in fluorescence intensity probably was targeting carbohydrate or lipid on the membrane. To further explore if the aptamers can penetrate into the cells via endocytosis by binding to the receptor, LoVo cells were first incubated with membrane protein-binding aptamers at 37°C and then with trypsin before being subjected to flow cytometry analysis. All aptamers showed total fluorescence loss, except one displayed only a decrease in fluorescence intensity which could be caused by the ingestion of aptamer molecules into the cells via endocytosis. This assumption was further confirmed by observing the fluorescence inside the cells under fluorescence microscope. Based on the different binding targets, aptamers were applied as either a carrier for specifically delivering the anticancer drug or a probe for fluorescence imaging of target cancer cells or tissues. Other binding molecules that have been determined by researchers include LPS (Lee et al., 2012), RET receptor tyrosine kinase (transmembrane molecule) (Cerchia et al., 2005) and so on.

1.1.3 Other methods of SELEX

1.1.3.1 Automated SELEX

The selection process of conventional SELEX is repetitive and time-consuming, taking weeks to months to complete. Cox et al. (1998) automated a protocol for in vitro selection using an augmented Beckman Biomek 2000 pipetting robot, which was interfaced with three other devices: a PTC-200 thermal cycler (for aptamer amplification), a magnetic bead separator (for partitioning target bound aptamers from free nucleic acids), and a Peltier cooler (for holding enzyme for amplification) via a Dimension XPS H266 computer. Five rounds of selection were accomplished using this automated SELEX procedure and each single round took only 212 min in total, greatly reduced labor and time. Instead of setting up large robotic workstations, Hybarger et al. (2006) established a smaller and simpler chip-based automated microfluidic SELEX prototype, consisting of reagent-loaded microlines, pressurized reagent reservoir manifold, thermocycler, and actuatable valves controlled by LabView. The utilizing of microlines and valves made the flowing of reagents more controllable and the speed of thermocycling faster because of smaller reaction volumes, which altogether caused this prototype to be less costly and more rapid.

1.1.3.2 Non-SELEX

Non-SELEX is a process involving repetitive steps of partitioning of aptamers from non-aptamers but with no amplification between them, which was first developed and named by Berezovski et al. in 2006. For the entire non-SELEX process, only three steps of partition by running non-equilibrium capillary electrophoresis of equilibrium mixtures (NECEEM) were conducted. In the first step, 150 µl mixture of 25 mM naive DNA library (2×10^{12} molecules)

and 0.5–500 nM target were injected into the capillary followed by incubation of 15 min. After

the running NECEEM and a fraction was collected in the outlet vial containing 5 µl of the target

(h-Ras protein) solution. The step was then repeated twice prior to the affinity analysis of

aptamer pool accomplished also by NECEEM. The exemption of repetitive steps of PCR proved

to accelerate the procedure of aptamer selection without compromising its efficiency, exclude

quantitative errors associated with the exponential nature of PCR amplification, and avoid the

bias related to differences in PCR efficiency with respect to different oligonucleotide sequences.

The lowest K_d value they obtained for an individual aptamer was 0.2 µM and the entire protocol

was completed in 1 week which is much shorter compared with conventional SELEX that takes

several weeks or months (Berezovski et al., 2006). Kupakuwana et al. combined over-

representation together with deep sequencing and dramatically shortened the discovery process

to one step of partitioning, which they called as acyclic identification. When the number of

randomized sequence is very large, almost all of the molecules in the pool occur as single copies.

By decreasing the number of randomized sequence, the representation of each different sequence

in the library of 0.1 nmol of total strands could be increased to 56, 000 copies, referred to as

over-representation. In addition, the use of deep sequencing in aptamer discovery allowed more

sequences to be sampled in the partitioned pool than Sanger sequencing and thus enabled the

distinguishing of aptamers from over-represented library after a single partitioning step

(Kupakuwana et al., 2011).

1.1.3.3 In vivo SELEX

On condition that the binding of aptamers is dependent on the 3D conformation of their

targets which varies in different environments, it won't be so practical for aptamers selected

against purified proteins or whole cells *in vitro* to be applied in cell and tissue imaging or tumor

treatment *in vivo*. To solve this problem, *in vivo* SELEX has been developed to generate

aptamers with better selectivity to target cells and much less binding to non-target cells in the

body. One example is the *in vivo* screen of RNA aptamers for CT26 tumor in tumor-bearing

mice via repetitive intravenous injection of random RNA library into the mice and extraction,

amplification of injected RNA molecules from liver tumors. By the excision of aptamer bound

proteins followed by peptide-mass fingerprinting and MS/MS peptide fragment ion-matching,

the target protein was identified to be mouse p68 helicase, which was further confirmed due to

the overlapping localization of the aptamers and p68 expression in tumor tissue sections (Mi et

al., 2010)

1.2. Aptamer based biosensors

1.2.1 Introduction to biosensors

A biosensor is an analytical device, composed of a bio-recognition element and a

transducer. A bio-receptor is a biologically derived material or biomimetic component, which

interacts, binds, or recognizes the target for detection. A bio-receptor could be enzymes,

antibodies, nucleic acids, cells, or phages to detect varied targets, including pathogens, proteins

and small molecules. Aptamers bind to the targets by their 3D structures instead of base-paring.

When nucleic acids are used in biosensors for the detection of genomic nucleic acids via

hybridization, the biosensors are called genosensors; while if aptamers are applied in biosensors

for the recognition of small molecules, proteins, or cells, the biosensors are called aptasensors.

While a transducer serves to convert a biological response into electrochemical, optical, thermal,

or mass signals which could be observed and displayed more easily. For optical biosensors, the

detection methods include fluorescence, calorimetry, chemiluminescence, surface plasmon

20

resonance (SPR), Raman spectroscopy, and so on. Optical aptasensors have been used for the detection of viruses (Bai et al., 2012) and foodborne pathogens (Chang et al., 2013; Xu et al., 2015). For electrochemical biosensors, the electroanalytical methods could be cyclic voltammetry (CV), amperometry, electrochemical impedance spectroscopy (EIS), and potentiometry. Using EIS method, the signal could be transduced as impedance, and it will be called an impedimetric biosensor. Electrochemical aptasensor have also been developed for the detection of viruses and pathogenic bacteria coupled with various nanomaterials (Wang et al., 2015; Labib et al., 2012; Zelada-Guillén et al., 2012). Mass-based biosensors include magnetoelastic and piezoelectric sensors, while QCM is a piezoelectric sensor. A thermal biosensor measures the amount of heat released during come chemical reactions (Yao et al., 2014; Wang et al., 2016).
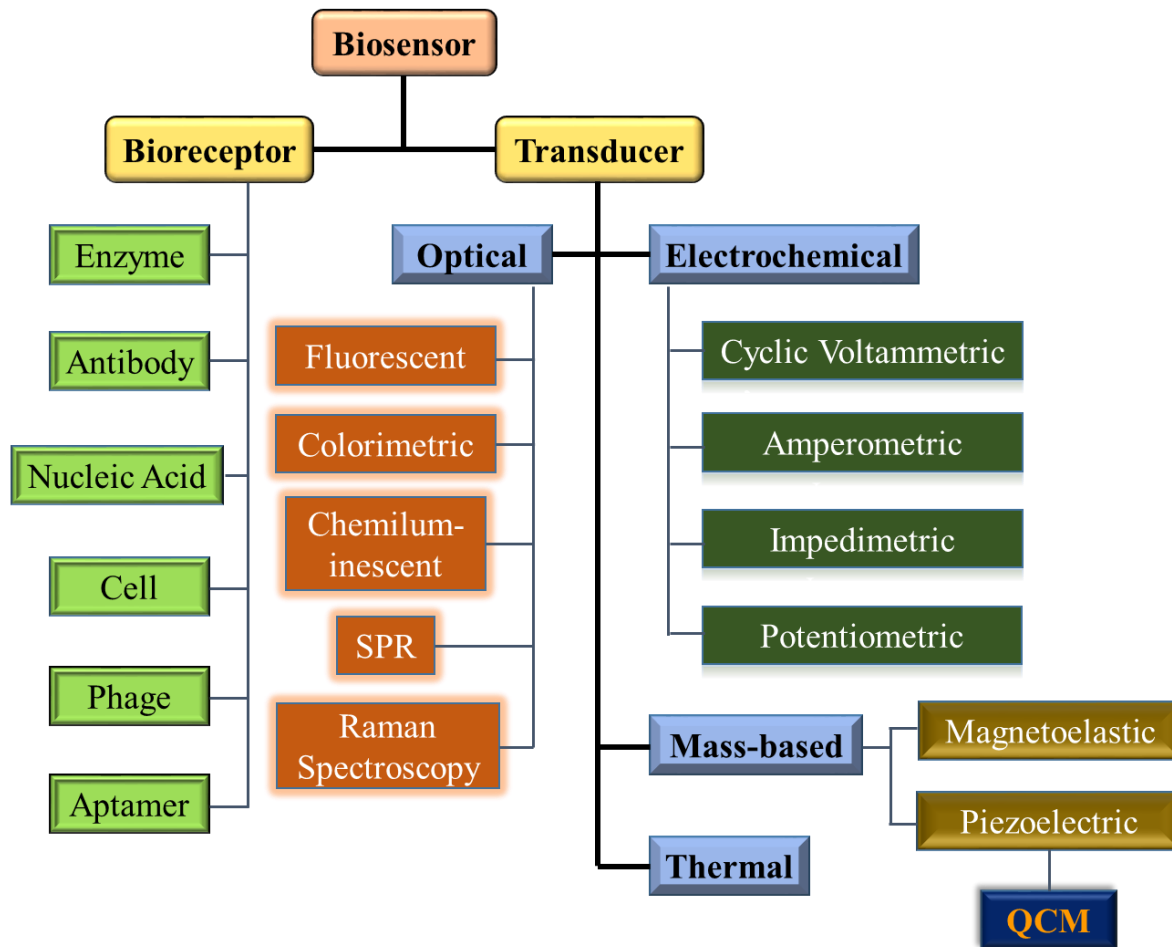
Fig. 1.1 Components and classification of biosensors.

1.2.2 QCM sensors

1.2.2.1 Theoretical principles of QCM

QCM is an acoustic (mass-based) piezoelectric biosensor. When an alternating potential (a sine wave) is applied to the quartz face, the quartz will oscillate (Jaiswal et al., 2008). If the thickness of the quartz is twice the acoustical wavelength, a standing wave can be established, half period of which equals to the inverse of the frequency - resonant frequency. A quartz crystal

has a complicated structure, and there are many ways to cut quartz crystal relative to the x, y, z, axes. Each cut has a different vibrational mode and is useful in particular ways. The AT-cut has gained the widest use for electronic instruments due to its low temperature coefficient at room temperature, which means the resonant frequency is not influenced much by small fluctuation in temperature.

QCM was first used to monitor the growth of thin film in vacuum, and later was used in liquid for monitoring of molecule interaction. For a thin and rigid film, the decrease in frequency is linearly proportional to adsorbed mass on the quartz surface based on the piezoelectric effect. The linear relationship has been defined by the Sauerbrey equation (Sauerbrey, 1959; Hengerer et al., 1999):

$$\Delta F = -2F_o^2 \frac{\Delta M}{A\sqrt{\rho\mu}} = -2.3 \times 10^6 F_o^2 \frac{\Delta M}{A} \qquad (1\text{-}1)$$

$$F_0 = \frac{\sqrt{\mu_q/\rho_q}}{2t} \qquad (1\text{-}2)$$

Where ΔF (Hz) is the measured frequency change, F_o (MHz) is the resonant frequency of the piezoelectric quartz crystal, ΔM (g) is the mass change on the electrode surface, A (cm^2) is the active area of the coated quartz surface (Kumar, 2000; Liss et al., 2002), ρ is the density of the crystal (2.648 g/cm^3), and μ is the shear modulus of the quartz (2.947 $\times$ 10^{11} g/cm^3/s^2) (Shan et al., 2014), t is the quartz crystal thickness (Liang et al, 2017). Obviously, ΔF is inversely proportional to the square of the thickness of the quartz, which indicates that thinner quartz gives higher sensitivity. However, thinning the oscillator will increase the inertia resistance of the

electrode layers deposited on the quartz, leading to deviation from the Sauerbrey equation. Au films were most commonly used as electrodes due to high biocompatibility and easy functionalization with thiola, but the density of Au is much larger than that of the quartz, causing very high inertia resistance (Ogi et al., 2008).

Since the Sauerbrey equation only applies to rigid films, when the adsorbed film is not rigid, the equation becomes invalid. The viscosity effect of the deposited layer also participates in the frequency shift, for elastic materials such as cells, protein, or polymer layers with entrapped water do not following the oscillations perfectly, which leads to internal frictions (motional resistance) and, therefore, energy dissipation. Dissipation factor is defined as energy loss per stored energy during one oscillation cycle (Kasper et al., 2016). The negligence of the viscosity effect can be a reason for the experimentally observed deviation from a linear relationship of QCM resonant frequency with mass change and can limit the sensitivity of QCM sensors (Voinova et al., 2002). QCM with Dissipation (QCM-D) is able to provide information about the viscoelastic properties as well as the mass change of adsorbed films in real time. (Jaiswal et al., 2008). Poitras and Tufenkji (2009) developed a QCM-D biosensor for detection of viable *E. coli* O157:H7. The polyclonal antibodies were immobilized onto gold-coated QCM-D quartz crystals via cysteamine. By conducting QCM-D measurement over a wide range of bacterial cell concentrations, the biosensor signal was set as the initial slope of the dissipation shift (D_{slope}). A linear response in the initial D_{slope} was obtained for detection of *E. coli* O157:H7 from 3×10^5 to 1×10^9 cells/ml, while linearly increasing frequency shifts were only observed from detection of *E. coli* O157:H7 of 10^6 cells/ml to 10^8 cells/ml.

As the density and viscosity of the deposited layer are greatly affected by the liquid environmental temperature, it is important to exclude the environmental factor in order to avoid

large frequency drift. One possible way to cancel out environmental factors is by arranging another QCM as a reference, however, separately arranged two QCM chip may receive slightly different environment influence, leading to un-precise cancellation. So Liang et al. (2017) designed the dual-channel QCM on one single quartz chip, where the two QCM resonators are supposed to have the same resonance characteristics. Then the frequency drift caused by the same environmental factors can be eliminated by taking the frequency difference between the two resonators. The performance of the fabricated dual-channel QCM was tested both in air and liquid. Highly improved frequency difference value was observed and suggested that the one chip dual channel QCM was very promising to be used a sensitive bio- or chemical- senor.

1.2.2.2 QCM based aptasensors

QCM sensors are nanogram mass sensing devices, possessing the advantages of simplicity, cost effectivity, label-free detection, and capability of for real-time monitoring (Marrazza, 2014). They have been used for studying the interactions of biomolecules, quantitative measurement for the binding affinity, and detection of a wide range of targets, such as ions, biomolecules, and cells.

Detection of small molecules. Neves et al. (2015) developed their own electromagnetic piezoelectric acoustic sensor (EMPAS) for the label-free detection of cocaine based on aptamers. The acoustic resonance of an electrode-free quartz crystal was excited through an external magnetic field produced by a spiral coil underneath the crystal. This design allowed the sensor to operate at ultra-high frequencies (860 MHz), which led to the ultra-sensitivity of the sensor. The quartz disc was coated with an S-(11-trichlorosilyl-undecanyl)-benzenethiosulfonate (BTS) adlayer followed by the immobilization of cocaine binding DNA aptamer, composing the

25

sensing platform for cocaine. Exposed to 100 µM cocaine, an EMPAS frequency shift of -1648 ± 260 Hz was generated. And the concentration limit of detection (C_{LoD}) was determined to be 0.9 µM using the regression parameters. No detectable response of the developed sensor was observed in contact with 100 µM of benzoylecgonine (BE) and 100 µM of ecgonine methylester (EME).

Detection of viruses. A nanowell-based QCM aptasensor was developed by Wang et al. (2017) for rapid and sensitive detection of AIV H5N1. The nanowell-based electrode was fabricated by immobilizing the nanoporous gold film prepared using a metallic corrosion method onto the QCM gold electrode via the cross-linker 1,6-hexanedithiol (HDT). The H5N1 AIV ssDNA aptamers labeled with amino groups were then immobilized on the carboxyl group functionalized gold nanowell layer. The binding of target viruses caused big drop of the resonant frequency of the quartz crystal, and a linear correlation was found between the frequency shift and the virus titer. The developed aptasensor achieved label-free detection of 2−4 HAU/50 µl in 10 min without interference from non-target AIV subtypes of H1N1, H2N2, H7N2 and H5N3.

Detection of bacterial cells. To minimize the influence of food matrices on the detection of foodborne pathogens, Ozalp et al. (2015) created a pre-purification system of aptamer-modified magnetic beads coupled to a QCM sensor for rapid detection of *Salmonella* Typhimurium in food samples. The magnetic p(Hydroxypropyl methacrylate (HPMA)/ ethyleneglycol dimetha-crylate (EGDMA) beads were functionalized with 2-bromo-2-methylpropionyl bromide (BMP) for creating hairy polymer on the bead surfaces. The beads were then used for graft polymerization with p(glycidyl methacrylate) (pGMA) in order for amino group labeled *Salmonella* aptamers to immobilized on the bead surface. Upon capture by the aptamer-immobilized magnetic beads, *Salmonella* cells were pre-concentrated and eluted

from the beads with NaOH treatment. The eluted bacterial cells were then subjected to QCM

sensing with aptamer immobilized QCM crystal. The QCM aptasensor showed rapid response

(less than 10 min) with a LOD of 100 cells. For milk samples contaminated with *Salmonella* or

E. coli, the aptasensor was able to distinguish *Salmonella* at 10^4 CFU/ml from *E. coli* at the same

concentration. In the study of Wang et al. (2017), QCM was used for the selection of aptamers

against *Salmonella* Typhimurium and development of an aptamer-based sensor for the rapid

detection of *S*. Typhimurium. After the kinetic analysis of all aptamer candidates using QCM,

the aptamer with highest binding affinity was selected and applied to the QCM sensor. The

developed aptasensor showed good sensitivity in detecting 10^3 CFU/mL of *S*. Typhimurium with

less than 1 h.

Detection of human cells. Shan et al., (2014) developed a strategy to significantly amplify

the signal of detection of target leukemia cells. Upon capture by the aptamer immobilized on the

QCM sensor surface, the leukemia cells were labeled by aminophenylboronic acid-modified gold

nanoparticles (APBA-AuNPs) through the formation of stable borate ester complexes between

sialic acids on cell membranes and phenylboronic acid (PBA). The following silver

enhancement is achieved by the catalysis of silver ion into metallic silver by AuNPs, which

resulted in great frequency change. A good linear relationship between the frequency shift and

cell concentration ranging from 2×10^3–1×10^5 cells/mL was obtained, with a LOD of 1160

cells/ml.

1.3 RCA

1.3.1 Fundamentals of RCA

In the mid-1990s, some particular DNA polymerases were found to continuously

lengthen a short DNA strand annealed to a small circular template (13-240 nt) by a process now

commonly called RCA (Zhao et al., 2008). This amplification technique exists naturally and is

utilized by bacteriophage, eukaryotic viruses and bacterial plasmids (Chandler et al., 2013). A

long ssDNA is yielded by the RCA reaction, which comprised of tens of thousands of

nucleotides corresponding to hundreds of nanometers to hundreds of microns in length. By

controlling RCA reaction time and dNTPs amount, the length of RCPs could be tuned

accordingly. The RCPs contain tandem repetitive sequence units complementary to the circular

tailor-designed DNA template, therefore they can be easily modified and applied to a RCA-based

sensor for signal amplification in detection of a wide range of targets.

RCA is one among isothermal amplification methods, which also include nucleic acid

sequence based amplification (NASBA), helicase-dependent amplification (HAD), strand

displacement amplification (SDA), and loop-mediated isothermal amplification (LAMP)

(Mayboroda et al., 2018). RCA relies on the activity of mesophilic polymerase (such as phi29

and Bst DNA polymerase), whose working temperature spans from 30–65°C and possessing

strand displacement activity. As for phi29 polymerase, the optimal activity is at temperature of

30°C, which makes it a perfect enzyme for the DNA amplification at environmental

temperatures. Polymerase-mediated elongation produces accumulating by-products of

pyrophosphate and protons, which results in the acidification of the reaction solution.
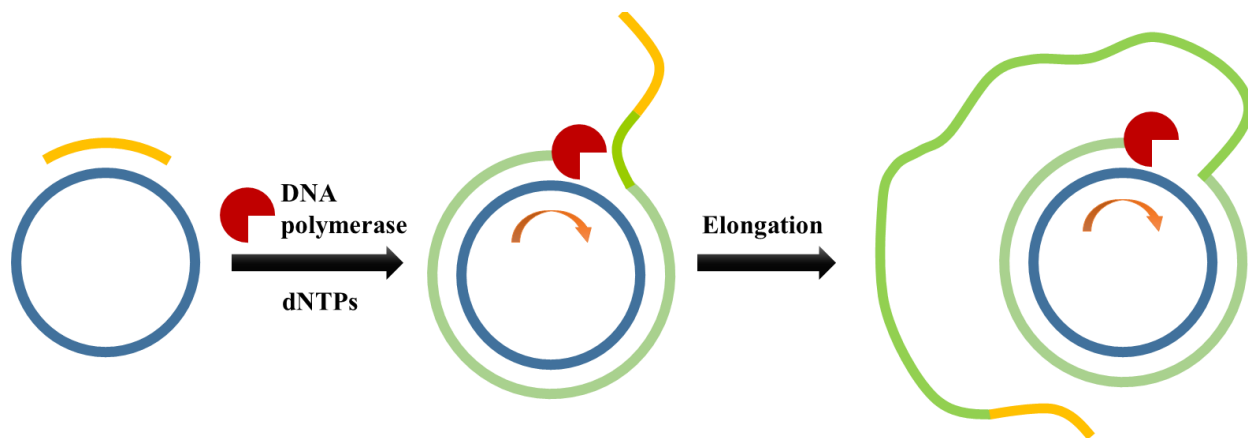
Fig. 1.2 Generation of long ssDNA by RCA reaction. Amplification initiates by a short DNA primer annealed to a circular DNA template in the presence of phi29 DNA polymerase and dNTP mix.

Although the polymerase chain reaction (PCR) is a detection method of high sensitivity, it requires sophisticated instrument for highly precise temperature cycling, complex sample preparation, strict laboratory conditions, and trained personnel, which hamper its widespread use for routine or in-field analysis. As an isothermal amplification method, RCA possesses unique characteristics, such as operation at a constant temperature, no need of thermally stable DNA polymerase or expensive instruments, high efficiency, and compatibility with biological systems (Zhao et al., 2008).

Yan et al. (2012) surveyed the effects of varied DNA circle size and varied polymerases on the RCA reaction. They found that T4, T7, Sequenase, Taq, Klenow, and Pol I DNA polymerases all produced RCPs longer than 2000 nt. There is a misconception that it is required for the polymerase to unwind the RCPs in front of the polymerase for efficient amplification. However, it is not true because a duplex is not likely to be made unstrained in a circle smaller than 120 nt. Circular templates ranging from 26 (smaller than the polymerase itself) to 74 nt had all been successfully amplified, indicating no topological issues limiting DNA strand elongation.

29

Polymerases have inherent processivity, which is the average length of DNA they synthesize before dissociating from the template. The smaller the circular template is, the more the copies of the template is completed. That is one reason that very small DNA templates are more useful. Phi29 polymerase, an enzyme from bacteriophage phi29, is one of the most processive polymerases, with a processivity of tens of thousands of nucleotides (Mohsen and Kool, 2016).

Recent developments of RCA include the improvement of amplification efficiency by "hyperbranched" RCA (HRCA), multiple displacement amplification or circle to circle amplification; the creation of the padlock process for detection of nucleic acids and proteins; the exploration of limited reverse transcriptase activity of phi29 DNA polymerase (Krzywkowski et al., 2018).

1.3.2 Application of RCA in biosensors

1.3.2.1 For signal amplification

Optical sensors. A dendrimer-aptamer based microfluidic detection platform coupled fluorescence signal amplification with RCA was developed. Carboxyl groups functionalized poly (amido amine) (PAMAM) dendrimers with ethylenediamine core were immobilized on amine functionalized inner surface of polydimethylsiloxane (PDMS) microchannel. PAMAM dendrimers were used on the one hand to prevent non-specific binding of non-target particles, and on the other hand to increase binding sites for NH_2- aptamer immobilization. Following capturing of *E. coli* O157:H7, aptamer-primer, padlock probe, and RCA reagents were introduced to the microchannel subsequently. After RCA reaction, Cy3 labeled DNA probes were injected to hybridize with RCPs for fluorescence signal amplification. With signal enhancement using RCA, the LOD was reduced from 10^3 cell/ml to 10^2 cells/ml (Jiang et al.,

2017). Yan et al. (2012) described a new approach based on nano rolling-circle amplification (nanoRCA) and nano hyperbranched rolling-circle amplification (nanoHRCA) for enhanced surface enhance Raman scattering (SERS) "hot spots" in protein microarrays. Biotinylated secondary antibodies were deposited on the chip, followed by the incubation with streptavidin conjugated AuNPs. The primer modified on the AuNPs would initiate the RCA reaction. For HRCA, the second primer, circle DNA, along with amplification mixture were added and reacted for another 30 min. AuNPs functionalized with Cy3-labeled oligonucleotide strands were then hybridizing with the complimentary sequences on the RCPs, and the subsequent Ag enhancement caused the number of hot spots to be largely increased. The enhancement factors (EF) for nanoHRCA-SERS and nanoRCA-SERS were approximately 1.3×10^8 and 3.7×10^7, respectively.

Electrochemical sensors. A disposable aptasensor with signal amplification was developed for the detection of prostate-specific antigen (PSA). PSA aptamer was immobilized on gold-coated magnetic NPs as the recognizing material, and then added into the sample solution containing artificial cDNA-primers. The designed cDNA-primer comprised a 27-mer sequence complementary to the PSA aptamer and a 9-mer primer sequence complementary to a circular RCA template. In the absence of PSA, the PSA aptamers on the magnetic NPs hybridized with the cDNA-primer, which would further initiate the RCA reaction. In the presence of PSA, the aptamer bound with PSA and less cDNA-primers, causing less RCA reaction. Following RCA reaction, the magnetic NPs were immobilized on a screen-printed electrode (SPE) modified with a DNA probe complimentary to RCA unit, and incubated with methylene blue (MB). MB can be bound specifically to guanine (G) in the RCPs and yield amplified electrochemical signal. The limit of detection (LOD) was determined to be 22.3 fM

31

and no significant interference was observed between PSA and four proteins found in human blood (IgE, IgG, globulin, albumin) based on the current response (Lee et al., 2018). A novel label-free electrochemical biosensor for highly sensitive and specific detection of *E. coli* was developed based on RCA coupled peroxidase-mimicking DNAzyme amplification. In a sandwich assay platform, *E. coli* were first captured by the polyclonal antibody immobilized on the electrode surface, and then bound by an aptamer-primer probe (APP), which contained anti-*E. coli* aptamer and a primer complementary to circular DNA probe. In the presence of phi29 DNA polymerase, a long DNA molecule comprising numerous G-quadruplex units was produced. With the help of hemin and K^+, G-quadruplex/hemin complex was formed and mimicked the peroxidase activity of horseradish peroxidase (HRP) to catalyze the reduction of H_2O_2, resulting in a significantly amplified current flow. A good linear relationship was displayed between the peak current intensity and the logarithm value of *E. coli* concentration ranging from 9.4 to 9.4×10^5 CFU/ml, with the LOD calculated to be 8 CFU/ml (Guo et al., 2016). An ultrasensitive electrochemical genosensor of Ebola virus cDNA was developed by rolling circle and circle to circle amplification (C2CA). Target Ebola cDNA was the product after retrotranscription of a specific *L-gene* sequence present in the five most common Ebola species. Upon hybridization of the padlock probes with the cDNA target, the probes were ligated with T4 ligase. Then the biotinylated cDNA was modified to the streptavidin conjugated magnetic particles (MPs) and RCA was performed on MPs for 60 min. After that, readout probes labeled with HRP were hybridized with the RCPs and produced electrochemical signal. For C2CA, RCPs after RCA reaction for 60 min were monomerized by the digestion of *AluI* restriction enzyme, and the monomers were religated and reamplified by RCA a second time. Different readout probes labeled with HRP were added and the electrochemical signals were

measured. The developed electrochemical genosensor exhibited ultrahigh sensitivity with a LOD of 33 cDNA molecules with a total assay time of less than 2.5 h (Carinelli et al., 2017).

QCM sensors. He et al. (2014) developed a QCM aptasensor combined with RCA and bio-bar-coated AuNP enhancement for the detection of thrombin. Primary aptamer probes were initially immobilized on the QCM electrode via Au-S binding. Upon the capture of thrombin, aptamer-primer complex, which contains a secondary aptamer and a primer, was added to form a sandwich assay platform. Following the hybridization and ligation of the padlock probe, the RCA reaction could be initiated in the presence of phi29 DNA polymerase and dNTPs. The generated long ssDNA, composed of hundreds of tandem-repeat sequences, would hybridize with the AuNP labeled bio-bar-coded probes, resulting in significant signal amplification. The developed QCM sensor exhibited an excellent specificity and ultrahigh sensitivity with a detection limit of 0.78 aM.

1.3.2.2 For generating recognition elements

Monovalent adhesion ligands, such as aptamers, extend only a few nanometers into the solution, fail to capture large-sized entities, such as human cells ($\sim$10–30 μm) with a high capture efficiency under high shear stress. Inspired by marine creatures that are capable of effectively capturing flowing food particulates with long tentacles containing repetitive adhesive domains, Zhao et al. (2012) developed 3D DNA network comprising repeating adhesive aptamer domains to capture CCRF-CEM cells. The 3D DNA network was produced by RCA reaction, the circular template of which was designed to be complimentary to the aptamer against protein tyrosine kinase 7 (PTK7) incorporated with a polyT spacer. RCA reaction was carried out at 37 °C for 30 min, which resulted in a length of tens of micrometers. They proved that target cells

bound more strongly to RCA-aptamers than to unit-aptamers via a peizo-controlled micropipette. They also demonstrated that the 3D DNA network could significantly improve the capture efficiency of CCRF-CEM cells over monovalent aptamers and antibodies on microfluidic test cell and herringbone chips. It was confirmed that a standard microscope slide ($\sim$10 cm^2) could harvest more than 100 target cells within 2 min of operation of the system. Having successfully captured leukemia cells, the next mission of the multivalent aptamer system would be to target and kill the cells. To solve the major problems associated with current chemotherapies, such as poor efficacy and off-target systemic toxicity, Zhang et al. (2013) developed a new form of polyvalent therapeutics by RCA, which is called "Poly-Aptamer-Drug". The Poly-Aptamer-Drug system is constructed by amplification of a DNA template composed of a PTK7 aptamer complimentary sequence and a spacer domain, which could hybridize with complementary strands to form duplex, doxorubicin-loading domains. RCA was carried out at 30°C for 10 min, producing a long ssDNA corresponding to approximately 30-40 aptamer units. Multivalent binding of Poly-Aptamer-Drug system on the cell membrane intensified endocytosis compared to monovalent binding, which lasted approximately 1 h and more than 3 h, respectively, in terms of the internalization half-time (defined as half of the time to reach the plateau). As for the toxicity followed the release of doxorubicin, treatment of leukemia cells with Poly-Aptamer-Drug (10 nM) for 24 h resulted in an approximately 50% loss of viability, which was significantly higher than that of Dox alone or Mono-Aptamer-Drug.

Table 1.3 Various RCA based biosensors with details of the RCA reaction.

Type of biosensors	Length of template (nt)	Spot where primer is tagged	RCA time (min)	Reference
Optical	61	Avidin on microfluidic cell	30	Zhao et al., 2012
Optical	60	AuNPs	30	Yan et al., 2012
Optical	60	Carbon nanotubes	90	Zhao et al., 2013
Optical	72	In the cell	90	Ge et al., 2014
Optical	79	Aptamer	120	Jiang et al., 2017
Electrochemical	73	Magnetic particles	20	Kühnemund and Nilsson, 2015
Electrochemical	78	Aptamer	80	Guo et al., 2016
Electrochemical	85	Magnetic particles	60	Carinelli et al., 2017
Electrochemical	45	Aptamer on MNBs	40	Lee et al., 2018
QCM	58	Secondary aptamer	90	He et al., 2014

1.3.3 Other applications of RCA

RCA has also been used to increase the complexity of periodic protein nanostructures (Cheglakov et al., 2008). Using RCA, linear DNA chains containing periodic repeats of aptamers for thrombin and for both thrombin and lysozyme were created. The length of these period DNA tapes could be controlled by the dNTPs to template ratio. The formed DNA-protein nanostructures were exploited for further hierarchical self-assembly by acting as anchoring sites for Au nanoparticles to form inorganic nanowires. These constructed nanoassemblies hold great promise in biosensing and enzymatic catalysis. DNA nanotubes have become increasingly attractive due to their great potential to be used for protein organization, as templates of nanowires and photonic systems, and for drug delivery. Hamblin et al. (2012) reported a strategy for the construction of DNA nanotubes, whose backbone was produced by RCA. The RCPs

produced in this study composed of two alternating regions: a binding region for attaching "rungs", and an intervening spacer region for hybridizing to spacers strand. With the addition of double-stranded linkers, the fully double-stranded triangular nanotube (RCA-NT) were formed. These nanotubes were found to be more resistant to nuclease degradation, and more capable of entering human cervical cancer (HeLa) cells than double-stranded DNA, which implied their unique potential for drug delivery and cell imaging.

1.4 Objectives

The overall goal of this research was to develop a QCM biosensor based on selected aptamers and a multivalent aptamer system for rapid and sensitive detection of *E. coli* O157:H7. Specifically the objectives of this research were:

1. To select DNA aptamers against *E. coli* O157:H7 with high affinity and specificity using whole-bacterium SELEX.

2. To design and construct a QCM sensor based on the selected aptamer for the sensitive and rapid detection of *E. coli* O157:H7

3. To creat a multivalent aptamer system using RCA and then integrate it into the QCM sensor for the ultrasensitive and rapid detection of *E. coli* O157:H7.

Chapter 2 Whole-bacterium SELEX of DNA Aptamers for Rapid Detection of *E. coli* O157:H7 Using a QCM Sensor

2.1 Abstract

The rapid detection of foodborne pathogens is critical to ensure food safety. The objective of this study is to select aptamers specifically bound to *Escherichia coli* O157:H7 using the whole-bacterium SELEX (Systematic Evolution of Ligands by Exponential Enrichment) and apply the selected aptamer to a QCM (quartz crystal microbalance) sensor for rapid and sensitive detection of target bacteria. A total of 19 rounds of selection against live *E. coli* O157:H7 and 6 rounds of counter selection against a mixture of *Staphylococcus aureus*, *Listeria monocytogenes*, and *Salmonella* Typhimurium, were performed. The aptamer pool from the last round was cloned and sequenced. One sequence S1 that appeared 16 (out of 20) times was characterized and a dissociation constant (K_d) of 10.30 nM was obtained. Subsequently, a QCM aptasensor was developed for the rapid detection of *E. coli* O157:H7. The limit of detection (LOD) and the detection time of the aptasensor was determined to be 1.46×10^3 CFU/ml and 40 min, respectively. This study demonstrated that the ssDNA aptamer selected by the whole-bacterium SELEX possessed higher sensitivity than previous work on SELEX (Lee et al., 2012) and the potential use of the constructed QCM aptasensor in rapid screening of foodborne pathogens.

2.2 Introduction

Each year, approximately 48 million people become sick from foodborne diseases. In 20 percent of these cases where a specific causative pathogen could be identified, over 90 percent are caused by only 15 pathogens (CDC, 2011). *E. coli* O157:H7 is one of them. Symptoms caused by *E. coli* O157:H7 infection include severe, acute hemorrhagic diarrhea,

abdominal cramps, and hemolytic uremic syndrome (HUS) particularly in children. Great

financial loss has been caused in terms of pain, suffering, reduced productivity, and medical

costs. To control outbreaks and disease progression in individuals infected, it is critical to rapidly

identify the pathogen using methods with high sensitivity and selectivity, in which a recognition

element that can specifically bind to the target is essentially required.

Aptamers are single-stranded DNA (ssDNA) or RNA oligonucleotides that are capable of

specifically binding to selected targets, including whole cells, proteins, peptides and small

molecules, through their folding into unique three-dimensional structures. Compared with

antibodies, aptamers show similarly high affinities to their targets, with dissociation constants

(K_d) ranging from nanomolar to picomolar. They also comprise a number of advantages over

antibodies, such as quick generation against a wider spectrum of targets, chemical synthesis with

low cost, easy modification, thermostability and non-immunogenicity (Hyeon et al., 2012; Joshi

et al., 2009; Keefe et al., 2010). Aptamers are usually selected through Systematic Evolution of

Ligands by Exponential Enrichment (SELEX), which was first developed by Tuerk and Gold

(1990). Whole-cell SELEX invented by Homann and Göringer (1999) is superior to conventional

SELEX in that molecules are targeted in their native conformations, complex purification is

avoided, and new biomarkers can be discovered (Hamula et al., 2011).

So far, more than ten aptamers developed for foodborne pathogens by whole-

cell/bacterium SELEX have been reported, including *E. coli* (Kim et al., 2013), *E. coli* O157:H7

(Lee et al., 2012), *E. coli* K88 (Peng et al., 2014), *Salmonella* spp. (Kolovskaya et al., 2013), *S.*

Typhimurium (Duan et al., 2013a; Dwivedi et al., 2013), *Salmonella* Paratyphi A (Yang et al.,

2013), *Listeria* spp. (Suh et al., 2014), *L. monocytogenes* (Duan et al., 2013b; Lee et al., 2015), *S.*

aureus (Turek et al., 2013), *Campylobacter jejuni* (Dwivedi et al., 2010), *Shigella dysenteriae*

(Duan et al., 2013c), *Streptococcus pyogenes* (Hamula et al., 2011), and *Vibrio parahemolyticus* (Duan et al., 2012). However, the RNA aptamer developed against *E. coli* O157:H7 by Lee et al. (2012) was less stable, harder to produce, and more costly if modified to be RNase-resistant compared to ssDNA aptamers. In addition, the equilibrium dissociation constant (K_d) of the developed aptamer was only 110 nM. And these aptamers have not been applied to any biosensor for the detection of *E. coli* O157:H7 yet. The ssDNA aptamers targeting *E. coli* selected by Kim et al. (2013) possessed lower K_d values ranging from 2.4 to 25.2 nM. Nevertheless, these aptamers were not specifically selected against *E. coli* O157:H7, and their binding affinity to *E. coli* O157:H7 was not characterized.

For rapid and sensitive detection of foodborne pathogens, aptamers have been incorporated into various biosensing platforms, such as fluorescence (Wang and Kang, 2016), resonance light-scattering (Chang et al., 2013), electrochemistry (Bagheryan et al., 2016), lateral flow (Wu et al., 2015), and QCM (Wang et al., 2017). QCM is an acoustic (mass-based) piezoelectric biosensor, which allows detection of small mass change down to the nanogram level. Based on the piezoelectric effect, the frequency shift of the quartz oscillation is proportional to the mass change deposited on the quartz surface. Therefore, QCM is highly suitable for real-time monitoring of molecular interactions on the crystal surface, and label-free detection (Marrazza, 2014). To the best of our knowledge, most QCM aptasensors were developed to target proteins and viruses, and only three works by Ozalp et al., (2015), Shan et al. (2014), and Wang et al. (2017) have reported to use QCM aptasensors for the detection of bacterial or human cells.

In this study, a whole-bacterium SELEX process for the selection of ssDNA aptamers with high affinity and specificity for live *E. coli* O157:H7 was described. The selection process

using antibody-conjugated magnetic beads for capturing target bacteria allowed the selected

aptamer to obtain a different binding site on the bacteria surface apart from that of anti-*E. coli*

antibodies. This feature of the aptamer would enable it to be employed in an aptamer-antibody

sandwich assay, avoiding the unsuccessful labeling due to the competition of binding sites

between ligands. The selected aptamer was further characterized for its affinity and specificity

and utilized in a QCM sensor for demonstrating its potential in the rapid detection of *E. coli*

O157:H7 at low concentrations.

2.3 Materials and methods

2.3.1 Bacterial strains and culture conditions

Stock cultures of *E. coli* O157:H7 (ATCC 43888), *S. aureus* (ATCC 27660), *L.*

monocytogenes (ATCC 43251), *S.* Typhimurium (ATCC 14028), and *E. coli* K12 (ATCC 29425)

were obtained from the American Type Culture Collection (ATCC, Manassas, VA, USA). Cells

were grown in 5 ml brain heart infusion (HBI) medium at 37°C, harvested upon reaching the log

phase by centrifugation. Then the cells were washed twice in $1 \times$ phosphate buffered saline

(PBS), and finally resuspended in 1 ml of $1 \times$ PBS. For bacterial enumeration, the bacterial

samples were 10-fold serially diluted with $1 \times$ PBS and were surface plated on the TSA (tryptic

soy agar) plates and incubated overnight before counting. Colony forming units (CFU) on the

agar plates were counted as CFU/ml.

2.3.2 Random DNA library and primers

A 90-nucleotide (nt) ssDNA library contained a 45-nt central random region flanked by

two primer binding sites: 5'-CAG TCC AGG ACA GAT TCG CGA G-N_{45}-CAC GTG GAT

TTC ATT CAG CGA TT-3'. The primers used for PCR amplification are: forward, 5'- CAG TCC AGG ACA GAT TCG CGA G - 3' and reverse, 5'-phos-AAT CGC TGA ATG AAA TCC ACG TG-3'. The phosphate-labeled reverse primer was used for the digestion with lambda exonuclease to obtain ssDNA from amplified dsDNA PCR (polymerase chain reaction) products, and the biotin-labeled forward primer was used for the aptamer blotting assay (the forward primer was not biotinylated in the process of SELEX). For the cloning of enriched aptamer pool, pGEM-T Easy Vector System II was used. The M13 primers: forward, 5'-GTA AAA CGA CGG CCA GT-3' and reverse, 5'-AGC GGA TAA CAA TTT CAC ACA GG-3' were used for verifying the existence of the insert in the plasmid after cloning. Both the library and the primers were synthesized by Integrated DNA Technologies, Inc. (Coralville, IA, USA).

2.3.3 Reagents and apparatus

Biotin-labeled rabbit antibodies to *E. coli* O and K Antigenic Serotypes and the biotin-labeled monoclonal antibodies to *S.* Typhimurium were purchased from Meridian (Memphis, TN, USA). Biotin-labeled rabbit anti-*S. aureus* antibodies and biotin-labeled rabbit anti-*L. monocytogenes* antibodies were obtained from Biodesign International (Saco, Maine). Streptavidin conjugated magnetic beads (MBs, 150 nm) were purchased from Ocean NanoTech (San Diego, CA, USA).

A QCA922 quartz crystal analyzer (Princeton Applied Research, Oak Ridge, TN, USA) was used for the analysis of the binding affinity of aptamer pools and the developed aptamer, and further for the detection of the target bacteria. AT-cut quartz crystals (International Crystal Manufacturing Co., Oklahoma city, OK, USA), whose resonant frequency was 7.995 MHz, were employed in the QCM tests. The quartz crystals were 14 mm in diameter and 100 nm in

41

thickness, with polished Au electrodes (5.1 mm in diameter and 100 nm in thickness) deposited on both sides. A methacrylate flow cell (International Crystal Manufacturing Co) was utilized for holding the crystal. The crystal was sealed between two O-rings attached to the upper and lower pieces of the cell held together with two screws. For QCM measurements, a quartz crystal is connect to the oscillator and then to the frequency counter of QCA922. WinEchem software on the computer was used to record the frequency change.

2.3.4 Whole-bacterium SELEX procedure

In the process of SELEX, whole cells of bacteria *E. coli* O157:H7 were used. For magnetic separation of target bacteria, immunomagnetic beads (IMBs) were freshly prepared before each round of SELEX. A scheme of the preparation of IMBs and the capturing of target bacteria is shown in Fig. 2.1. Briefly, 20 µl of streptavidin conjugated MBs (1 mg/ml) were washed with 180 µl PBS in a 1.5 ml 3% BSA (bovine serum albumin) blocked tube. After magnetic separation for 3 min using the magnetic separator (1.3 Tesla [T]) (Aibit Biotech Instrument, LLC, China), the solution was pipetted out and the beads were resuspended in 180 µl PBS. The beads were then mixed with 20 µl biotinylated anti-*E. coli* antibodies (Ab) (0.5 mg/ml) and incubated using a rotating mixer (Grant Instruments, U.K.) at 15 rpm for 45 min (all the following incubation was carried out in this way). After magnetic separation, the excess antibodies in the solution were removed. The IMBs were then washed in 200 µl PBS and incubated with 200 µl of bacterial solution (10^8 CFU/ml) for 45 min. The IMBs-cell complexes were subsequently collected by magnetic separation (Xu et al., 2015).
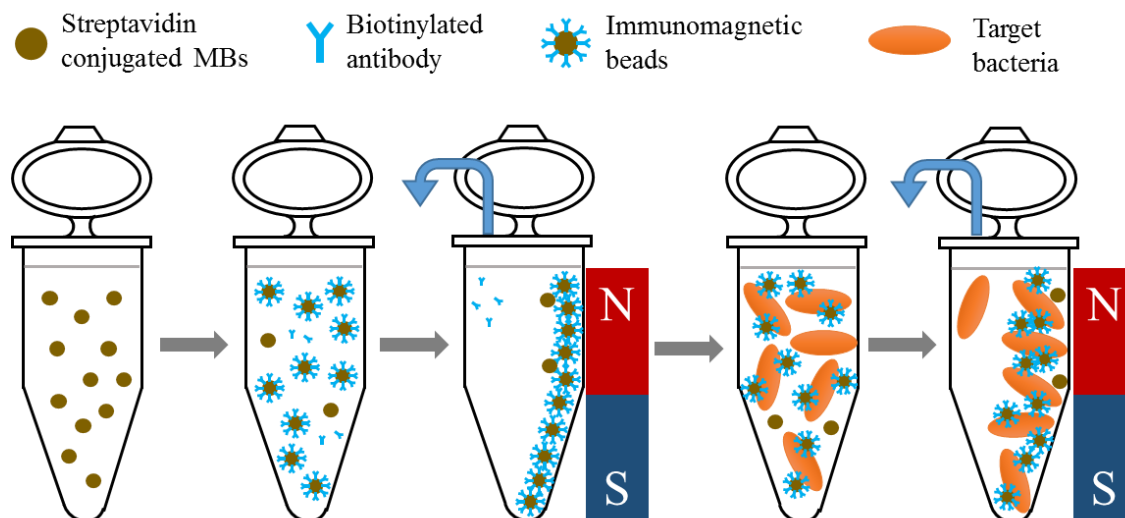
Fig. 2.1 Schematic diagram of the preparation of immunomagnetic beads and the capture of target bacteria.

A scheme of the whole-bacterium SELEX process is shown in Fig. 2.2. The process was initiated with 2 nmol of the ssDNA random library, and the aptamer pool of 1-100 pmol (from previous round) was used as the input in subsequent rounds. Before incubating with target bacteria, the ssDNA (0.03-2.63 µM) dissolved in 38 µl binding buffer (BB: 50 mM Tris-HCl, pH 7.5, 25 mM NaCl, 5 mM MgCl$_2$) were denatured by heating at 95°C for 10 min and then renatured to its secondary structure by cooling down at room temperature for 30 min. Then ssDNA dissolved in the incubation buffer (PBS with 0.05% BSA) were incubated with IMBs captured bacteria of 10^8 CFU/ml for 45 min. The unbound ssDNA in the solution were removed after magnetic separation. The IMBs-cell-ssDNA complexes were washed in PBS twice and resuspended in 20 µl PBS. To elute the bound ssDNA, the IMBs-cell-ssDNA complexes were heated at 95°C for 10 min and placed on ice immediately for 10 min, then the denatured ssDNA would dissociate from the surface of bacteria and could be collected after magnetic separation. To remove the ssDNA that have bound to IMBs instead of target bacteria, the elution was

subsequently subject to a negative selection, in which the elution was incubated with the IMBs for 30 min, and the unbound ssDNA in the solution after magnetic separation were retained and used for further PCR amplification.
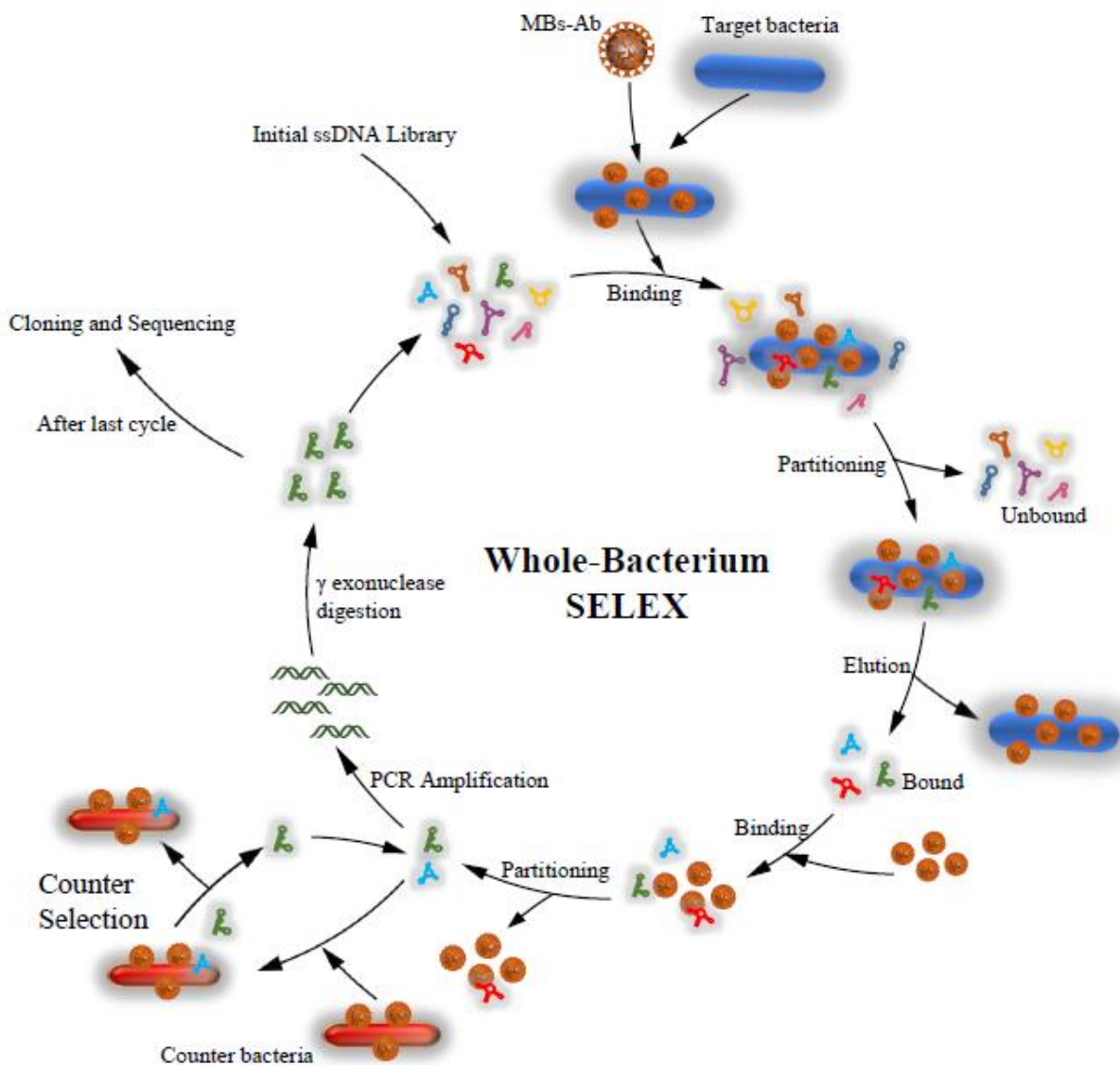
Fig. 2.2 The process of the whole-bacterium SELEX against *E. coli* O157:H7.

Each 50 µl reaction of PCR amplification contained 5 µl 10 × AccuPrime PCR buffer, 1 µl 2 U/µl AccuPrime *Taq* DNA polymerase (Life Technologies, Grand Island, NY), 1 µl 100 µM

forward primer, 1 µl 100 µM phosphate-labeled reverse primer, 0.1-1 µl of aptamer pool, and DNase-free distilled water. PCR conditions were as follows: initial denaturation at 94°C for 5 min, followed by 20 or 25 cycles (Savory et al., 2014) of denaturation at 94°C for 30 s, annealing at 55°C for 20 s, and extension at 68°C for 30 s. A final extension step at 68°C for 5 min was carried out after the last cycle. Electrophoresis on 1.5% agarose gel at 130 V for 35 min was used to confirm the purity and the size of PCR products. All PCR products were purified using MinElute PCR Purification Kit (Qiagen, Valencia, CA).

To obtain aptamer pool as the input for the next round, ssDNA was generated from dsDNA PCR products via lambda exonuclease digestion, in which the 5'-phosphorylated strand of dsDNA was digested. 1 unit of lambda exonuclease (5,000 U/ml) was used for digestion of 1 µg PCR products. Lambda exonuclease, 10× lambda exonuclease buffer, purified PCR product, and DNase-free water made up a total reaction volume of 50 µl. The reaction was carried at 37°C for 30 min and the enzyme was heat-inactivated at 75°C for 10 min. The obtained ssDNA was finally purified by ethanol precipitation with glycogen as a carrier, and the purified ssDNA was dissolved in distilled water. Agarose gel electrophoresis was used to determine if the restriction digest was complete. The concentration of the precipitated ssDNA was measured by Synergy HT multi-mode microplate reader (BioTek Instruments, Inc., Winooski, VT, USA) using BioTek's Take3 multi-volume plate.

To eliminate nonspecific-binding ssDNA from the pool, four and another two counter selection rounds were introduced after SELEX round 9 and 14, respectively. In the counter selection, the aptamer pool was incubated with a mixture of non-target bacterial cells (*S. aureus*, *S.* Typhyimurium and *L. monocytogens*) at a concentration of 10^8 CFU/ml for 45 min. After magnetic separation, the cell-bound ssDNA were discarded and the unbound aptamer pool in the

solution was collected for subsequent PCR amplification. The details on the procedures of all

selection and counter selection rounds are listed in Table 1.1.

Table 2.1 Details on procedures of all selection and counter selection rounds.

Selection (S) or counter selection (CS) round	Concentration of bacteria (CFU/ml)	Amount of ssDNA (pmol)	BSA in the incubation buffer (%)	Incubation time of ssDNA (min)	Times of washing
S1	10^8	2000	0.05	75	2
S2	10^8	7.5	0.05	45	2
S3	10^8	14.65	0.05	45	3
S4	10^6	8.69	0.05	45	3
S5	10^6	16.97	0.05	45	3
S6	10^5	5.57	0.05	30	3
S7	10^4	12.12	1	30	3
S8	10^4	14.79	1	30	3
S9	10^3	17.86	1	30	3
CS1	10^8	4.58	1	45	1
CS2	10^8	9.33	1	45	1
CS3	10^8	1.88	1	45	1
CS4	10^8	1.27	1	45	1
S10	10^3	101.22	1	20	3
S11	10^3	28.62	1	20	3
S12	10^3	37.78	1	20	3
S13	10^3	3.25	1	20	3
S14	10^3	27.88	1	20	3
CS5	10^8	53.74	1	45	1
CS6	10^8	6.45	1	45	1
S15	10^3	33.85	1	15	3
S16	10^3	7.25	1	15	3
S17	10^3	33.46	1	15	4
S18	10^3	17.66	1	15	4
S19	10^3	42.64	1	15	4

The aptamer pool from the last round was selected for cloning to obtain unique aptamer

sequences. Briefly, the aptamer pool was ligated into pGEM®-T Easy Vector System II

(Promega, Madison, WI), which were then transformed into JM109 High Efficiency Competent

Cells. After growing on LB (Luria-Bertani)/ampicillin/IPTG (Isopropyl β-D-1-

thiogalactopyranoside)/X-Gal plates overnight, white colonies were randomly picked out. PCR

using M13 primers were used to identify the positive inserts. Then the competent cells transformed with the clones having positive inserts were growing in LB broth with 50 µg/ml ampicillin and the plasmid were purified by QIAprep® Spin Miniprep Kit. PCR was then conducted with biotinylated forward primer and phosphorylated reverse primer and ssDNA was generated by lambda exonuclease digestion. Following the screening of the binding affinity of around 100 clones via dot blot assay, twenty aptamer clones with the highest binding affinities were chosen for sequencing by Eurofins Genomics (Huntsville, AL, USA). Secondary structures of sequenced aptamers were predicted by web-based OligoAnalyzer 3.1 program from IDT.

2.3.5 Analysis of the binding affinity using QCM

Before use, the crystal was immersed in 1 M NaOH for 30 min and 1 M HCl for 5 min to obtain a clean Au surface. Then the crystal was rinsed with pure water and absolute ethanol for three times (Su and Li, 2005). After drying with a stream of nitrogen, the crystal was submerged in 20 mM MHDA (16-Mercaptohexadecanoic acid) for 24 h at room temperature in the dark to form self-assembled monolayers (SAMs) terminated with carboxyl groups via gold-thiolate bonds (Xue et al., 2014). The unreacted MHDA was removed by three washes with absolute ethanol and pure water. The functionalized electrode was then mounted in the methacrylate flow cell with only one side exposed to the solution and was connected to the QCA922 quartz crystal analyzer.

Fig. 2.3 shows the procedure of the gold surface immobilization and the binding of aptamers to target bacteria: first, 200 µl of deionized water was added into the cell to obtain a stable baseline. Then, 300 µl of the freshly prepared EDC (*N*-(3-Dimethylaminopropyl)-*N′*-ethylcarbodiimide hydrochloride)/NHS (N-Hydroxysuccinimide) (original concentrations: 75

mM/30 mM, v/v, 1:1, final concentrations: 37.5 mM/15 mM) solution was added and reacted for

10 min to convert the terminal carboxylic group to an amine-reactive NHS-ester. After that, 400

µl of *E. coli* O157:H7 (10^6 CFU/ml) was added and incubated for 45 min to be immobilized on

the electrode surface. Next, 200 µl of BB was used to flush the cell for four times to rinse off the

excess bacteria. And another 200 µl BB was added to get the baseline. Afterwards, 200 µl of heat

denatured (95˚C for 10 min) aptamer pool diluted in BB was added and incubated for 45 min.

After flushing out the unbound aptamers, 200 µl binding buffer was added again to get the

baseline. The frequency change (ΔF) caused by aptamer binding was calculated by measuring

the difference of the baselines before and after the incubation of aptamer pools (Wang and Li,

2013).
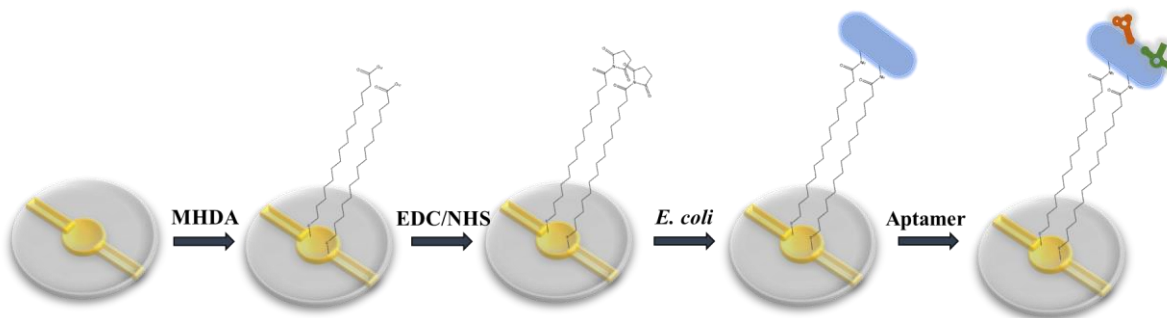
Fig. 2.3 Schematic diagram of the QCM electrode modification and the binding of aptamers to target bacteria.

To determine the K_d of the aptamer candidate, 10^7 CFU/ml *E. coli* O157:H7 were

immobilized on the electrode. Different concentrations of aptamer solution (0, 5 nM, 50 nM, 100

nM, and 1 µM) were used in the binding assays. Regeneration of the electrode was carried out by

reacting with 400 µl of different concentrations of NaOH (1, 2, 5, 7.5, and 10 mM) for 2 min. A

nonlinear regression curve was fitted to the frequency shifts corresponding to the varied aptamer

concentration. And the K_d value was estimated using the equation $Y = B_{max} \times X/(K_d + X)$ (Bing et al., 2010) by GraphPad Prism 5.0 software.

2.3.6 Analysis of the specificity using dot blot assay

Non-target bacteria - *E. coli* K12, *S.* Typhimurium, and *L. monocytogenes* were used to examine the specificity of the aptamer candidate by dot blot assay. The procedure of the assay was as follows. First, 3 µl of target bacteria *E. coli* O157:H7 (suspended in 1× PBS) and non-target bacteria (suspended in 1× PBS) at 10^8 CFU/ml were spotted onto a piece of BioRad zeta-probe blotting nylon membrane (BioRad, Hercules, CA). While 3 µl of 1 × PBS was spotted as a negative control (NC). After the spots were air dried, the membrane was immersed in KPL blocking buffer for 30 min and then allowed to air dry. 50 µl of 40 µM biotinylated aptamer S1 (diluted in KPL blocking buffer) were added to cover the whole membrane and incubated for 30 min. Subsequently, four times of washing were applied with washing buffer (1 × PBS with 0.1% Tween-20) for 20 min to remove the unbound aptamers. Then the membrane was incubated with three drops of alkaline phosphatase-labeled streptavidin (approximately 2 µg/ml) for 25 min. After excess enzymes were removed with the same washing step, 500 ml of phosphatase substrate BCIP (5-bromo-4-chloro-3-indolyl-phosphate)/NBT (nitro blue tetrazolium) (KPL, Gaithersburg, MD) were added to react with the phosphate for 10 min in the dark for color development. Finally, water was added to stop the reaction, and the membrane was kept in the dark overnight.

2.3.7 A QCM aptasensor for the detection of *E. coli* O157:H7

200 µl 1 mg/ml streptavidin (Rockland, Limerick, PA) were immobilized on the MHDA-SAMs modified electrode for 30 min following the activation of carboxyl groups with 300 µl of

EDC/NHS (original concentrations: 400 mM/100 mM, v/v, 1:1, final concentrations: 200 mM/50 mM) for 10 min. After washing with 300 µl of deionized water twice and 300 µl of BB, 100 µl of 5'-biotin - labeled aptamer S1 (20 µM in BB) was added and incubated for 45 min. Then the flow cell was washed with 300 µl of deionized water twice and 300 µl of PBS, and 200 µl of 0.1 mg/mL poly (ethylene glycol) (PEG) methyl ether thiol (Brockman et al., 2013) dissolved in PBS was added to block the unmodified electrode gold surface for 20 min. Following the same washing step, 200 µl of PBS was added to get a baseline. Subsequently, 200 µl of *E. coli* O157:H7 (1 ml of 10^2-10^7 CFU/ml cells were pelleted by centrifugation and resuspended in 200 µl PBS) was added and incubated for 30 min. After washing for the removal of unbound bacterial cells, 200 µl of PBS was added to get a baseline. The frequency change (ΔF) caused by the target bacterial binding was calculated by measuring the difference of the baselines before and after the incubation of *E. coli* O157:H7. The scheme of the process of the detection of *E. coli* O157:H7 using a QCM aptasensor is shown in Fig. 2.4. For the specificity test, 200 µl of *E. coli* K12, *S.* Typhimurium, *L. monocytogenes*, or *S. aureus* (1 ml 10^7 CFU/ml cells were pelleted by centrifugation and resuspended in 200 µl PBS) was added and incubated for 30 min.
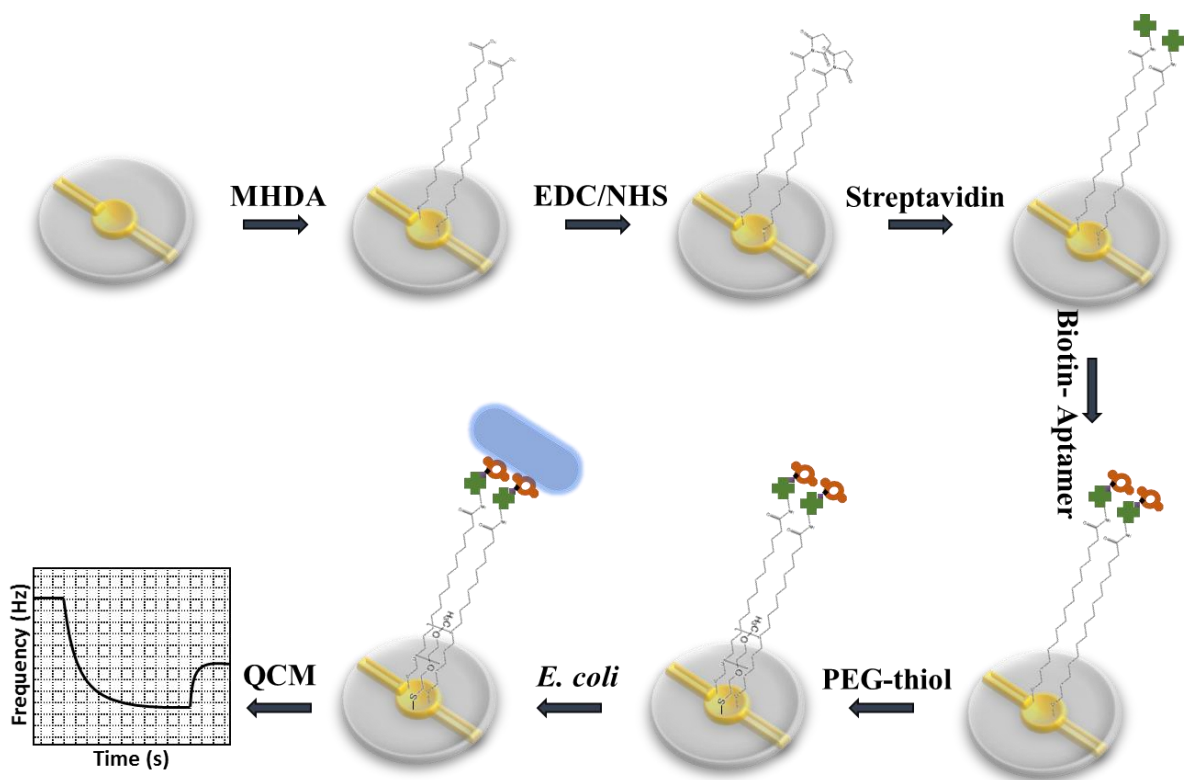
Fig. 2.4 Schematic diagram of the QCM aptasensor for the rapid detection of *E. coli* O157:H7.

2.3.8 Scanning electron microscopy (SEM) imaging

SEM imaging was performed to confirm the binding of target bacteria onto the aptamer immobilized QCM electrode using the high-resolution scanning electron microscope FEI Nova NanoLab 200 (FEI, Hillsboro, OR).

2.4 Results and discussion

2.4.1 Selection of ssDNA aptamers against *E. coli* O157:H7

In the SELEX, MBs served as the solid support for the partitioning of aptamers from the target bacteria. Compared with other partitioning methods, such as centrifugation and filtration, MBs possess several advantages, including fast separation, ease of extensive washing, and

applicability for a wide range of targets. The capture efficiency of IMBs for *E. coli* O157:H7 at a concentration of 10^3 CFU/ml was over 90% (Xu et al., 2015).

In each round of selection, the sizes of both the PCR products and lambda exonuclease digested ssDNA fragments were determined by running agarose gel electrophoresis (AGE). As seen in Fig. 2.5, the bands of the PCR products were at around 90 bp, and those of digested ssDNA fragments were smeared in the range of 100 - 200 bp or were invisible. Meanwhile, two patterns of PCR by-products were observed: ladder-like bands over 90 bp and a single band slightly smaller than 90 bp (see Fig. 2.6). A molecular mechanism to explain this phenomena was proposed by Tolle et al. (2014) via sequence identification of the corresponding PCR products after PCR condition alteration. They suggested that the generated short and ladder-like by-products were results of primer-primer hybridization and product-product or product-primer base paring in the random region of ssDNA, respectively. By-product formation could be decreased by the reduction of the amount of DNA template and the number of thermal cycles (He et al., 2013) or better primer design (Tolle et al., 2014). In this study, the short by-products were possibly generated by the hybridization between forward primer and the central random region of the product instead. The right PCR products were obtained by means of DNA template dilution, thermocycling number decreasing, or gel extraction of the correctly sized band, so as to avoid the failure of aptamer selection.
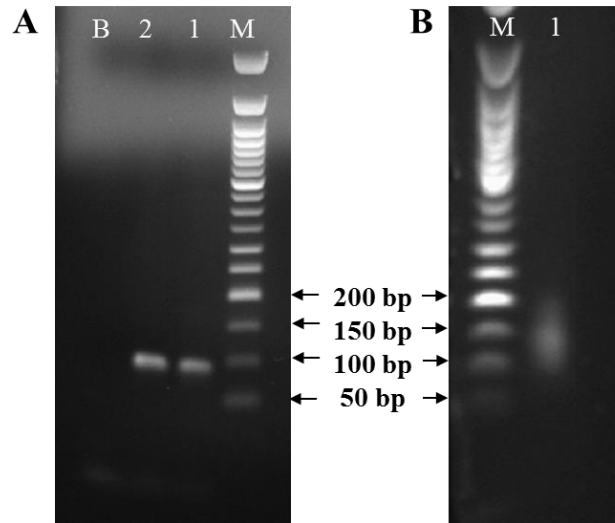
Fig. 2.5 Agarose gel electrophoresis of A) PCR products: M is 50 bp ladder, 1 and 2 are samples, B is blank control; B) digested ssDNA: M is 50 bp ladder, and 1 is the sample.
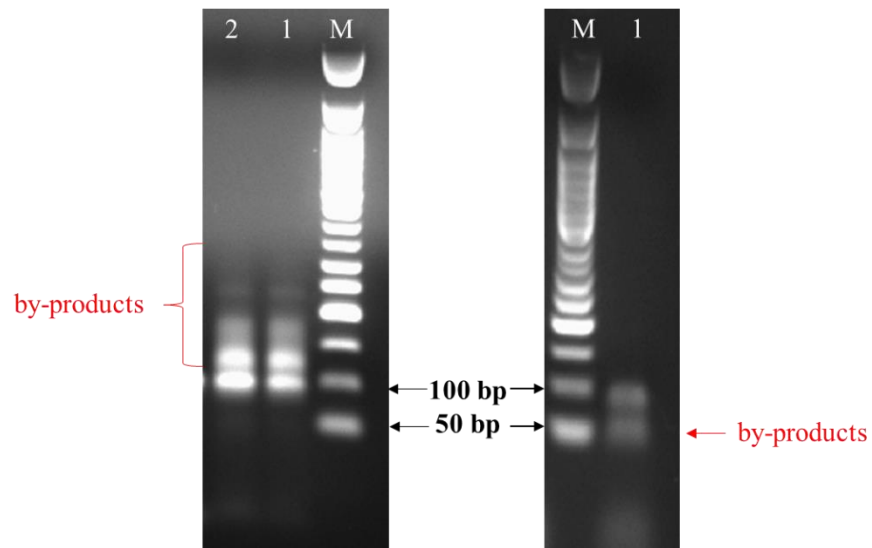
Fig. 2.6 Agarose gel electrophoresis of PCR by-products of two patterns: one is ladder-like and all above the correct band (left); the other is lower than the correct band (right). M is 50 bp ladder, and 1 and 2 are the PCR products.

In order to select aptamers sensitively and specifically recognizing *E. coli* O157:H7, the

selection pressure was progressively enhanced by: 1) decreasing the concentration of bacteria

from 10^8 to 10^3 CFU/ml, 2) decreasing the incubation time with the target bacteria from 45 min to 15 min, 3) increasing the amount of BSA in the incubation buffer from 0.05% to 1%, 4) increasing times of washing after the incubation from two to four, 5) increasing washing duration from 10 seconds to 1 min (Table 1.1).

2.4.2 Affinity analysis of aptamer pools

In the whole process of whole-bacterium SELEX, nineteen rounds of positive selection and six rounds of counter selection were conducted. To monitor the enrichment of aptamer pools during selection, the binding affinity of aptamer pools was evaluated by bot blot assay (data not shown) and QCM. The typical response course of frequency shifts for the stepwise immobilization of the QCM electrode and the binding of the aptamer pool is shown in Fig. 2.7. The frequency changes in response to the binding of the initial ssDNA library, and the aptamer pools from rounds 13, 14, and 19 are illustrated in Fig. 2.8. As indicated in the figure, no detectable signal was obtained for the original random ssDNA library. For the aptamer pools from round 13, 14, and 19, frequency changes of -17 Hz, -37 Hz, and -60 Hz, respectively, were obtained. The larger the change of frequency, the larger the amount of aptamers bound to the target bacteria, and the higher the binding affinity of the aptamer pool. It was also observed that after two rounds of counter selection following round 14, the binding affinity of the aptamer pool from round 17 was decreased (data not shown). This phenomenon was likely due to the removal of aptamer candidates non-specifically binding to the non-target bacteria from the pool. These eliminated aptamer candidates might have occupied different sites on the target surface and contributed to the total binding affinity of the aptamer pool from round 14.
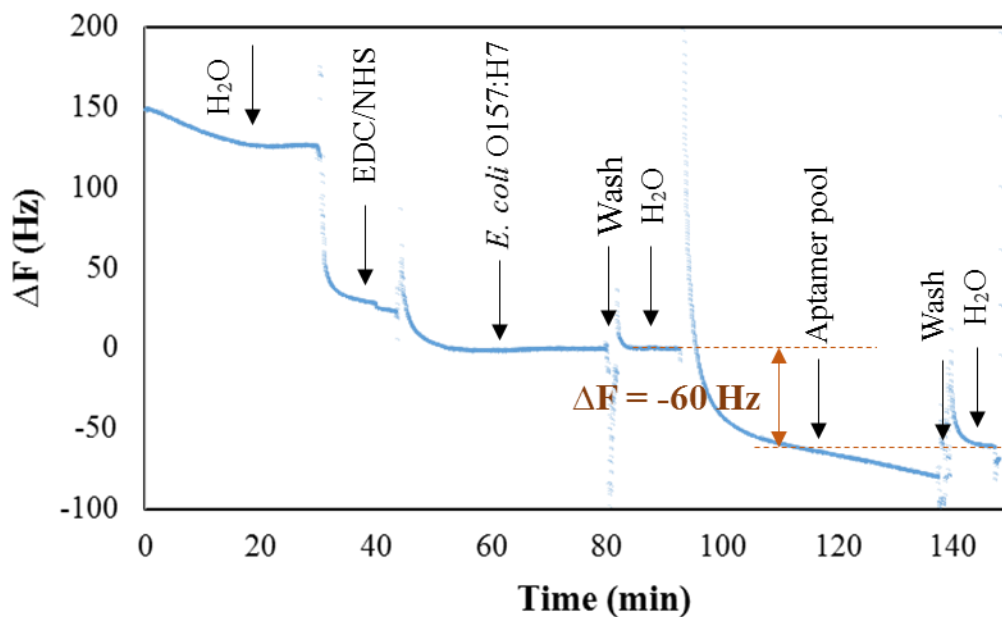
Fig. 2.7 Frequency shifts (ΔF) corresponding to each step of modification on QCM electrode for the affinity test of the aptamer pool from SELEX round 19.
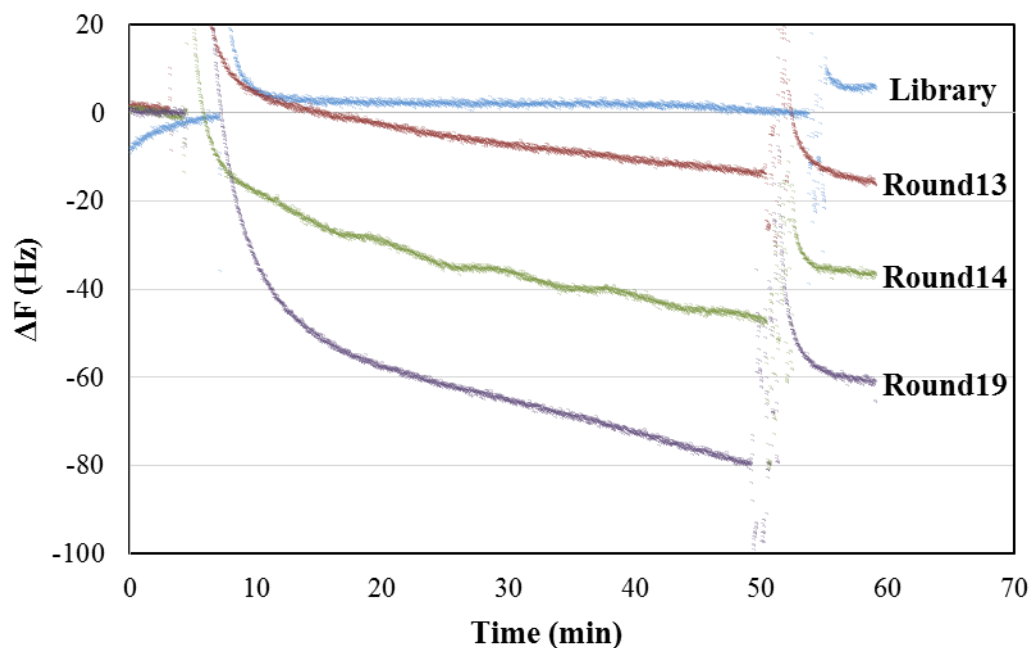
Fig. 2.8 Frequency changes in response to the binding of initial ssDNA library, and aptamer pools from rounds 13, 14, and 19 to *E. coli* O157:H7 measured by QCM.

The process of SELEX is usually repeated for 5-12 times (rounds) (Dwivedi et al., 2010, 2013; Suh et al., 2014) in order to enrich the aptamer pool. The reason that it took as many as 19 rounds of selection in this study is probably that the remained binding sites on the target bacteria for aptamers were limited after the binding of anti-*E. coli* antibodies on the bacteria surface. This SELEX format is capable of isolating aptamers sharing no competitive binding sites with antibodies, which can be employed in an aptamer-antibody sandwich assay. The reason why the selected aptamer is unlikely to share the same binding site with the antibody is that the whole surface of the bacterial cell was exposed and occupied with over a hundred of IMBs when the bacteria were captured by IMBs in the solution during SELEX (Fig. 2.9). As a result, a great majority of the O (somatic lipopolysaccharide) and K (capsular) antigens on the bacterial surface had been bound by the antibodies on IMBs, leaving negligible free epitopes for aptamers to interact with. Even if some aptamer candidates did bind to some free epitopes in the earlier rounds of SELEX, they would have been sifted out during the enrichment of the aptamer pool by PCR, in which the aptamer candidates that bound to more available binding sites with stronger affinities would dominate the pool.
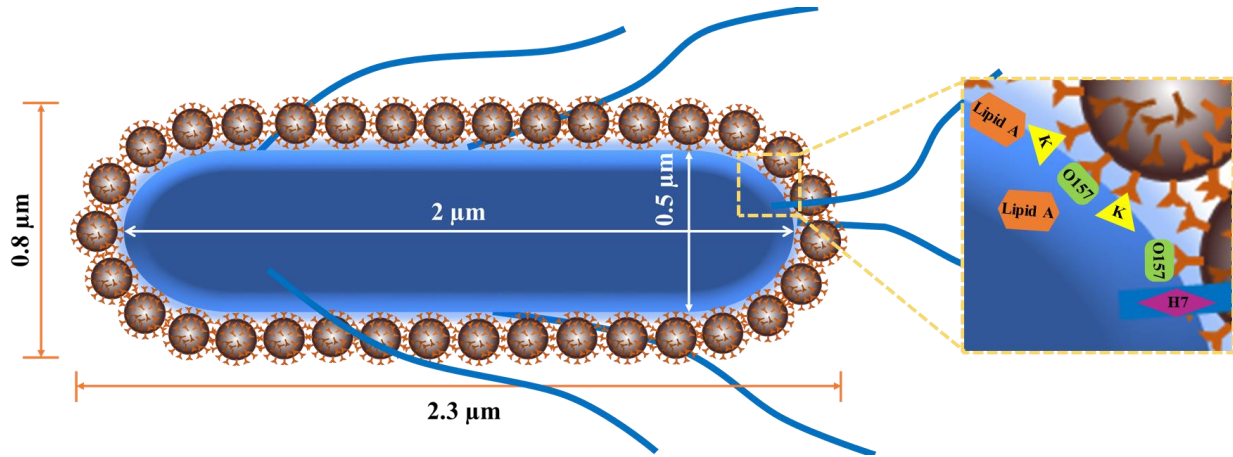
Fig. 2.9 Schematic diagram of an *E. coli* O157:H7 cell captured and surrounded by IMBs. On the cell surface, a great majority of the O and K antigens were bound by the anti-*E. coli* polyclonal antibodies on IMBs, and the potential binding sites for aptamers could be flagellar (H7) antigen or other components on the outer membrane, such as lipid A.

The Sauerbrey equation (Sauerbrey, 1959) is used to describe a linear relationship between the shift in resonant frequency of a quartz crystal and the change in mass loading to its surface and thus can be utilized to calculate the mass of molecules deposited to the QCM electrode surface. The equation (Hengerer et al., 1999; Shan et al., 2014) is as follows:

$$\Delta F = -2F_o^2 \frac{\Delta M}{A\sqrt{\rho\mu}} = -2.3 \times 10^6 F_o^2 \frac{\Delta M}{A} \qquad (2\text{-}1)$$

Where ΔF (Hz) is the measured frequency change, F_o (MHz) is the resonant frequency of the piezoelectric quartz crystal (7.995 MHz in this case), ΔM (g) is the mass change on the electrode surface, and A (cm^2) is the active area of the coated quartz surface (Kumar, 2000; Liss et al., 2002), which is 0.2 cm^2 in this case (Wang et al., 2017), ρ is the density of the crystal (2.648

g/cm^3), and μ is the shear modulus of the quartz (2.947×10^{11} g/cm^3/s^2) (Shan et al., 2014).

According to the equation above, the binding amount of aptamers - ΔM (g) was calculated based

on the measured value of ΔF (Hz) for each specific round. The results of the calculation are

shown in Table 2.2. As SELEX proceeded, increasing amounts of aptamers were bound to the

target bacteria, as an indication of the improvement of the binding affinity of aptamer pools.

Table 2.2 The calculations of the amount of aptamers bound to target bacteria by Sauerbrey equation using the frequency change measured in QCM tests. The concentrations of the aptamers from all rounds used for QCM tests were constantly 11.4 ng/µl.

Aptamer pool	ΔF (Hz)	ΔM (g)	Binding amount (pmol)
Library	0	0	0
Round 13	-17	2.31×10^{-8}	0.82
Round 14	-37	5.00×10^{-8}	1.79
Round 19	-60	8.16×10^{-8}	2.91

The molecular weight of the aptamer is 2.80×10^{-8} g/pmol.

2.4.3 Cloning and sequence analysis

Twenty clones presenting the highest binding affinities by dot blot assay (data not shown)

were sequenced. Table 2.3 shows the three different sequences obtained from these twenty

clones, among which 16 clones had the identical sequence S1, 3 clones had the identical

sequence S2, and the one clone had the sequence S3. The large percentage of identical sequences

in 20 clones might have resulted from the high enrichment of the aptamer pool via 19 rounds of

selection, which proved that the enrichment was accomplished successfully.

Table 2.3 A list of the three sequences identified from the 45-nt randomized region of the library after nineteen rounds of whole-cell SELEX against *E. coli* O157:H7.

Name	Occurrence	Sequences of N$_{45}$ random region (5' to 3')	ΔG (kcal/mol)	T_m (°C)
S1[a]	16X	TGGTCGTGGTGAGGTGCGTGTATGGGTGGTGGATGAGTGTGTGGC	-4.72	42.6
S2	3X	GCGGGAATAGGATGCGGCTGGAAGGAGAGGTGTTGGTGGGTGGTG	-4.76	41.3
S3	1X	GTGCGGTGACGTGAGGGGGAGAGGCGTTGGTGTAGGCTGTTGGTG	-6.00	42.1

[a] The sequence used for binding analysis was shown in red.

The secondary structures of all sequenced aptamers were predicted by web-based IDT OligoAnalyzer 3.1, which was based on free energy minimization algorithm. The structures of S1, S2, and S3 possess one external loop, one interior loop (except S3), and several hairpin loops (shown in Fig. 2.10). It has been known that aptamers bind to the target through molecular structure compatibility, precise stacking of flat moieties, electrostatic and van der Waals interactions, and hydrogen bonding (Hermann and Patel, 2000). So the stem-loop structures of aptamers must have played an important role as binding motifs in the target recognition (Kim et al., 2013).
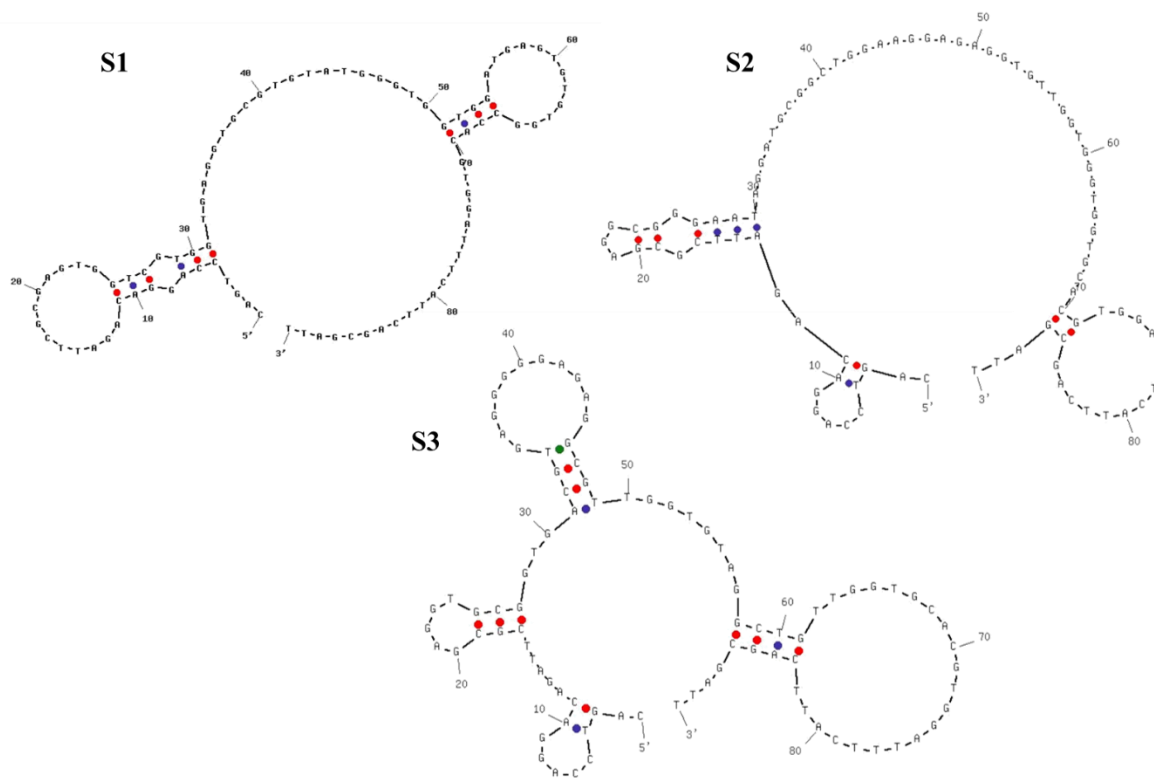
Fig. 2.10 Predicted secondary structures of aptamers S1, S2 and S3 using IDT OligoAnalyzer 3.1.

2.4.4 Determination of K_d and specificity of aptamer S1

Considering that the most frequently repeated sequence has been found to have the highest binding affinity (Hamula et al., 2008), sequence S1 with repetition of 16 times was chosen to be synthesized for further characterization. Fig. 2.11 shows the binding saturation curve from QCM-based assay of aptamer S1 and the target *E. coli* O157:H7 cells. A nonlinear regression curve was fit to the data using GraphPad Prism 5.0 based on the equation $Y = B_{max} \times X/(K_d + X)$. The K_d value of aptamer S1 was determined to be 10.30 nM.
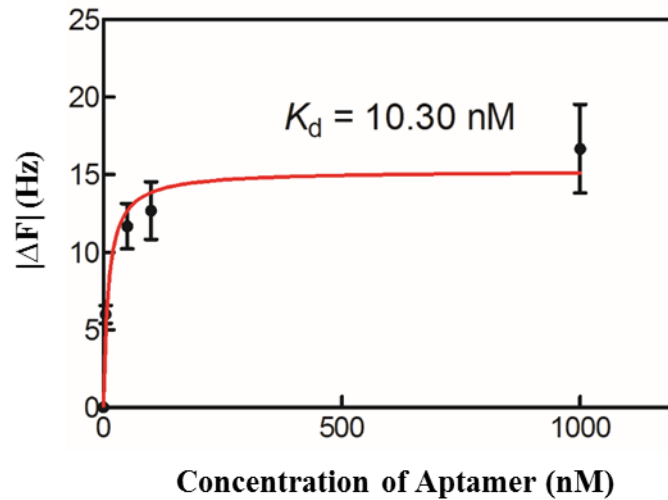
Fig. 2.11 Binding characteristics of aptamer S1 as determined by QCM. The data were fitted to a non-interacting binding sites model, which yielded a dissociation constant of 10.30 nM. Error bars are standard diviations from triplicate analyses.

During the tests characterizing the binding affinity of aptamer S1, the reusability of the QCM electrode was investigated. A previous research by our group found out that the regeneration of a QCM immunosensor by applying 10 mM NaOH for 10 min could cause 20% loss of activity (Li et al., 2011). According to that, we investigated the regeneration efficiency by using NaOH starting from a low concentration of 1 mM to 10 mM with a regeneration time from 2 min to 4 min. As in the test using 100 nM aptamers, the first and second regeneration was carried out by incubation with 400 µl 5 mM NaOH for 3 min and with 400 µl 7.5 mM NaOH for 2 min, resulting in a binding signal variation of 7.1 % and 35.7%, respectively. It was also found that it became difficult to regenerate the electrode for a 3rd time on all tested concentrations of aptamers. Thus, each electrode was only regenerated twice and the first three data were recorded.

The specificity of aptamer S1 in recognizing *E. coli* O157:H7 was examined using dot blot assay. Non-target bacteria *E. coli* K12 (gram-negative non-pathogenic), *S.* Typhimurium

(gram-negative pathogenic), and *L. monocytogenes* (gram-positive pathogenic) were tested to check any cross-reactivity. Fig. 2.12 shows that aptamer S1 had the best binding affinity to target *E. coli* O157:H7, while no notable binding to two non-target pathogenic bacteria. Some degree of cross-reactivity with *E. coli* K12 was observed, which is probably due to the similar cell surface structure between *E. coli* K12 and *E. coli* O157:H7. And as we know, *E. coli* K12 was not included in counter selection in the whole-bacterium SELEX process. Nevertheless, the high binding affinity and specificity of aptamer S1 to *E. coli* O157:H7 over other two pathogenic bacteria still prove its great potential to be applied in distinguishing *E. coli* O157:H7 from other foodborne pathogens.
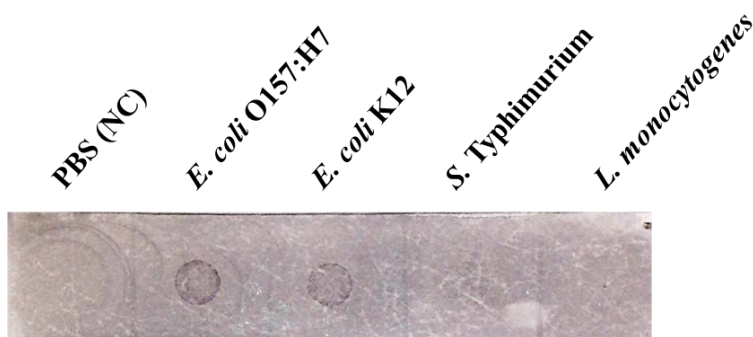
Fig. 2.12 The binding specificity of selected aptamer S1 for *E. coli* O157:H7 over three other bacteria evaluated by dot blot assay.

In comparison with the RNA aptamer developed by Lee et al. (2012) ($K_d = 110$ nM), the selected ssDNA aptamer in this study possessed stronger binding affinity against *E. coli* O157:H7. The aptamers for *E. coli* selected by Kim et al. (2013) showed similar affinities ($K_d = 2.4 \sim 25.2$ nM), but were not specific for *E. coli* O157:H7. And the affinity of the aptamer to *E.coli* O157:H7 was not evaluated. Besides, in the SELEX process, the aptamer was only counter-selected against four non-foodborne pathogens - *Klebsiella pneumoniae, Citrobacter*

freundii, Enterobacter aerogenes, and *Staphylococcus epidermidis.* Thus, a potential problem lies in the application of these aptamers to the discrimination of *E. coli* in food samples. It may also indicates that these aptamers were not developed for the purpose of detecting foodborne pathogens.

Some researchers have endeavored to discover possible binding sites of aptamers on target cells through binding affinity analysis of aptamers with either extracted cell surface protein (Hamula et al., 2008) or intact or enzyme-pretreated cell membranes (Li et al., 2014). According to the SELEX procedure in this study, before the incubation of the aptamer pools, a great majority of the O and K antigens on the cell surface had already been bound by the anti-*E. coli* polyclonal antibodies on IMBs for the capture of target bacteria. And some aptamer candidates that did bind to the limited free epitopes in the earlier rounds of SELEX would be sifted out during the enrichment of the aptamer pool by PCR. So it is not very likely that the aptamer we selected shared the binding sites (O and K antigens) with the antibodies. The potential binding sites for aptamers could be H (flagellar) antigen or other components on the outer membrane, such as lipid A (Fig. 2.9). Based on that the developed QCM aptasensor had some cross-reaction with *E. coli* K12 (Fig. 2.14), it could be implied that the epitope that the selected aptamer binds to is more abundant on the *E. coli* O157:H7 surface than on *E. coli* K12 surface.

2.4.5 Application of aptamer S1 to *E. coli* O157:H7 detection

To demonstrate the potential application of the selected aptamer to the detection of live *E.coli* O157:H7, a QCM-based aptasensor was fabricated by the successive immobilization of streptavidin and biotinylated aptamer S1 on the QCM electrode surface. *E. coli* O157:H7

cultures of 10-fold serial dilution from 10^2 to 10^7 CFU/ml were detected by incubating with the immobilized aptamers for 30 min. The decrease of frequency caused by the binding of various concentrations of *E. coli* O157:H7 was shown in Fig. 2.13 A. The standard deviations (S.D.) calculated from triplicate tests are shown as error bars in the figure. Good linear relationships were found between the frequency change and the logarithm of the cell concentration from 10^2 to 10^5 CFU/ml and from 10^5 to 10^7 CFU/ml. The corresponding regression equations were y = -1.65x + 2.22 ($R^2 = 0.96$) and y = -9.19x + 43.80 ($R^2 = 0.99$), respectively. PBS without target bacteria was detected as a negative control (NC), which resulted in frequency change of 0 ± 1 Hz. The LOD (as 3 times the S. D. of the NC) was thus determined to be 1.46×10^3 CFU/ml based on the regression equation. The total detection time was 40 min including the baseline stabilization after the incubation with target bacteria. SEM imaging was used to check the binding of *E. coli* O157:H7 cells onto the aptamer - immobilized gold surface of the QCM electrode (Fig. 2.13 B).
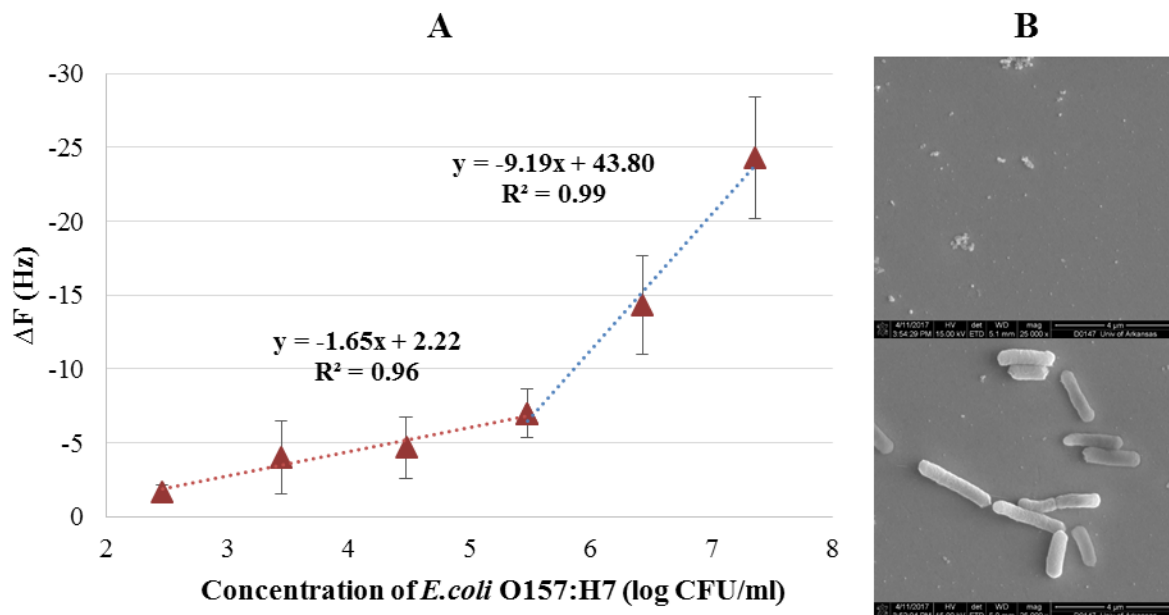
Fig. 2.13 (A) The calibration curves of frequency changes verses *E. coli* O157:H7 concentrations from 10^2 to 10^7 CFU/ml detected by QCM-based aptasensor. Each value is presented as mean ± S. D. (n=3). (B) SEM images of the QCM gold surface immobilized with streptavidin and biotinylated aptamers before (top), and after (bottom) the detection of *E. coli* O157:H7.

The capability of the QCM-based aptasensor to discriminate *E. coli* O157:H7 from other non-target bacteria were investigated under the same experimental conditions as those for *E. coli* O157:H7. Frequency shifts after incubation with 10^7 CFU/ml *E. coli* K12, *S.* Typhimurium, *L. monocytogenes*, and *S. aureus* for 30 min were measured and the S.D. calculated from triplicate tests are shown as error bars in Fig. 2.14. The results showed that the aptasensor had some affinity to *E.coli* K12, and negligible or no cross-reactivity to *S.* Typhimurium, *S. aureus*, and *L. monocytogenes*. The frequency change corresponding to the LOD of 1.46×10^3 CFU/ml is -3 Hz, which is larger than the detection signal for *E.coli* K12 at 10^7 CFU/ml (-7 Hz). It was a pity that *E.coli* K12 was not used for counter-selection of SELEX because of the lack of anti- *E.coli* antibody, which should be used to coat the magnetic beads for the capture of *E.coli* K12 cells. Since the species of *E.coli* share similar epitopes more than with other genus of bacteria, it's

possible that the selected aptamer will have some degree of affinity to other strains of *E.coli*. Thus, the QCM aptasensor is not capable of discriminating *E. coli O157:H7* from 10^7 CFU/ml *E.coli* K12, but has good specificity for *E. coli* O157:H7 against the other three pathogenic bacteria.
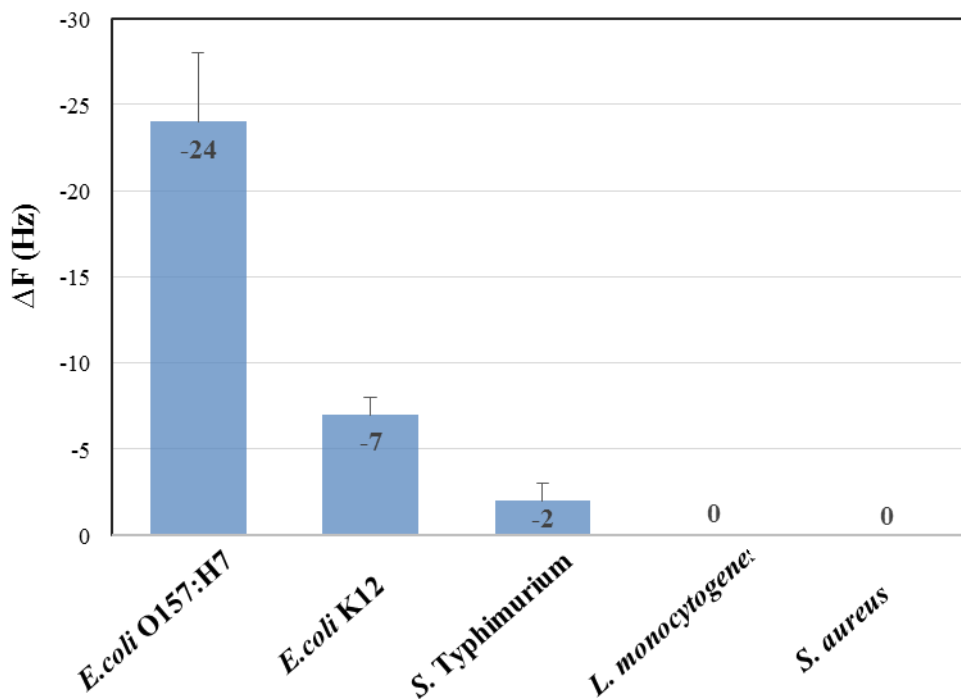
Fig. 2.14 Specificity of the QCM-based aptasensor for the detection of *E. coli* O157:H7 at concentration of 10^7 CFU/ml. Each value is presented as mean $\pm$ S. D. (n=3).

There are some published studies of label-free QCM sensors using the Ab or the aptamer as the recognition element for the detection of bacterial cells. The LOD for immunosensors was from 10^3-10^7 CFU/ml (Buchatip et al., 2010; Liu et al., 2007; Su and Li, 2005), and that for aptasensors was from 10^2-10^3 CFU/ml (Ozalp et al., 2015; Wang et al., 2017). It has been reported that the average height of Ab is 7.1 nm (Dong and Shannon, 2000), and the diameter of the folded aptamer is around 3 nm (White and Plaxco, 2009). As the Sauerbrey equation is only

applicable to uniform, rigid, thin-film deposits (Buttry, 1989), the relatively thicker layer of immobilized Ab might not have caused as large a signal as the thinner layer of aptamers for the detection of target bacteria. The sensitivity of the QCM-based immunosensor decreased especially when the immobilization layer was further increased by using protein A as a crosslinker.

The sensitivities of the QCM instrument and the quartz crystal themselves now need to be considered. The resolution of the QCA922 instrument is down to 1 Hz, which corresponds to 1.3 ng of mass change on the quartz surface of 0.2 cm^2. Since a single *E. coli* cell has a mass of approximate 1 pg (Milo and Phillips, 2015), the detection limit of the label-free QCM sensor will be around 1.3×10^3 *E. coli* cells, that is 1.3×10^3 CFU/ml (1 ml). From the Sauerbrey equation *(2-1)*, we can see that the sensitivity of QCM can be improved by increasing the primary resonant frequency of the quartz crystal F_o (MHz). When F_o is doubled, ΔF (Hz) – the signal will be increased by a factor of four (Afzal et al., 2017). For example, if the F_o of the quartz utilized in this study were 15.99 MHz instead of 7.995 MHz, the LOD would have been lowered to 3.65 $\times 10^2$ CFU/ml. However, crystals with high fundamental frequencies will be thin and fragile (Vashist and Vashist, 2011). When both the QCM instrument and the quartz crystal are fixed, one way to amplify the signal is by labeling the target with antibody conjugated magnetic beads or gold nanoparticles (AuNPs) (Jiang et al., 2011; Masdor et al., 2016; Salam et al., 2013). For example, in the ultra-sensitive QCM-based immunosensor developed for the detection of *E. coli* O157:H7 (Shen et al., 2014), the amplification was carried out by 3 times labeling of biotinylated IMBs, streptavidin conjugated gold nanoparticles (AuNPs), and gold growth on the AuNPs. The LOD of the developed immunosensor was lowered to 23 CFU/ml, but the detection time was

increased to 4 h and the detection procedure was much more complex, which made this sensor

inappropriate for the rapid and in-field detection of *E. coli* O157:H7 (Table 2.4).

Table 2.4 Reported studies of labeled and label-free QCM sensors for the detection of *E. coli* O157:H7.

Recognition element	Label	Immobilization method	LOD (CFU/ml)	Detection time	Reference
Antibody	Label-free	Polyclonal Ab to protein A	10^7	~50 min	Liu et al., 2007
	Label-free	Ab to protein A	10^6	~50 min	Jiang et al., 2011
	Label-free	Polyclonal Ab to protein A	10^5	1 h	Su and Li, 2005
	Label-free	Ab	10^2	50 min	Ngo et al., 2014
	Ab-conjugated magnetic nanoparticles	Polyclonal Ab to protein A	10^2	~90 min	Liu et al., 2007
	Ab-modified magnetic/silica/polymer beads	Ab to protein A	10^3	~90 min	Jiang et al., 2011
	3 times mass enhancement of BIMPs, streptavidin-gold, and growth solution.	Monoclonal Ab	23	4 h	Shen et al., 2011
	Ab-functionalized AuNPs	Ab for enriched bacterial culture	1-10	24 h	Guo et al., 2012
DNA probe	Label-free	Thiolated ssDNA probe for *eaeA* gene (PCR amplified)	1×10^6	> 120 min	Wu et al., 2007
	Streptavidin-coated ferrofluid nanoparticles	Thiolated ssDNA probe for *eaeA* gene (PCR amplified)	2.67×10^2	> 130 min	Mao et al., 2006
	Thiolated ssDNA probe-conjugated AuNPs	Thiolated ssDNA probe for *eaeA* gene (PCR amplified)	1.2×10^2	~170 min	Chen et al., 2008
	Avidin-coated AuNPs	Thiolated ssDNA probe for amplified *eaeA* gene to AuNPs	2×10^3	~220 min	Wang et al., 2008
Aptamer	Label-free	Biotinylated aptamer to streptavidin	1.46×10^3	40 min	This work

In the present study, *E. coli* O157:H7 cells were suspended in 1× PBS to be detected by

the developed QCM-based aptasensor. But for real application of the aptasensor, food sample

pretreatment will be conducted before the detection of the target bacteria, such as magnetic

separation. By using magnetic separation, only target bacteria will be isolated and concentrated

from the complicated impurities, such as biomaterials. Then, the isolated *E. coli* cells will be

resuspended in $1\times$ PBS and the detection procedure will be the same as what was provided in

this study.

2.5 Conclusions

In this study, ssDNA aptamers were selected the first time by a whole-bacterium SELEX

technique against *E. coli* O157:H7 with high affinity (K_d =10.30 nM) and specificity. The

selected aptamer was further applied to the development of a QCM aptasensor for the detection

of *E. coli* O157:H7. The LOD of the aptasensor was as low as 1.46×10^3 CFU/ml, superior to

most QCM-based immunosensors for pathogen detection. In addition, the fast response time of

40 min demonstrated the potential of the selected aptamer to be incorporated into various formats

of biosensors for rapid detection and investigation of *E. coli* O157:H7 outbreaks.

Chapter 3 Sensitive and Rapid Detection of *E. coli* O157:H7 Using a QCM Sensor based on a Multivalent Aptamer System

3.1 Abstract

E. coli O157:H7 is one of the top foodborne pathogens that cause illnesses more likely to lead to hospitalization. For rapid and sensitive detection of foodborne pathogens, some aptamers have been developed and incorporated into various biosensing systems. With advantages such as high affinity, low cost of chemical synthesis, and thermo-stability, however, aptamers suffer from monovalency and small size, which limit their binding efficiency of bacterial cells. The objective of this study is to create a multivalent aptamer system based on rolling circle amplification (RCA), which comprises repetitive aptamer sequences that are against *E. coli* O157:H7. The system is then applied to a quartz crystal microbalance (QCM) sensor for sensitive and rapid detection of *E. coli* O157:H7. The single-stranded (ss) 105-nt DNA template was circularized by ligation and then was immobilized on the electrode surface via streptavidin-biotin interaction. RCA reaction was then initiated with the catalysis of phi29 DNA polymerase using a biotinylated primer, generating a very long ssDNA product. Following the incubation with *E. coli* O157:H7 for 30 min, the frequency shift was measured. The ligation process and the RCA reaction were performed at 16°C for 8 h and at room temperature (RT) for 1 h, respectively. The RCA products (RCPs) were analyzed by agarose gel electrophoresis, indicating that the size of the RCPs was larger than 48.5 kb. After immobilization on the QCM electrode, the RCPs at the concentration of 8.33 µM (concentration of the DNA template) were able to produce much larger signals than the aptamers at 20 µM for the detection of *E. coli* O157:H7 cells at the same concentration. The limit of detection (LOD) of the aptasensor was determined to be 34 CFU/ml. The whole detection procedure was completed in 40 min. The developed QCM

sensor showed negligible cross-activity to *Listeria monocytogenes*, *Listeria innocua*, *E. coli* K12, *Salmonella* Typhimurium, or *Staphylococcus aureus.* It is the first time that RCA was utilized to produce a multivalent aptamer system for the detection of *E. coli* O157:H7 using a QCM sensor. The RCPs-based aptamer sensor developed in this study manifested a much better sensitivity than a regular aptasensor.

3.2 Introduction

As one of the top foodborne pathogens, *E. coli* O157:H7 is related to 73,000 illnesses in the US each year. *E. coli* O157:H7 produces Shiga toxins (Stxs) and can cause hemorrhagic colitis (HC) and the life-threatening hemolytic uremic syndrome (HUS) in humans. The annual cost of illness due to *E. coli* O157:H7 infections was 405 million dollars, including lost productivity, medical care, and premature death (CDC).

Conventional detection methods for foodborne pathogens, being time-consuming, labor-intensive, or complex sample preparation required, failed to meet the urgent need of rapid and sensitive detection of *E. coli* O157:H7 to monitor and control outbreaks. A biosensor is an analytical device, composed of a bio-recognition element and a transducer, which is able to realize fast and sensitive detection of targets. A bio-recognition element or a bioreceptor that acts as the sensor could be enzymes, antibodies, nucleic acids, cells, or phages, while a transducer serves to convert a biological response into electrochemical, optical, thermal, or mass signals which could be observed and displayed more easily. QCM is an acoustic (mass-based) piezoelectric biosensor. The decrease in resonant frequency of the quartz is linearly proportional to adsorbed mass on the quartz surface based on the piezoelectric effect. QCM sensors possess

71

the advantages of simplicity, cost effectiveness, label-free detection, and real-time monitoring, and are able to detect mass change down to nanogram level (Marrazza, 2014).

Aptamers are a class of small single-stranded DNA or RNA oligonucleotides that are capable of binding to selected targets, including whole cells, proteins, peptides and small molecules with high specificity and affinity, through their folding into unique three-dimensional (3D) structures. As substitute of antibodies, aptamers have advantages such as high affinity, low cost of chemical synthesis, easy modification, and thermo-stability. However, aptamers suffer from monovalency and small size, which limit their binding efficiency to large entities. RCA is an isothermal amplification method, which is initiated by a primer hybridized to a small circular template in the presence of some polymerase with strand-displacement activity (e.g. phi29 DNA polymerase) (Mayboroda et al., 2018). The RCPs are tens of thousands of nucleotide long, containing tandem repetitive sequences complimentary to the circular template. RCA has been widely used in biosensors for signal amplification due to its high efficiency of amplification, no requirement for thermal cycling instrument, no significant damage to biological molecules or environment, and easy modification of RCPs with fluorescence or nanoparticles labeled short complimentary DNA strands (Zhao et al., 2008).

So far, only two biosensors based on multivalent aptamer system by RCA have been reported, which are used to capture and deliver drugs into leukemia cells (Zhao et al., 2012; Zhang et al., 2013). The circular templates were designed to include a complimentary sequence to the aptamer against protein tyrosine kinase 7 (PTK7) for the recognition of leukemia cells, a polyT spacer for separating two aptamer sequences, and/or with a short DNA domain for drug loading. The established 3D DNA network and Poly-Aptamer-Drug system were demonstrated

to have much higher capture efficiency of leukemia cells under high shear stress and notably enhanced endocytosis and drug release efficiency than monovalent aptamers.

Herein, a novel multivalent aptamer system was constructed based on RCA, which comprises repetitive aptamer sequences against *E. coli* O157:H7. The system is then applied to a QCM sensor for sensitive, rapid, and label-free detection of *E. coli* O157:H7.

3.3 Materials and methods

3.3.1 Bacterial cell preparation

Stock cultures of *E. coli* O157:H7 (ATCC 43888), *S. aureus* (ATCC 27660), *L. monocytogenes* (ATCC 43251), *L. innocua* (ATCC 33090), *S.* Typhimurium (ATCC 14028), and *E. coli* K12 (ATCC 29425) were obtained from the American Type Culture Collection (ATCC, Manassas, VA, USA). Pure cultures were maintained at -80°C with glycerol, then were grown in 5 ml HBI medium at 37°C and harvested upon reaching the log phase (usually 3-4 h) by centrifugation. Subsequently the cells were washed in $1 \times$ PBS, and finally resuspended in the same volume of $1 \times$ PBS. For bacterial enumeration, the bacterial samples were 10-fold serially diluted with $1 \times$ PBS and were surface plated on the TSA plates and incubated overnight before counting. Colony forming units (CFU) on the agar plates were counted as CFU/ml.

3.3.2 Materials

Deoxynucleotide (dNTP) solution mix, phi 29 DNA polymerase, DNA T4 ligase, 50 bp DNA ladder, and Quick-Load® 1 kb extend DNA ladder were purchased from New England BioLabs (Ipswich, MA). Streptavidin was purchased from Rockland Immunochemical Inc. (Limerick, PA). 16-Mercaptohexadecanoic acid (MHDA), poly(ethylene glycol) methyl ether

thiol, N-Hydroxysuccinimide (NHS), and ethidium bromide were obtained from Sigma (St.

Louis, MO). N-(3-Dimethylaminopropyl)-N'-ethylcarbodiimide hydrochloride (EDC·HCl) was

purchased from Merck KGaA (Darmstadt, Germany). Certified molecular biology agarose was

purchased from BioRad (Hercules, CA), and $10 \times$ Tris/Boric Acid/EDTA (TBE) buffer was

purchased from Life Technologies (Grand Island, NY). Milli-Q water purified by the system

from MillliporeSigam (Burlington, MA) was used in all experiments. All DNA (names and

sequences in Table 3.1) were synthesized by Integrated DNA Technologies.

Table 3.1 Oligonucleotide sequences of ssDNA aptamer, circular template, and primer[a].

Name	Sequences (5' – 3')
Aptamer	CAG TCC AGG ACA GAT TCG CGA GTG GTC GTG GTG AGG TGC GTG TAT GGG TGG TGG ATG AGT GTG TGG CCA CGT GGA TTT CAT TCA GCG ATT
Circular Template	*Phosphate –* **AAT** CGC TGA ATG AAA TCC ACG TGG CCA CAC ACT CAT CCA CCA CCC ATA CAC GCA CCT CAC CAC GAC CAC TCG CGA ATC TGT CCT GGA C**TG** ATG AGG ATC CGA TCG
Primer	*Biotin –* **ATT CGA TCG GAT CCT CAT CA**

[a] The red sequence in the circular template was designed to be complimentary to the sequence of the aptamer to *E. coli* O157:H7. The blue sequence in the circular template was spacer. And the underlined and bold sequences of both ends of the circular template were designed to be complementary to the sequence of the primer.

3.3.3 QCM system

A QCA922 quartz crystal analyzer (Princeton Applied Research, Oak Ridge, TN) was

used for the detection of target bacteria. AT-cut quartz crystals with resonant frequency of 7.995

MHz were obtained from CH Instruments, Inc. (Austin, TX). The size of the quartz crystal was

13.7 mm in diameter and 208 μm in thickness. The polished Au electrodes deposited on both

sides of the crystal were 5.1 mm in diameter and 100 nm in thickness. A methacrylate flow cell

(International Crystal Manufacturing Co, Oklahoma City, OK) was utilized for mounting the crystal. The crystal was sealed between two O-rings attached to the upper and lower pieces of the flow cell held together with two screws. Two sides of the QCM electrode created the base of a cylindrical well and the base of a 70-µl flow-through detection chamber, respectively (see Fig. 3.1).
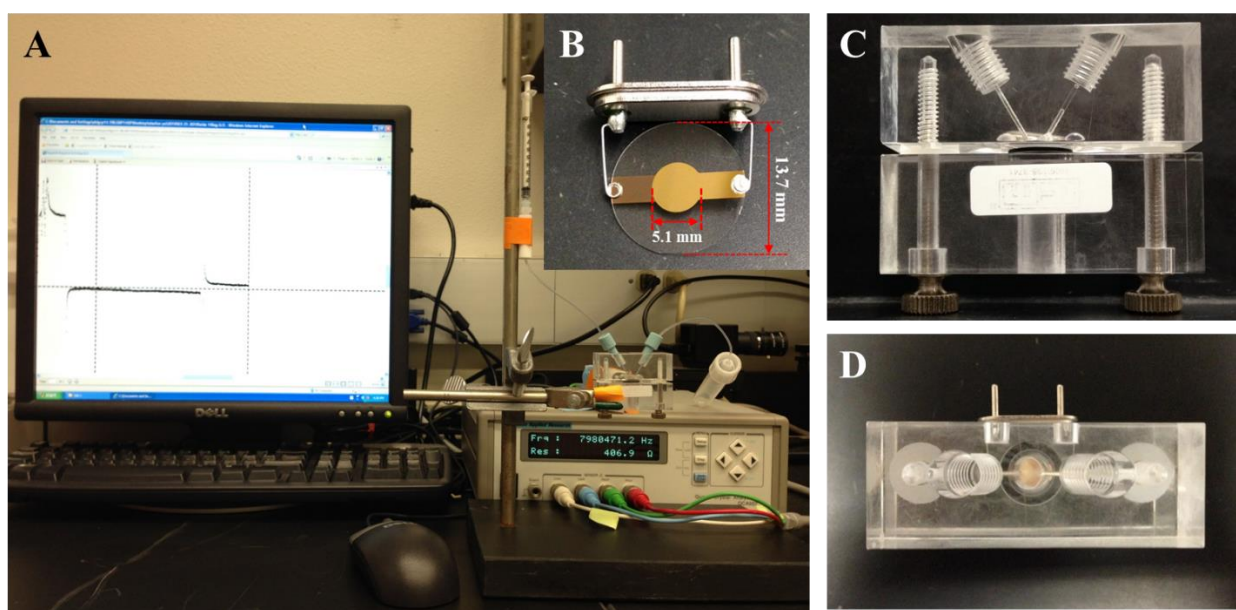
Fig. 3.1 (A) Princeton Applied Research QCA922 quartz crystal analyzer; (B) The dimensions of the AT-cut quartz crystals (7.995 MHz); (C) The front view of the methacrylate flow cell; (D) The top view of the flow cell

3.3.4 RCA reaction in the solution and gel electrophoresis characterization

Phosphorylated linear DNA template (100 µM, 2.5 µl) and biotinylated primer (100 µM, 2.5 µl) dissolved in Milli-Q water were mixed, denatured at 95°C for 10 min, and annealed at 54 °C for 5 min. After that, T4 DNA ligase (400 units/µl, 1 µl), 10 × T4 ligase reaction buffer (2 µl), and Milli-Q water (12 µl) were added to make a 20 µl ligation system. The ligation reaction

was carried out at 16°C for 8 h, and the enzyme was heat inactivated at 65°C for 10 min. The ligated circular DNA templates hybridized with primers were then purified by standard ethanol precipitation and the pellet after centrifugation was dissolved in 29 µl Milli-Q water and stored at 4°C for later use. For RCA reaction in the solution, the ligated circular template hybridized with the primer (29 µl) was mixed with phi29 DNA polymerase (10 units/µl, 2 µl), 10 × phi29 DNA polymerase reaction buffer (7 µl), 10 × bovine serum albumin (BSA, 7 µl), and dNTPs (10 mM, 7 µl). RCA reaction was performed at RT for 1 h, and the resulting RCPs were purified by standard ethanol precipitation. The size of the RCPs were characterized by 0.5% agarose gel electrophoresis which was stained by ethidium bromide and imaged using ultraviolet light.

3.3.5 Preparation of QCM electrodes

The crystal was cleaned by immersing in 1 M NaOH for 30 min and 1 M HCl for 5 min to remove inorganic contaminants, and then the crystal was rinsed with Milli-Q water and 95% ethanol for three times to remove organic residues (Su and Li, 2005). After drying with a stream of nitrogen, the crystal was submerged in 20 mM MHDA at room temperature in the dark for 24 h to functionalize the gold surface with carboxyl groups via gold-thiolate bonds (Xue et al., 2014). The unreacted MHDA was rinsed off with 95% ethanol and Milli-Q water for three times. After drying, the crystal was placed horizontally on the countertop with a clamp for immobilization at RT. 100 µl mixture of 75 mM EDC and 30 mM NHS at a volume ration of 1:1 was dropped on the electrode surface to active the carboxyl groups for 10 min. After that, 100 µl 1 mg/ml streptavidin were dropped on the electrode surface and incubated for 30 min. After each incubation step, the electrode was rinsed with Milli-Q water and dried.

3.3.6 RCA reaction on the electrode surface

The ligated circular template hybridized with biotinylated primer was immobilized on the gold electrode via biotin-streptavidin interaction at RT for 45 min. Rinsed with water and dried, the electrode then incubated with 50 µl RCA reaction mixture, containing phi29 DNA polymerase (10 units/µl, 2 µl), 10 × phi29 DNA polymerase reaction buffer (7 µl), 10 × BSA (7 µl), dNTPs (10 mM, 7 µl), and Milli-Q water (29 µl). After RCA reaction at RT for 1 h, the electrode was rinsed with water and dried.

3.3.7 Detection of *E. coli* O157:H7 cells using QCM sensors based on a multivalent aptamer system

The multivalent aptamer system for QCM sensing was fabricated by immobilizing RCPs using two different methods (as seen Fig. 3.2). In the first method, the reactions of ligation and RCA were both carried out in the solution inside a centrifuge tube. The produced long ssDNA RCPs were directly immobilized on the electrode surface via biotin-streptavidin interaction. In the second method, the ligated circular template with biotinylated primer was first immobilized on the electrode surface, and then the RCA reaction mixture was added to the electrode surface, initiating the primer-induced ssDNA elongation in situ.

Following the creation of the multivalent aptamer system by RCA, the electrode was rinsed by Milli-Q water (heated to 95°C) for the denaturation and reformation into proper 3D structure of RCPs. To block the remaining binding sites on the surface of the gold electrode, 500 µl of 0.1 mg/mL PEG methyl ether thiol (Brockman et al., 2013) dissolved in PBS was added and incubates for 20 min. After rinsing with water, the electrode was subjected to the detection of *E. coli* O157:H7.

By mounting the electrode into the flow cell, the immobilized side of the electrode was made exposed to the 70-μl flow-through chamber, whose inlet fluid channel was connected to a 1 ml syringe. 1 ml PBS was injected into the liquid chamber by the syringe manually and a baseline in PBS was obtained in 10 min. Subsequently, 0.1 ml of *E. coli* O157:H7 at different concentrations ($10^1 - 10^7$ CFU/ml) was injected into the chamber and incubated for 30 min. Next, the liquid chamber was flushed with 1 ml PBS again to remove the unbound *E. coli* cells and a baseline in PBS was obtained in 10 min. The frequency change (ΔF) caused by the binding of target bacteria was calculated by measuring the difference of the baselines before and after the incubation of *E. coli* O157:H7.
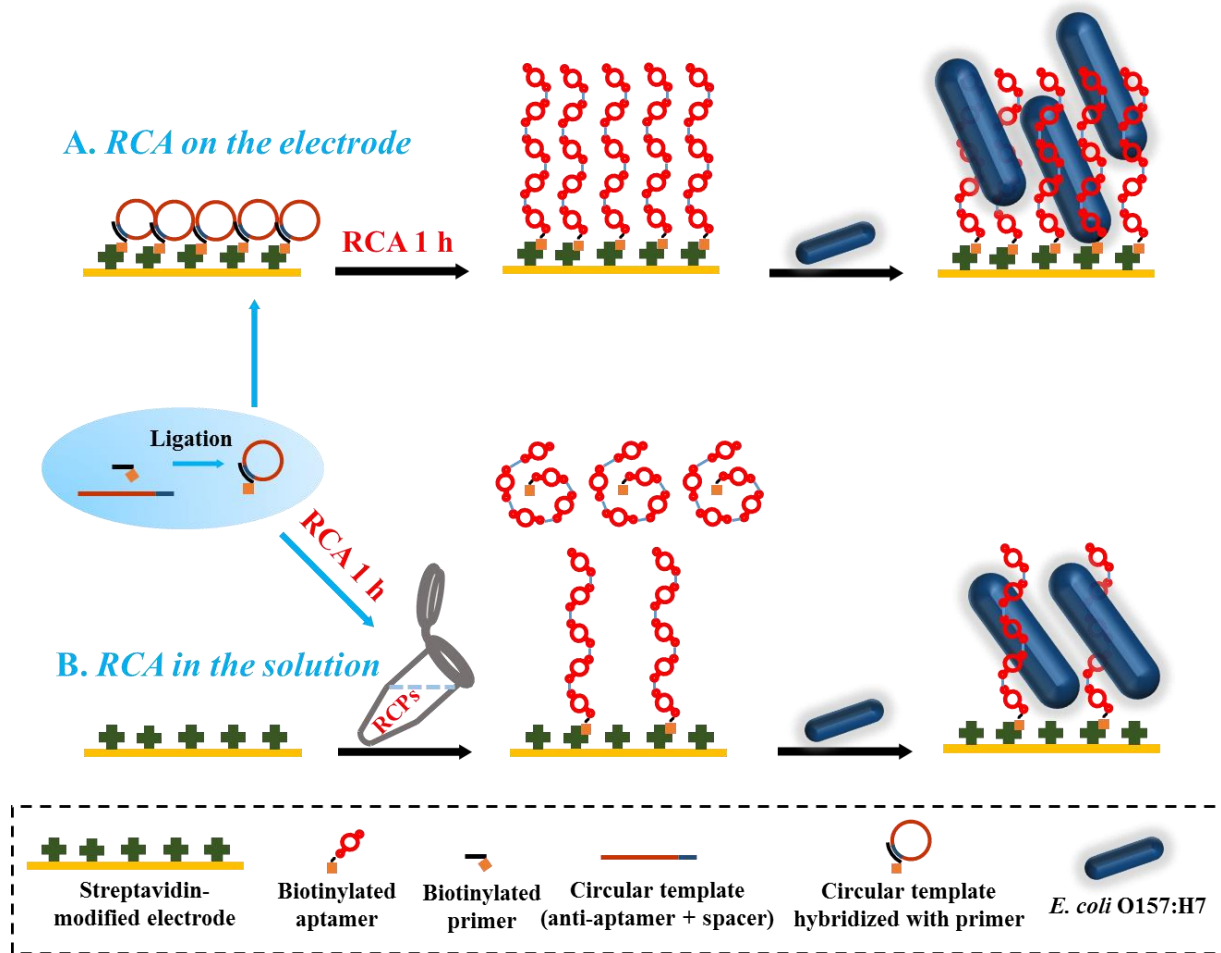
Fig. 3.2 Detection of *E. coli* O157:H7 cells using QCM sensors based on RCA on the electrode surface (A) and RCPs produced in the solution (B).

3.3.8 Specificity tests

For the specificity test, 0.1 ml of *E. coli* K12, *S.* Typhimurium, *L. monocytogenes*, *L. innocua* or *S. aureus* (10^6 CFU/ml in PBS) was injected into the liquid chamber and incubated for 30 min. The frequency change (ΔF) of the baselines before and after the incubation of the non-target bacteria was measured.

3.3.9 Atomic force microscopy (AFM) characterization

Atomic force microscope is one of the scanning probe microscopes, which is based on the invention of the scanning tunneling microscope (Rugar and Hansma, 1990). It is a technique that is capable of investigating the surface on a nanoscale and mapping the topography. The AFM is composed of a cantilever with a sharp tip (probe). The cantilever is made with a spring constant weaker than the equivalent spring between atoms, and the sharp tip can be used to image conducting and nonconducting samples at atomic resolution. Micas with atomically smooth surface and stable properties are ideal for studying the DNA confirmation and interaction. However, negatively charged DNA molecules repulse with the same negatively charged mica surfaces. So addition of divalent cations has become a common way to improve the adsorption of DNA on a mica surface (Kan et al., 2015).

Thin iron disks for the attachment of micas were first polished by sand paper, immersed in acetone for 7 min, rinsed with excessive distilled and Milli-Q water, and then dried. Micas were attached to the iron disks via double-sided adhesive tapes. The top few layers on the surface of micas were removed by tapes.10 µl of 12.5 µM ligated template and primer mix and 10 µl of 12.5 µM RCPs after RCA reaction at RT for 1 h dissolved in 10 mM $MgCl_2$ and 10 mM HEPES were deposited on the mica surface for DNA adsorption. After an incubation of 20 min, micas were rinsed with Milli-Q to remove unbound DNA molecules. Finally, the micas were left for air dry in a chemical hood overnight.

AFM observations were carried out using an AFM (Agilent SPM 5500) in contact mode with a silicon probe (BudgetSensors, Sofia, Bulgaria), whose resonant frequency is 190 kHz. The mica was installed on a sample holder. Applied experimental parameters were driving frequency

(162 kHz), driving amplitude (1 V), and set point (0.78 V). A 10 µm × 10 µm sample area was observed with a 256 × 256 pixel resolution. The AFM images were processed by software Gwyddion.

3.4 Results and discussion

3.4.1 Design of circular DNA template and primer

The size of the circular DNA template was 105 nt, containing an aptamer-complementary sequence and a spacer region. Concerning the length design of the template, it was found that circular templates ranging from 26 to 74 nt could all be successfully amplified, even when the polymerase was larger than the template (26 nt). Besides, with a smaller circular template, more copies of the template could be amplified due to the inherent processivity of polymerases. The inherent processivity of polymerase is the average length of DNA they synthesize before dissociating from the template (Mohsen and Kool, 2016). Some researchers have designed the circular template to include two identical or different aptamer-complimentary sequences (Cheglakov et al., 2008). But in our case, if two aptamer-complimentary sequences and two spacers were incorporated into the template, the size of the template would exceed 200 nt, which cannot be easily chemically synthesized based on current techniques. However, very small circular templates (2-10 nt) are also unsuitable for RCA (Mohsen and Kool, 2016). RCA showed a sinusoidal template length-dependent amplification bias. Joffroy et al. (2017) examined the amplification efficiency of a pool of 29 oligonucleotides with a total size of 67–95 nt. Their results confirmed the low sequence-dependent amplification bias of RCA, and suggested that an increased strain-promoted fraying probability could improve the polymerization rate compared to a relaxed template.

The 20-nt primer was designed to be complimentary to the both ends of the circular template. The primer was labeled with biotin in order to bind to streptavidin immobilized on the electrode surface. The reason why primer was not labeled with thiol group to directly be immobilized on the gold surface is that the streptavidin-biotin crosslinker can help the template-primer duplex more flexible for DNA strand elongation by the polymerase and cause the resulting RCPs to be more flexible in the solution for the capturing of target bacteria.

3.4.2 Optimization of ligation and RCA reaction

3.4.2.1 Optimization of ligation time

DNA ligases are critical to *in vivo* genome integrity, in that they catalyze the formation of a phosphodiester bond between adjacent 3'-hydroxyl and 5'-phosphate termini at single-strand nicks, as well as cohesive or blunt ends at dsDNA. The process of nick-sealing by DNA ligases involves three nucleotidyl-transfer chemical steps: first, the formation of an adenylylated ligase intermediate (an open form); second, the binding of the adenylylated ligase to the 5'-phosphorylated nick site (a closed form); third, the formation of a phosphodiester bond. After dissociating from the phosphodiester bond and the product AMP, ligases are free to start next reaction (Bauer et al., 2017; Crut et al., 2008). For different ends, the best temperature for ligation is different. As recommended by NEB, the ligation in our study was performed at 16℃. Under the condition that the amounts of T4 DNA ligase and DNA were fixed, the ligation efficiency of different ligation time was investigated through agarose gel electrophoresis. The circular template ligated for 4 h or 8 h was used for RCA reaction at 30°C for 24 h, and the RCPs were verified by the agarose (1%) gel electrophoresis. As seen from Fig. 3.3, the two bands (lane 1 and 2) represented the RCPs remained in the gel wells were very bright, indicating the

successful reaction of RCA and ligation. The bands around 100 bp (enclosed by the blue square) represented the templates that were not ligated nor amplified. Compared to the bands of the template in Fig. 3.3 A, the bands in Fig. 3.3 B were much darker, which implied that the efficiency of ligation was greatly improved after increasing the ligation time from 4 h to 8 h. Thus, 8 h was chosen for ligation in the future experiments.

3.4.2.2 Optimization of concentration of dNTPs

dNTPs are the building blocks added one at a time to the elongated ssDNA strand by the DNA polymerase. The amount of dNTPs in the RCA reaction mixture plays an important role in the elongation of the RCPs. To obtain the largest output of RCPs within a fixed reaction time, the concentration of dNTPs were optimized by verifying the size of RCPs on agarose gel (0.5%). Two different concentrations of dNTPs - 250 µM and 10 mM - were examined, and the corresponding RCPs after RCA reaction at 30°C of 24 h were characterized as shown in Fig. 3.3 C. The band stuck in the gel well (lane 2) representing the RCPs produced with 10 mM dNTPs was much brighter than that (lane 1) representing the RCPs produced with 250 µM dNTPs. It suggested that in the presence of 10 mM dNTPs, longer RCPs could be produced in a reaction time of 24 h. Therefore, 10 mM was chosen as the concentration of dNTPs in later RCA reactions.
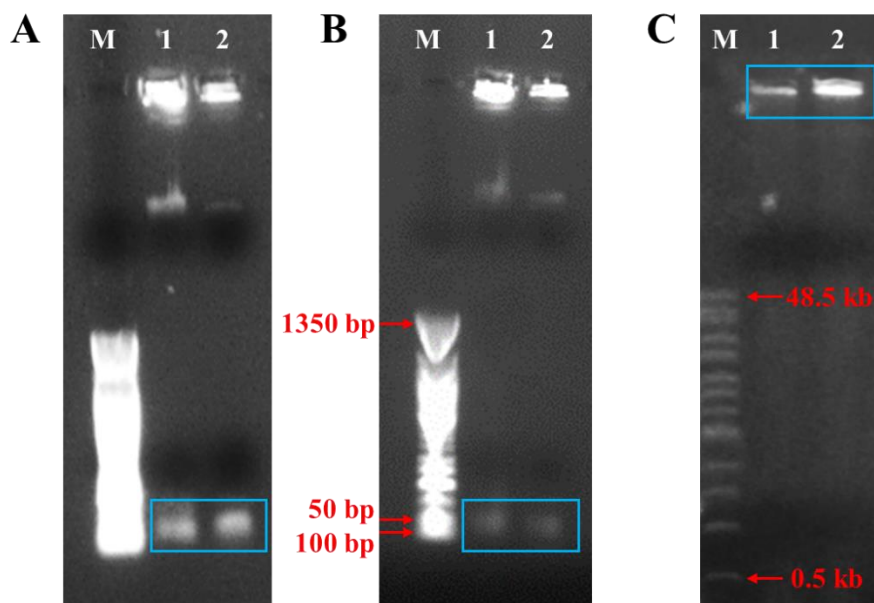
Fig. 3.3 Agarose gel (1%) electrophoresis of 50 bp marker (M) and RCPs of RCA reaction (concentration of dNTPs was 200 µM) was 200 at 30°C of 24 h after ligation of circular template at 16°C for 4 h (lane 1 and 2) (A) and 8 h (lane 1 and 2) (B); Agarose gel (0.5%) electrophoresis of 1 kb extended marker (M) and RCPs of RCA reaction at 30°C of 24 h in the presence of 250 µM dNTPs (lane 1) and 10 mM dNTPs (lane 2) (C).

3.4.3 Optimization of fabrication of the multivalent aptamer system by RCA

2.4.3.1 Immobilization in the flow cell (RCA at 30°C)

To monitor the immobilization of the QCM electrode in real time, the step-wise immobilization was conducted inside the flow cell. After the electrode was cleaned and modified by 20 mM MHDA for 24 h, the electrode was mounted between the two parts of the flow cell and connected to the QCA, with the side for immobilization facing the cylindrical well. 300 µl mixture of 75 mM EDC and 30 mM NHS at a volume ration of 1:1 was added for the activation of carboxyl groups for 10 min, followed by the addition of 200 µl 1 mg/ml streptavidin to incubate with the electrode for 30 min.

The optimal activity of phi29 polymerase is at temperature of 30°C. For RCA in the solution, the RCPs produced by RCA reaction in the solution within in a tube at 30°C for different time periods were dissolved in 100 µl Milli-Q water, and added to the flow cell followed by incubation for 45 min. The unbound RCPs were rinsed off by 400 µl PBS for three times. For RCA on the electrode, 100 µl of the ligated circular template with biotinylated primer were first immobilized on the electrode surface, and then 50 µl of the RCA reaction mixture were added to the electrode surface. To prevent the RCA solution from evaporation, the opening of the cylindrical well was sealed by parafilm and then the flow cell was left in the incubator for reaction at 30°C. A small amount of Milli-Q was added into the cell every now and then to replenish the water that was evaporated.

After the creating of a multivalent aptamer system, the flow cell was flushed with PBS at RT and PBS heated to 95°C. Then 200 µl of 0.1 mg/mL PEG methyl ether thiol was added to block the unmodified electrode gold surface for 20 min. Following the washing step with 400 µl PBS for six times, 200 µl of PBS was added to get a baseline. Subsequently, 200 µl of *E. coli* O157:H7 of 10^7 CFU/ml was added and incubated for 30 min. After the removal of unbound bacterial cells, 200 µl of PBS was added to get a baseline. The frequency change (ΔF) caused by the target bacterial binding was calculated by measuring the difference of the baselines before and after the incubation of *E. coli* O157:H7.

As seen from Fig. 3. 4 A, the detection signals of *E. coli* O157:H7 at 10^7 CFU/ml by RCA either in the solution or on the electrode for various hours were between -11 to -16 Hz. There was no significant difference between these two methods. Furthermore, when RCA reaction was directly performed on the electrode in the cell, the baselines during QCM sensing

became very unstable typified by the large fluctuation of the frequency. The possible reason for this phenomenon was that the dNTPs, polymerases, and BSA in the RCA reaction mixture non-specifically bound to the wall of the cylindrical well, causing interference with the oscillation of the quartz by wavering in the liquid upon the electrode. The reason why the detection signals with RCA in the solution were not large either could be that the RCPs added to the flow cell also bound to the wall of the cylindrical well non-specifically, resulting in the huge drop of the amount of RCPs immobilized on the electrode surface.
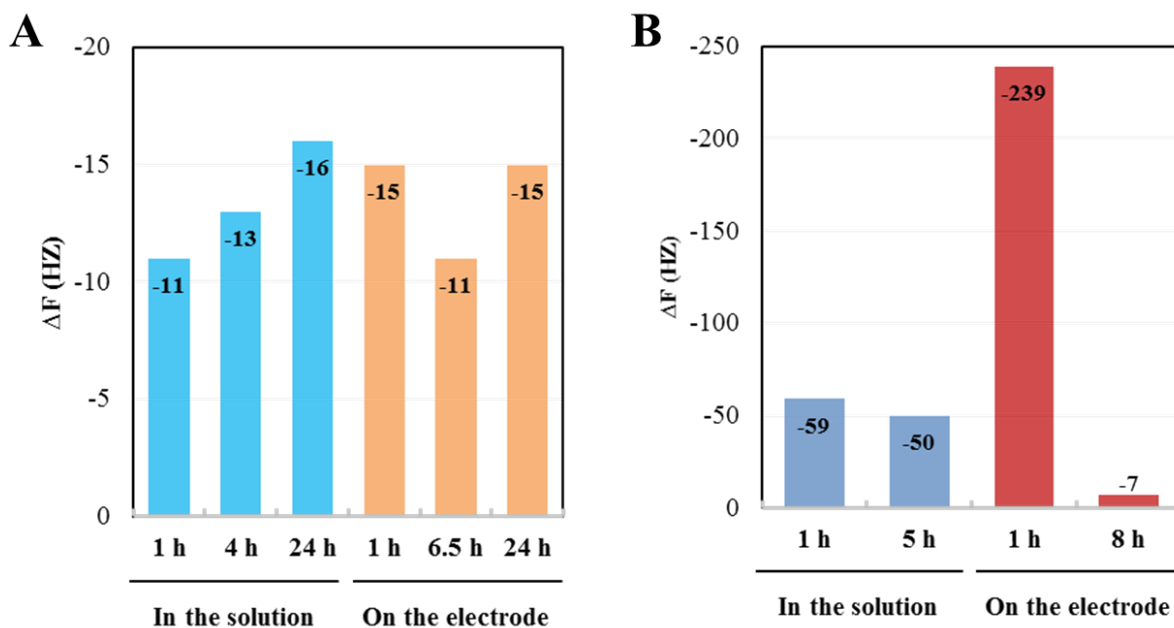

Fig. 3.4 (A) Frequency shifts after the detection of 10^7 CFU/ml *E. coli* O157:H7 using RCPs from RCA reaction at 30°C of different hours in the solution or on the electrode; (B) Frequency shifts after the detection of 10^6 CFU/ml *E. coli* O157:H7 using RCPs from RCA reaction at RT of different hours in the solution or on the electrode.

2.4.3.2 Immobilization outside the flow cell (RCA at RT)

To determine which method - RCA in solution or RCA on the electrode - is more superior, the multivalent aptamer system established by each of them was used for the detection of *E. coli* O157:H7 at 10^6 CFU/ml. As seen from Fig. 3.4 B, the detection signal acquired by the method of performing RCA on the electrode was much larger than that acquired by the method of conducting RCA in the solution, which were -239 Hz (1 h) and -59 Hz (1 H), respectively. The possible reason could be that long ssDNA strands of RCPs produced in the solution were self-folding into coils and the biotin molecules at the end of the stands might have been embedded inside the coils. Without enough interaction between biotin and streptavidin, the amount of RCPs immobilized on the electrode surface was greatly reduced. Therefore, RCA on the electrode at RT was selected to be used for further QCM sensing of *E. coli* O157:H7 at various concentrations.

By extending the time of RCA in solution from 1 h to 5 h, no significant change in detection signal was observed. As the time of RCA on the electrode was increased from 1 h to 8 h, the concentrated solution formed a white stain in the center of the quartz, which could hardly be rinsed off by Milli-Q water (at RT or 95°C) or PBS. That might have been the reason for the extremely low detection signal. Long RCPs produced with long reaction time may contain more intra- and inter-molecular interactions, which could inverse limit the accessibility of aptamers to the target (Zhao et al., 2012). Based on the reported various biosensors based on RCA (Yan et al., 2012; Zhao et al., 2013; Ge et al., 2014; Kühnemund and Nilsson, 2015; Guo et al., 2016; Carinelli et al., 2017; He et al., 2014), the RCA reaction for no more than 1 h was enough for signal enhancement. Therefore, in this study, 1 h was chosen for RCA reaction.

In order to check the size of the RCA products, the agarose gel electrophoresis was performed under 120 V for 45 min. As seen from Fig. 3.5, clear bands stuck in the gel wells represented the RCPs produced at RT or 30°C for 1 h or 5 h. However, the size of RCPs cannot be estimated by the location of the bands, because the RCPs might not have been able to migrate in the gel due to the intra- and inter-molecular interactions.

Although the preferred temperature for RCA reaction was 30°C, the RCA reaction mixture dropped on the electrode surface could be quickly evaporated at 30°C in an incubator, which would largely influence the amplification efficiency. So for the convenience of the whole immobilization process of the electrode, RCA was conducted at RT (~23°C) as other steps of modification and blocking. Compared with the band of RCPs generated at 30°C for 1 h (or 5 h), the band of the RCPs generated at RT for 1 h (or 5 h) showed slightly lower intensity, indicating that the amplification efficiency of the polymerase was not significantly affected by performing RCA at RT.
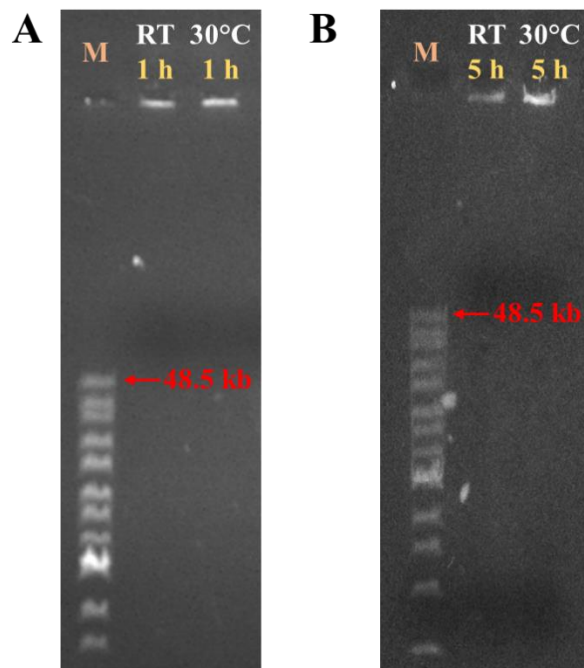
Fig. 3.5 Agarose gel (0.5%) electrophoresis of 1 kb extended marker (M) and RCPs of RCA reaction at RT and 30°C for 1 h (A) or 5 h (B).

To be noted, there was a problem related to performing RCA on the electrode, which was that the RCA reaction solution appeared to have better "affinity" to the electrode surface than other solutions and would spread to the edge of the quartz and even flow to the other side of the quartz when the quartz was not placed entirely horizontally. Once that happened, the polymerization efficiency was decreased and the other side of the electrode was also contaminated. Thus, it was critical to make sure the electrode is completely dry before the addition of RCA reaction mixture and to adjust the position of the electrode from any tilt.

3.4.4 Highly sensitive and specific QCM sensor based on the multivalent aptamer system

After the optimization of RCA reaction, RCA on the electrode at RT for 1 h was used as the approach for building the multivalent aptamer system, which was incorporated into the QCM

sensor for sensitive, rapid, and label-free detection of *E. coli* O157:H7. The frequency shifts caused by the incubation of *E. coli* O157:H7 with the QCM sensor for 30 min are plotted versus the logarithm of the bacterial concentrations (Fig. 3.6 A). The standard deviations (S.D.) calculated from triplicate tests are shown as error bars in the figure. Good linear relationships were found between the frequency shift (ΔF) and the logarithm of the bacterial concentrations from 10^2 to 10^5 CFU/ml and from 10^5 to 10^7 CFU/ml, respectively. The corresponding regression equations were y = -13.711x + 12 (R^2 = 0.998) and y = -305.27x + 1696.7 (R^2 = 0.9677), respectively. PBS without target bacteria was detected as a negative control (NC), which resulted in frequency change of -3 ± 2 Hz. The LOD (as 3 times of the S. D. of the NC) was thus determined to be 34 CFU/ml based on the regression equation. Compared to the QCM sensor based on monovalent aptamers developed in Chapter 2 for the detection of *E. coli* O157:H7, the sensitivity of the multivalent aptamer system based QCM sensor was approximately 8-fold higher at low concentrations and 33-fold higher at high concentrations of *E. coli* O157:H7 (the sensitivity corresponds at the slope of the calibration curve). The LOD was also lowered from 1.46×10^3 CFU/ml to 34 CFU/ml by 2 orders of the magnitude (Yu et al., 2018).

The specificity of the proposed QCM sensor was demonstrated by using five different strains of non-pathogenic or pathogenic bacteria, which were *E. coli* K12, *S.* Typhimurium, *L. monocytogenes*, *L. innocua* and *S. aureus*. Frequency shifts after incubation with 10^6 CFU/ml non-target bacteria for 30 min were measured. The mean and S.D. calculated from triplicate tests are shown in Fig. 3.6 B. The detection signals for the non-target bacteria at a concentration of 10^6 CFU/ml were much smaller than that for *E. coli* O157:H7 at a concentration of 10^4 CFU/ml, suggesting that the developed QCM sensor has a high selectivity for *E. coli* O157:H7.

The regeneration of the QCM sensor was carried out by injecting 0.1 ml 1, 10, or 100

mM NaOH solution into the chamber and reacted for 1-10 min to remove the bound bacterial

cells. The regeneration solution was then flushed out by PBS. The recovery of the baseline in

PBS to its original frequency before the binding of bacteria indicated successful regeneration

process. One side of the QCM electrode could usually be used for 3-5 measurements.
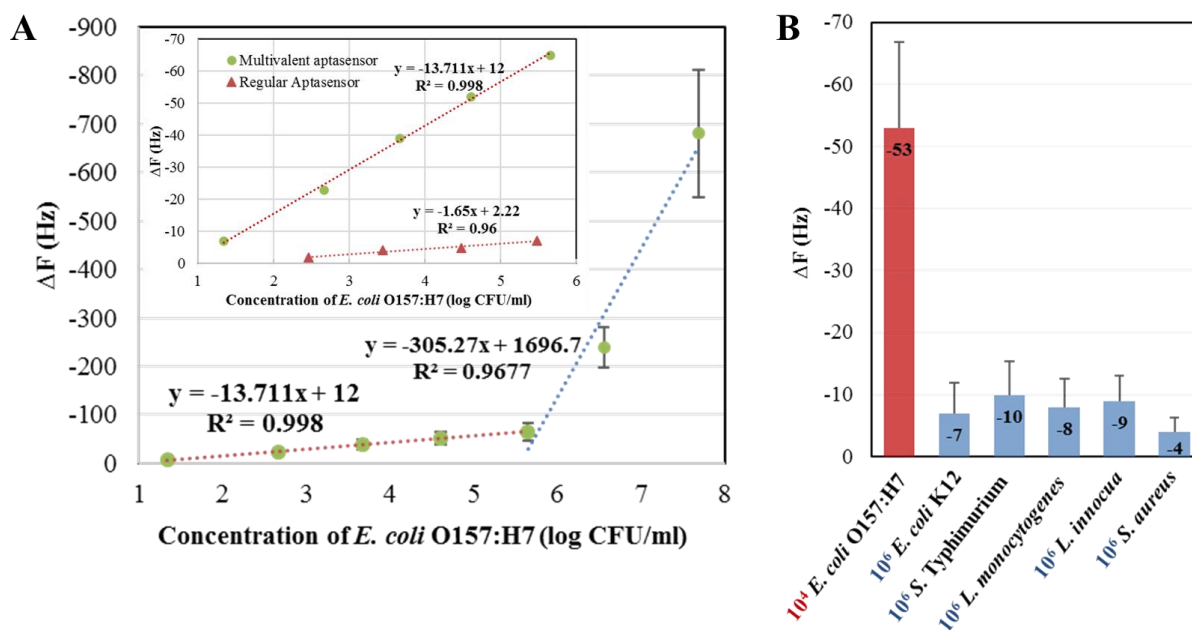
Fig. 3.6 (A) The two linear calibration curves of frequency changes verses the logarithm of *E. coli* O157:H7 concentrations from 10^1 to 10^5 CFU/ml and from 10^5 to 10^7 CFU/ml detected by the QCM based on a multivalent aptamer system by RCA on the electrode. Each value is presented as mean $\pm$ S. D. (n=3). The figure at the left corner compares the detection signals of *E. coli* O157:H7 at lower concentrations by QCM based multivalent and regular aptasensors. (B) Specificity of the multivalent aptamer system based QCM sensor for the detection of *E. coli* O157:H7. The values presented corresponded to *E. coli* O157:H7 at 10^4 CFU/ml, and the non-target bacteria at 10^6 CFU/ml.

3.4.5 AFM imaging

The RCPs produced at RT for 1 h were also characterized by AFM. The bright dots as

seen in Fig. 3.7 A were around 3 nm in height. The dots possibly represent the ligated template

hybridized with primer, the ligases, or some contaminates. In comparison with the image of circular template-primer, the images of RCPs showed long stands, which were about 0.8 nm in height (data didn't show) and a few microns in length (Fig. 3.7 C and E). The long strands of RCPs were broken at some points probably due to the strong charge of the buffer solution and the drying process of the samples. The lumps shown in Fig. 3.7 C and E are 20 - 30 nm in height, which might have be caused by the incomplete drying of the surface of micas. The preparation of the AFM samples needs to be further optimized.
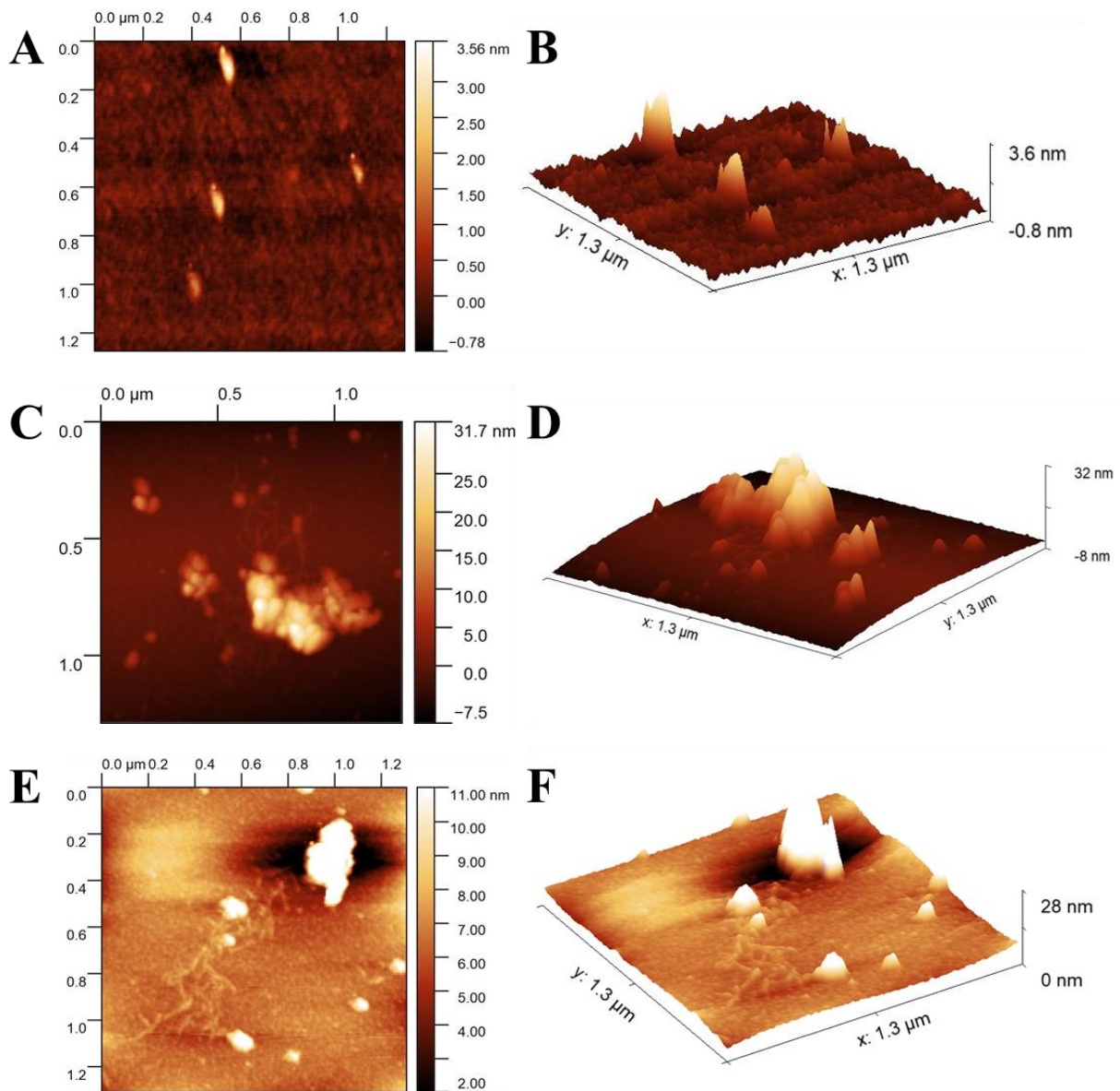
Fig. 3.7 AFM measurements of different DNA samples: (A) circular template-primer and its 3D image (B); (C) and (E) RCPs produced at RT for 1 h in the solution and their 3D images (D) and (F), respectively.

3.5 Conclusions

It is the first time that RCA was utilized to produce a multivalent aptamer system for the

detection of *E. coli* O157:H7 using a QCM sensor. The RCP-based aptamer sensor developed in

this study manifested a much better sensitivity than a regular aptasensor with the LOD of 34

CFU/ml. By tailor designing the unit aptamer, the multivalent aptamer system can be

incorporated into different biosensors for sensitive detection of a variety of bacterial or human

cells.

Conclusions

In this study, ssDNA aptamers were selected the first time by a whole-bacterium SELEX technique against *E. coli* O157:H7 with high affinity (K_d =10.30 nM) and specificity. The selected aptamer was further applied to the development of a QCM aptasensor for the detection of *E. coli* O157:H7. The LOD of the aptasensor was as low as 1.46×10^3 CFU/ml, superior to most QCM-based immunosensors for pathogen detection. The sequence complementary to the selected aptamer was used as the circular template for RCA to create a multivalent aptamer system, which was intergrated with the QCM sensor, for the detection of *E. coli* O157:H7. The RCP-based aptamer sensor developed in this study manifested a much better sensitivity than a regular aptasensor with the LOD of 34 CFU/ml. By tailor designing the unit aptamer, the multivalent aptamer system can be incorporated into different biosensors for sensitive and selective detection of a variety of bacterial pathogens.

Recommendations for future research

1. More related bacteria strains, such as *E. coli* K12, can be used in counter selection in order to increase the specificity of aptamer pools. Also, the binding of the aptamer pools to other bacteria should be evaluated after counter selection, so that the number of counter selection rounds could be determined.

2. The dissociation constants (K_d) for all three sequences of aptamers could be determined. The binding motifs of aptamers can also be determined by various ways of truncation.

3. The binding sites on the target bacteria could be investigated by purifying proteins and other molecules, such as flagella antigens and lipid A, and their binding affinity with selected aptamers could be characterized.

4. In order to increase the capture efficiency of aptamers immobilized on the electrode, a panel of aptamers with different binding sites can be used to capture the target bacteria in the aptasenor.

5. The RCPs could be verified by the digestion of BamH1 digestion, the restriction site of which is at the spacer. The ladder-like bands on the agarose gel will prove the successful amplification of the template.

6. The 3D structure of RCPs could be simulated via the software called oxDNA. We can also check if the hybridization of the RCPs with spacers will improve the correct folding of RCPs into tandem aptamer structures.

7. The circular template can be tailor designed for detection of different targets. By incorporating different multivalent aptamer systems specific for different bacteria, multiplex detection could be achieved by the labeling of reporters in electrochemical or optical sensors.

References

Afzal, A., Mujahid, A., Schirhagl, R., Bajwa, S.Z., Latif, U. and Feroz, S., 2017. Gravimetric viral diagnostics: QCM based biosensors for early detection of viruses. *Chemosensors*, *5*(1), p.7.

Atay, S., Pişkin, K., Yılmaz, F., Çakır, C., Yavuz, H. and Denizli, A., 2016. Quartz crystal microbalance based biosensors for detecting highly metastatic breast cancer cells via their transferrin receptors. *Analytical Methods*, *8*(1), pp.153-161.

Avci-Adali, M., Paul, A., Wilhelm, N., Ziemer, G. and Wendel, H.P., 2009. Upgrading SELEX technology by using lambda exonuclease digestion for single-stranded DNA generation. *Molecules*, *15*(1), pp.1-11.

Bai, H., Wang, R., Hargis, B., Lu, H. and Li, Y., 2012. A SPR aptasensor for detection of avian influenza virus H5N1. *Sensors*, *12*(9), pp.12506-12518.

Bagheryan, Z., Raoof, J.B., Golabi, M., Turner, A.P. and Beni, V., 2016. Diazonium-based impedimetric aptasensor for the rapid label-free detection of *Salmonella* Typhimurium in food sample. *Biosensors and Bioelectronics*, *80*, pp.566-573.

Bauer, R.J., Jurkiw, T.J., Evans Jr, T.C. and Lohman, G.J., 2017. Rapid time scale analysis of T4 DNA ligase–DNA binding. *Biochemistry*, *56*(8), pp.1117-1129.

Berezovski, M., Musheev, M., Drabovich, A. and Krylov, S.N., 2006. Non-SELEX selection of aptamers. *Journal of the American Chemical Society*, *128*(5), pp.1410-1411.

Bing, T., Yang, X., Mei, H., Cao, Z. and Shangguan, D., 2010. Conservative secondary structure motif of streptavidin-binding aptamers generated by different laboratories. *Bioorganic & Medicinal Chemistry*, *18*(5), pp.1798-1805.

Birch, C.M., Hou, H.W., Han, J. and Niles, J.C., 2015. Identification of malaria parasite-infected red blood cell surface aptamers by inertial microfluidic SELEX (I-SELEX). *Scientific reports*, *5*, p.11347.

Brockman, L., Wang, R., Lum, J., and Li, Y., 2013. QCM aptasensor for rapid and specific detection of avian influenza virus. *Open Journal of Applied Biosensor, 2*, pp.97-103.

Buchatip, S., Ananthanawat, C., Sithigorngul, P., Sangvanich, P., Rengpipat, S. and Hoven, V.P., 2010. Detection of the shrimp pathogenic bacteria, Vibrio harveyi, by a quartz crystal microbalance-specific antibody based sensor. *Sensors and Actuators B: Chemical*, *145*(1), pp.259-264.

Buttry, D.A., 1989. *Applications of the quartz crystal microbalance to electrochemistry*. University of Wyoming, Laramie, MY.

Carinelli, S., Kühnemund, M., Nilsson, M. and Pividori, M.I., 2017. Yoctomole electrochemical genosensing of Ebola virus cDNA by rolling circle and circle to circle amplification. *Biosensors and Bioelectronics*, *93*, pp.65-71.

Cerchia, L., Ducongé, F., Pestourie, C., Boulay, J., Aissouni, Y., Gombert, K., Tavitian, B., De Franciscis, V. and Libri, D., 2005. Neutralizing aptamers from whole-cell SELEX inhibit the RET receptor tyrosine kinase. *PLoS Biology*, *3*(4), p.e123.

Chandler, M., De La Cruz, F., Dyda, F., Hickman, A.B., Moncalian, G. and Ton-Hoang, B., 2013. Breaking and joining single-stranded DNA: the HUH endonuclease superfamily. *Nature Reviews Microbiology*, *11*(8), p.525.

Chang, Y.C., Yang, C.Y., Sun, R.L., Cheng, Y.F., Kao, W.C. and Yang, P.C., 2013. Rapid single cell detection of *Staphylococcus aureus* by aptamer-conjugated gold nanoparticles. *Scientific Reports*, *3*, p.1863.

Cheglakov, Z., Weizmann, Y., Braunschweig, A.B., Wilner, O.I. and Willner, I., 2008. Increasing the complexity of periodic protein nanostructures by the rolling-circle-amplified synthesis of aptamers. *Angewandte Chemie International Edition*, *47*(1), pp.126-130.

Chen, S.H., Wu, V.C., Chuang, Y.C. and Lin, C.S., 2008. Using oligonucleotide-functionalized Au nanoparticles to rapidly detect foodborne pathogens on a piezoelectric biosensor. *Journal of Microbiological Methods*, *73*(1), pp.7-17.

Cox, J.C., Rudolph, P. and Ellington, A.D., 1998. Automated RNA selection. *Biotechnology Progress*, *14*(6), pp.845-850.

Crut, A., Nair, P.A., Koster, D.A., Shuman, S. and Dekker, N.H., 2008. Dynamics of phosphodiester synthesis by DNA ligase. *Proceedings of the National Academy of Sciences*, *105*(19), pp.6894-6899.

Dong, Y. and Shannon, C., 2000. Heterogeneous immunosensing using antigen and antibody monolayers on gold surfaces with electrochemical and scanning probe detection. *Analytical Chemistry*, *72*(11), pp.2371-2376.

Duan, N., Ding, X., He, L., Wu, S., Wei, Y. and Wang, Z., 2013. Selection, identification and application of a DNA aptamer against *Listeria monocytogenes*. *Food Control*, *33*(1), pp.239-243.

Duan, N., Ding, X., Wu, S., Xia, Y., Ma, X., Wang, Z. and Chen, J., 2013. In vitro selection of a DNA aptamer targeted against *Shigella dysenteriae*. *Journal of Microbiological Methods*, *94*(3), pp.170-174.

Duan, N., Wu, S., Chen, X., Huang, Y. and Wang, Z., 2012. Selection and identification of a DNA aptamer targeted to *Vibrio parahemolyticus*. *Journal of Agricultural and Food Chemistry*, *60*(16), pp.4034-4038.

Duan, N., Wu, S., Chen, X., Huang, Y., Xia, Y., Ma, X. and Wang, Z., 2013. Selection and characterization of aptamers against *Salmonella* Typhimurium using whole-bacterium systemic

evolution of ligands by exponential enrichment (SELEX). *Journal of Agricultural and Food Chemistry*, *61*(13), pp.3229-3234.

Dwivedi, H.P., Smiley, R.D. and Jaykus, L.A., 2010. Selection and characterization of DNA aptamers with binding selectivity to Campylobacter jejuni using whole-cell SELEX. *Applied Microbiology and Biotechnology*, *87*(6), pp.2323-2334.

Dwivedi, H.P., Smiley, R.D. and Jaykus, L.A., 2013. Selection of DNA aptamers for capture and detection of Salmonella Typhimurium using a whole-cell SELEX approach in conjunction with cell sorting. *Applied Microbiology and Biotechnology*, *97*(8), pp.3677-3686.

Ellington, A.D. and Szostak, J.W., 1990. In vitro selection of RNA molecules that bind specific ligands. *Nature*, *346*(6287), p.818.

Ellington, A.D. and Szostak, J.W., 1992. Selection in vitro of single-stranded DNA molecules that fold into specific ligand-binding structures. *Nature*, *355*(6363), p.850.

Ellington, A.D. and Szostak, J.W., 1992. Selection in vitro of single-stranded DNA molecules that fold into specific ligand-binding structures. *Nature*, *355*(6363), p.850.

Ge, J., Zhang, L.L., Liu, S.J., Yu, R.Q. and Chu, X., 2014. A highly sensitive target-primed rolling circle amplification (TPRCA) method for fluorescent in situ hybridization detection of microRNA in tumor cells. *Analytical Chemistry*, *86*(3), pp.1808-1815.

Gopinath, S. C. B., 2007. Methods developed for SELEX. *Analytical and Bioanalytical Chemistry*, *387*(1), 171-182.

Guo, X., Lin, C.S., Chen, S.H., Ye, R. and Wu, V.C., 2012. A piezoelectric immunosensor for specific capture and enrichment of viable pathogens by quartz crystal microbalance sensor, followed by detection with antibody-functionalized gold nanoparticles. *Biosensors and Bioelectronics*, *38*(1), pp.177-183.

Guo, Y., Wang, Y., Liu, S., Yu, J., Wang, H., Wang, Y. and Huang, J., 2016. Label-free and highly sensitive electrochemical detection of E. coli based on rolling circle amplifications coupled peroxidase-mimicking DNAzyme amplification. *Biosensors and Bioelectronics*, *75*, pp.315-319.

Hamblin, G.D., Carneiro, K.M., Fakhoury, J.F., Bujold, K.E. and Sleiman, H.F., 2012. Rolling circle amplification-templated DNA nanotubes show increased stability and cell penetration ability. *Journal of the American Chemical Society*, *134*(6), pp.2888-2891.

Hamula, C.L., Le, X.C. and Li, X.F., 2011. DNA aptamers binding to multiple prevalent M-types of *Streptococcus pyogenes*. *Analytical Chemistry*, *83*(10), pp.3640-3647.

Hamula, C.L., Zhang, H., Guan, L.L., Li, X.F. and Le, X.C., 2008. Selection of aptamers against live bacterial cells. *Analytical Chemistry*, *80*(20), pp.7812-7819.

Hamula, C.L., Zhang, H., Li, F., Wang, Z., Le, X.C. and Li, X.F., 2011. Selection and analytical applications of aptamers binding microbial pathogens. *TrAC Trends in Analytical Chemistry*, *30*(10), pp.1587-1597.

He, C.Z., Zhang, K.H., Wang, T., Wan, Q.S., Hu, P.P., Hu, M.D., Huang, D.Q. and Lv, N.H., 2013. Single-primer-limited amplification: A method to generate random single-stranded DNA sub-library for aptamer selection. *Analytical Biochemistry*, *440*(1), pp.63-70.

He, P., Liu, L., Qiao, W. and Zhang, S., 2014. Ultrasensitive detection of thrombin using surface plasmon resonance and quartz crystal microbalance sensors by aptamer-based rolling circle amplification and nanoparticle signal enhancement. *Chemical Communications*, *50*(12), pp.1481-1484.

Hengerer, A., Kösslinger, C., Decker, J., Hauck, S., Queitsch, I., Wolf, H. and Dübel, S., 1999. Determination of phage antibody affinities to antigen by a microbalance sensor system. *Biotechniques*, *26*, pp.956-965.

Hermann, T. and Patel, D.J., 2000. Adaptive recognition by nucleic acid aptamers. *Science*, *287*(5454), pp.820-825.

Homann, M., & Göringer, H. U., 1999. Combinatorial selection of high affinity RNA ligands to live African trypanosomes. *Nucleic Acids Research*, *27*(9), 2006-2014.

Hybarger, G., Bynum, J., Williams, R.F., Valdes, J.J. and Chambers, J.P., 2006. A microfluidic SELEX prototype. *Analytical and Bioanalytical Chemistry*, *384*(1), pp.191-198.

Hyeon, J.Y., Chon, J.W., Choi, I.S., Park, C., Kim, D.E. and Seo, K.H., 2012. Development of RNA aptamers for detection of *Salmonella Enteritidis*. *Journal of Microbiological Methods*, *89*(1), pp.79-82.

Iwagawa, T., Ohuchi, S.P., Watanabe, S. and Nakamura, Y., 2012. Selection of RNA aptamers against mouse embryonic stem cells. *Biochimie*, *94*(1), pp.250-257.

Jaiswal, A., Smoukov, S., Poggi, M. and Grzybowski, B., 2008. Quartz crystal microbalance with dissipation monitoring (QCM-D): Real-time characterization of nano-scale interactions at surfaces. *Nsti Nanotech*, *1*, pp.855-858.

Jiang, X., Wang, R., Wang, Y., Su, X., Ying, Y., Wang, J. and Li, Y., 2011. Evaluation of different micro/nanobeads used as amplifiers in QCM immunosensor for more sensitive detection of *E. coli* O157: H7. *Biosensors and Bioelectronics*, *29*(1), pp.23-28.

Jiang, Y., Zou, S. and Cao, X., 2017. A simple dendrimer-aptamer based microfluidic platform for *E. coli* O157: H7 detection and signal intensification by rolling circle amplification. *Sensors and Actuators B: Chemical*, *251*, pp.976-984.

Joffroy, B., Uca, Y.O., Prešern, D., Doye, J.P. and Schmidt, T.L., 2017. Rolling circle amplification shows a sinusoidal template length-dependent amplification bias. *Nucleic Acids Research*, *46 (2),* pp.538-545.

Joshi, R., Janagama, H., Dwivedi, H.P., Kumar, T.S., Jaykus, L.A., Schefers, J. and Sreevatsan, S., 2009. Selection, characterization, and application of DNA aptamers for the capture and detection of Salmonella enterica serovars. *Molecular and Cellular Probes*, *23*(1), pp.20-28.

Kan, Y., Tan, Q., Wu, G., Si, W. and Chen, Y., 2015. Study of DNA adsorption on mica surfaces using a surface force apparatus. *Scientific Reports*, *5*, p.8442.

Kasper, M., Traxler, L., Salopek, J., Grabmayr, H., Ebner, A. and Kienberger, F., 2016. Broadband 120 MHz impedance quartz crystal microbalance (QCM) with calibrated resistance and quantitative dissipation for biosensing measurements at higher harmonic frequencies. *Biosensors*, *6*(2), p.23.

Keefe, A.D., Pai, S. and Ellington, A., 2010. Aptamers as therapeutics. *Nature Reviews Drug Discovery*, *9*(7), p.537.

Kim, A., Won, Y., Woo, K., Kim, C.H. and Moon, J., 2013. Highly transparent low resistance ZnO/Ag nanowire/ZnO composite electrode for thin film solar cells. *ACS Nano*, *7*(2), pp.1081-1091.

Kim, Y.S., Song, M.Y., Jurng, J. and Kim, B.C., 2013. Isolation and characterization of DNA aptamers against Escherichia coli using a bacterial cell–systematic evolution of ligands by exponential enrichment approach. *Analytical Biochemistry*, *436*(1), pp.22-28.

Kim, E.Y., Kim, J.W., Kim, W.K., Han, B.S., Park, S.G., Chung, B.H., Lee, S.C. and Bae, K.H., 2014. Selection of aptamers for mature white adipocytes by Cell SELEX using flow cytometry. *PloS One*, *9*(5), p.e97747.

Kolovskaya, O.S., Savitskaya, A.G., Zamay, T.N., Reshetneva, I.T., Zamay, G.S., Erkaev, E.N., Wang, X., Wehbe, M., Salmina, A.B., Perianova, O.V. and Zubkova, O.A., 2013. Development of bacteriostatic DNA aptamers for *Salmonella*. *Journal of Medicinal Chemistry*, *56*(4), pp.1564-1572.

Krzywkowski, T., Kühnemund, M., Wu, D. and Nilsson, M., 2018. Limited reverse transcriptase activity of phi29 DNA polymerase. *Nucleic Acids Research, 46(7),* pp.3625-3632.

Kühnemund, M. and Nilsson, M., 2015. Digital quantification of rolling circle amplified single DNA molecules in a resistive pulse sensing nanopore. *Biosensors and Bioelectronics*, *67*, pp.11-17.

Kumar, A., 2000. Biosensors based on piezoelectric crystal detectors: Theory and application. *JOM-e*, *52*(10), pp.1-6.

Kupakuwana, G.V., Crill II, J.E., McPike, M.P. and Borer, P.N., 2011. Acyclic identification of aptamers for human alpha-thrombin using over-represented libraries and deep sequencing. *PloS One*, *6*(5), p.e19395.

Labib, M., Zamay, A.S., Kolovskaya, O.S., Reshetneva, I.T., Zamay, G.S., Kibbee, R.J., Sattar, S.A., Zamay, T.N. and Berezovski, M.V., 2012. Aptamer-based impedimetric sensor for bacterial typing. *Analytical Chemistry*, *84*(19), pp.8114-8117.

Lee, C.Y., Fan, H.T. and Hsieh, Y.Z., 2018. Disposable aptasensor combining functional magnetic nanoparticles with rolling circle amplification for the detection of prostate-specific antigen. *Sensors and Actuators B: Chemical*, *255*, pp.341-347.

Lee, S.H., Ahn, J.Y., Lee, K.A., Um, H.J., Sekhon, S.S., Park, T.S., Min, J. and Kim, Y.H., 2015. Analytical bioconjugates, aptamers, enable specific quantitative detection of *Listeria monocytogenes. Biosensors and Bioelectronics*, *68*, pp.272-280.

Lee, Y.J., Han, S.R., Maeng, J.S., Cho, Y.J. and Lee, S.W., 2012. In vitro selection of *Escherichia coli* O157: H7-specific RNA aptamer. *Biochemical and Biophysical Research Communications*, *417*(1), pp.414-420.

Li, D., Wang, J., Wang, R., Li, Y., Abi-Ghanem, D., Berghman, L., Hargis, B. and Lu, H., 2011. A nanobeads amplified QCM immunosensor for the detection of avian influenza virus H5N1. *Biosensors and Bioelectronics*, *26*(10), pp.4146-4154.

Li, M., Li, Y.T., Li, D.W. and Long, Y.T., 2012. Recent developments and applications of screen-printed electrodes in environmental assays—A review. *Analytica Chimica Acta*, *734*, pp.31-44.

Li, W.M., Bing, T., Wei, J.Y., Chen, Z.Z., Shangguan, D.H. and Fang, J., 2014. Cell-SELEX-based selection of aptamers that recognize distinct targets on metastatic colorectal cancer cells. *Biomaterials*, *35*(25), pp.6998-7007.

Li, Y., Afrasiabi, R., Fathi, F., Wang, N., Xiang, C., Love, R., She, Z. and Kraatz, H.B., 2014. Impedance based detection of pathogenic *E. coli* O157: H7 using a ferrocene-antimicrobial peptide modified biosensor. *Biosensors and Bioelectronics*, *58*, pp.193-199.

Li, Y., Cheng, P., Gong, J., Fang, L., Deng, J., Liang, W. and Zheng, J., 2012. Amperometric immunosensor for the detection of *Escherichia coli* O157: H7 in food specimens. *Analytical Biochemistry*, *421*(1), pp.227-233.

Liang, J., Zhang, J., Zhou, W. and Ueda, T., 2017. Development of a flow injection based high frequency dual channel quartz crystal microbalance. *Sensors*, *17*(5), p.1136.

Liss, M., Petersen, B., Wolf, H. and Prohaska, E., 2002. An aptamer-based quartz crystal protein biosensor. *Analytical Chemistry*, *74*(17), pp.4488-4495.

Liu, F., Li, Y., Su, X.L., Slavik, M.F., Ying, Y. and Wang, J., 2007. QCM immunosensor with nanoparticle amplification for detection of *Escherichia coli* O157: H7. *Sensing and Instrumentation for Food Quality and Safety*, *1*(4), pp.161-168.

Mao, X., Yang, L., Su, X.L. and Li, Y., 2006. A nanoparticle amplification based quartz crystal microbalance DNA sensor for detection of *Escherichia coli* O157: H7. *Biosensors and Bioelectronics*, *21*(7), pp.1178-1185.

Marrazza, G., 2014. Piezoelectric biosensors for organophosphate and carbamate pesticides: a review. *Biosensors*, *4*(3), pp.301-317.

Masdor, N.A., Altintas, Z. and Tothill, I.E., 2016. Sensitive detection of *Campylobacter jejuni* using nanoparticles enhanced QCM sensor. *Biosensors and Bioelectronics*, *78*, pp.328-336.

Mayboroda, O., Katakis, I. and O'Sullivan, C.K., 2018. Multiplexed isothermal nucleic acid amplification. *Analytical Biochemistry*, *545*, pp.20-30.

Mi, J., Liu, Y., Rabbani, Z.N., Yang, Z., Urban, J.H., Sullenger, B.A. and Clary, B.M., 2010. In vivo selection of tumor-targeting RNA motifs. *Nature Chemical Biology*, *6*(1), p.22.

Milo, R., and Phillips, R., 2015. Cell Biology by the Numbers, first ed. Garland Ccience, New York.

Mohsen, M.G. and Kool, E.T., 2016. The discovery of rolling circle amplification and rolling circle transcription. *Accounts of Chemical Research*, *49*(11), pp.2540-2550.

Moon, J., Kim, G., Lee, S. and Park, S., 2013. Identification of *Salmonella* Typhimurium-specific DNA aptamers developed using whole-cell SELEX and FACS analysis. *Journal of Microbiological Methods*, *95*(2), pp.162-166.

Neves, M.A., Blaszykowski, C., Bokhari, S. and Thompson, M., 2015. Ultra-high frequency piezoelectric aptasensor for the label-free detection of cocaine. *Biosensors and Bioelectronics*, *72*, pp.383-392.

Ngo, V.K.T., Nguyen, D.G., Nguyen, H.P.U., Nguyen, T.K.M., Huynh, T.P., Lam, Q.V., Huynh, T.D. and Truong, T.N.L., 2014. Quartz crystal microbalance (QCM) as biosensor for the detecting of *Escherichia coli* O157: H7. *Advances in Natural Sciences: Nanoscience and Nanotechnology*, *5*(4), p.045004.

Ogi, H., Fukunishi, Y., Omori, T., Hatanaka, K., Hirao, M. and Nishiyama, M., 2008. Effects of flow rate on sensitivity and affinity in flow injection biosensor systems studied by 55-MHz wireless quartz crystal microbalance. *Analytical Chemistry*, *80*(14), pp.5494-5500.

Ozalp, V.C., Bayramoglu, G., Erdem, Z. and Arica, M.Y., 2015. Pathogen detection in complex samples by quartz crystal microbalance sensor coupled to aptamer functionalized core–shell type magnetic separation. *Analytica Chimica Acta*, *853*, pp.533-540.

Peng, Z., Ling, M., Ning, Y. and Deng, L., 2014. Rapid fluorescent detection of *Escherichia coli* K88 based on DNA aptamer library as direct and specific reporter combined with immuno-magnetic separation. *Journal of Fluorescence*, *24*(4), pp.1159-1168.

Poitras, C. and Tufenkji, N., 2009. A QCM-D-based biosensor for *E. coli* O157: H7 highlighting the relevance of the dissipation slope as a transduction signal. *Biosensors and Bioelectronics*, *24*(7), pp.2137-2142.

Procek, M., Stolarczyk, A., Pustelny, T. and Maciak, E., 2015. A study of a QCM sensor based on TiO_2 nanostructures for the detection of NO_2 and explosives vapours in air. *Sensors*, *15*(4), pp.9563-9581.

Ray, P.C., Khan, S.A., Singh, A.K., Senapati, D. and Fan, Z., 2012. Nanomaterials for targeted detection and photothermal killing of bacteria. *Chemical Society Reviews*, *41*(8), pp.3193-3209.

Rugar, D. and Hansma, P., 1990. Atomic force microscopy. *Physics Today*, *43*(10), pp.23-30.

Salam, F., Uludag, Y. and Tothill, I.E., 2013. Real-time and sensitive detection of *Salmonella* Typhimurium using an automated quartz crystal microbalance (QCM) instrument with nanoparticles amplification. *Talanta*, *115*, pp.761-767.

Sauerbrey, G., 1959. Verwendung von Schwingquarzen zur Wägung dünner Schichten und zur Mikrowägung. *Zeitschrift für Physik A Hadrons and Nuclei*, *155*(2), pp.206-222.

Savory, N., Nzakizwanayo, J., Abe, K., Yoshida, W., Ferri, S., Dedi, C., Jones, B.V. and Ikebukuro, K., 2014. Selection of DNA aptamers against uropathogenic *Escherichia coli* NSM59 by quantitative PCR controlled Cell-SELEX. *Journal of Microbiological Methods*, *104*, pp.94-100.

Sefah, K., Shangguan, D., Xiong, X., O'donoghue, M.B. and Tan, W., 2010. Development of DNA aptamers using Cell-SELEX. *Nature Protocols*, *5*(6), p.1169.

Shan, W., Pan, Y., Fang, H., Guo, M., Nie, Z., Huang, Y. and Yao, S., 2014. An aptamer-based quartz crystal microbalance biosensor for sensitive and selective detection of leukemia cells using silver-enhanced gold nanoparticle label. *Talanta*, *126*, pp.130-135.

Shangguan, D., Li, Y., Tang, Z., Cao, Z.C., Chen, H.W., Mallikaratchy, P., Sefah, K., Yang, C.J. and Tan, W., 2006. Aptamers evolved from live cells as effective molecular probes for cancer study. *Proceedings of the National Academy of Sciences*, *103*(32), pp.11838-11843.

Shangguan, D., Tang, Z., Mallikaratchy, P., Xiao, Z. and Tan, W., 2007. Optimization and modifications of aptamers selected from live cancer cell lines. *ChemBioChem*, *8*(6), pp.603-606.

Shen, Z.Q., Wang, J.F., Qiu, Z.G., Jin, M., Wang, X.W., Chen, Z.L., Li, J.W. and Cao, F.H., 2011. QCM immunosensor detection of *Escherichia coli* O157: H7 based on beacon immunomagnetic nanoparticles and catalytic growth of colloidal gold. *Biosensors and Bioelectronics*, *26*(7), pp.3376-3381.

Su, X.L. and Li, Y., 2005. A QCM immunosensor for *Salmonella* detection with simultaneous measurements of resonant frequency and motional resistance. *Biosensors and Bioelectronics*, *21*(6), pp.840-848.

Suh, S.H., Dwivedi, H.P., Choi, S.J. and Jaykus, L.A., 2014. Selection and characterization of DNA aptamers specific for *Listeria* species. *Analytical Biochemistry*, *459*, pp.39-45.

Sun, H., Zhu, X., Lu, P.Y., Rosato, R.R., Tan, W. and Zu, Y., 2014. Oligonucleotide aptamers: new tools for targeted cancer therapy. *Molecular Therapy-Nucleic Acids*, *3*.

Tang, Z., Parekh, P., Turner, P., Moyer, R.W. and Tan, W., 2009. Generating aptamers for recognition of virus-infected cells. *Clinical Chemistry*, *55*(4), pp.813-822.

Tolle, F., Wilke, J., Wengel, J. and Mayer, G., 2014. By-product formation in repetitive PCR amplification of DNA libraries during SELEX. *PloS one*, *9*(12), p.e114693.

Torres-Chavolla, E. and Alocilja, E.C., 2009. Aptasensors for detection of microbial and viral pathogens. *Biosensors and Bioelectronics*, *24*(11), pp.3175-3182.

Tuerk, C. and Gold, L., 1990. Systematic evolution of ligands by exponential enrichment: RNA ligands to bacteriophage T4 DNA polymerase. *Science*, *249*(4968), pp.505-510.

Turek, D., Van Simaeys, D., Johnson, J., Ocsoy, I. and Tan, W., 2013. Molecular recognition of live methicillin-resistant *Staphylococcus aureus* cells using DNA aptamers. *World Journal of Translational Medicine*, *2*(3), p.67.

Vashist, S.K. and Vashist, P., 2011. Recent advances in quartz crystal microbalance-based sensors. *Journal of Sensors*, *2011*.

Voinova, M.V., Jonson, M. and Kasemo, B., 2002. 'Missing mass' effect in biosensor's QCM applications. *Biosensors and Bioelectronics*, *17*(10), pp.835-841.

Wang, D., Chen, G., Wang, H., Tang, W., Pan, W., Li, N. and Liu, F., 2013. A reusable quartz crystal microbalance biosensor for highly specific detection of single-base DNA mutation. *Biosensors and Bioelectronics*, *48*, pp.276-280.

Wang, G., Dewilde, A.H., Zhang, J., Pal, A., Vashist, M., Bello, D., Marx, K.A., Braunhut, S.J. and Therrien, J.M., 2011. A living cell quartz crystal microbalance biosensor for continuous monitoring of cytotoxic responses of macrophages to single-walled carbon nanotubes. *Particle and Fibre Toxicology*, *8*(1), p.4.

Wang, L., Wei, Q., Wu, C., Hu, Z., Ji, J. and Wang, P., 2008. The *Escherichia coli* O157: H7 DNA detection on a gold nanoparticle-enhanced piezoelectric biosensor. *Chinese Science Bulletin*, *53*(8), pp.1175-1184.

Wang, L., Wang, R., Chen, F., Jiang, T., Wang, H., Slavik, M., Wei, H. and Li, Y., 2017. QCM-based aptamer selection and detection of *Salmonella* Typhimurium. *Food Chemistry*, *221*, pp.776-782.

Wang, Q.Y. and Kang, Y.J., 2016. Bioprobes based on aptamer and silica fluorescent nanoparticles for bacteria *Salmonella* Typhimurium detection. *Nanoscale Research Letters*, *11*(1), pp.1-9.

Wang, R. and Li, Y., 2013. Hydrogel based QCM aptasensor for detection of avian influenzavirus. *Biosensors and Bioelectronics*, *42*, pp.148-155.

Wang, R., Wang, L., Callaway, Z.T., Lu, H., Huang, T.J. and Li, Y., 2017. A nanowell-based QCM aptasensor for rapid and sensitive detection of avian influenza virus. *Sensors and Actuators B: Chemical*, *240*, pp.934-940.

Wang, R., Xu, L. and Li, Y., 2015. Bio-nanogate controlled enzymatic reaction for virus sensing. *Biosensors and Bioelectronics*, *67*, pp.400-407.

Wang, Z., Kimura, M., Inomata, N. and Ono, T., 2016, April. A freestanding microfluidic-based thermocouple biosensor for enzyme-catalyzed reaction analysis. In *Nano/Micro Engineered and Molecular Systems (NEMS), 2016 IEEE 11th Annual International Conference on* (pp. 58-61). IEEE.

Wu, V.C., Chen, S.H. and Lin, C.S., 2007. Real-time detection of *Escherichia coli* O157: H7 sequences using a circulating-flow system of quartz crystal microbalance. *Biosensors and Bioelectronics*, *22*(12), pp.2967-2975.

Wu, W., Zhao, S., Mao, Y., Fang, Z., Lu, X. and Zeng, L., 2015. A sensitive lateral flow biosensor for *Escherichia coli* O157: H7 detection based on aptamer mediated strand displacement amplification. *Analytica Chimica Acta*, *861*, pp.62-68.

Xu, L., Callaway, Z.T., Wang, R., Wang, H., Slavik, M.F., Wang, A. and Li, Y., 2015. A fluorescent aptasensor coupled with nanobead-based immunomagnetic separation for simultaneous detection of four foodborne pathogenic bacteria. *Transactions of the ASABE*, *58*(3), pp.891-906.

Xue, Y., Li, X., Li, H. and Zhang, W., 2014. Quantifying thiol–gold interactions towards the efficient strength control. *Nature Communications*, *5*, pp.43-48.

Yan, J., Su, S., He, S., He, Y., Zhao, B., Wang, D., Zhang, H., Huang, Q., Song, S. and Fan, C., 2012. Nano rolling-circle amplification for enhanced SERS hot spots in protein microarray analysis. *Analytical Chemistry*, *84*(21), pp.9139-9145.

Yao, N., Wang, J. and Zhou, Y., 2014. Rapid determination of the Chemical Oxygen Demand of water using a thermal biosensor. *Sensors*, *14*(6), pp.9949-9960.

Yang, M., Peng, Z., Ning, Y., Chen, Y., Zhou, Q. and Deng, L., 2013. Highly specific and cost-efficient detection of *Salmonella Paratyphi* A combining aptamers with single-walled carbon nanotubes. *Sensors*, *13*(5), pp.6865-6881.

Yildirim, N., Long, F., Gao, C., He, M., Shi, H.C. and Gu, A.Z., 2012. Aptamer-based optical biosensor for rapid and sensitive detection of 17β-estradiol in water samples. *Environmental Science & Technology*, *46*(6), pp.3288-3294.

Yilmaz, E., Majidi, D., Ozgur, E. and Denizli, A., 2015. Whole cell imprinting based *Escherichia coli* sensors: A study for SPR and QCM. *Sensors and Actuators B: Chemical*, *209*, pp.714-721.

Yu, X., Chen, F., Wang, R. and Li, Y., 2018. Whole-bacterium SELEX of DNA aptamers for rapid detection of *E. coli* O157: H7 using a QCM sensor. *Journal of Biotechnology*, *266*, pp.39-49.

Zelada-Guillén, G.A., Sebastián-Avila, J.L., Blondeau, P., Riu, J. and Rius, F.X., 2012. Label-free detection of *Staphylococcus aureus* in skin using real-time potentiometric biosensors based on carbon nanotubes and aptamers. *Biosensors and bioelectronics*, *31*(1), pp.226-232.

Zhang, Z., Ali, M.M., Eckert, M.A., Kang, D.K., Chen, Y.Y., Sender, L.S., Fruman, D.A. and Zhao, W., 2013. A polyvalent aptamer system for targeted drug delivery. *Biomaterials*, *34*(37), pp.9728-9735.

Zhao, B., Yan, J., Wang, D., Ge, Z., He, S., He, D., Song, S. and Fan, C., 2013. Carbon nanotubes multifunctionalized by rolling circle amplification and their application for highly sensitive detection of cancer markers. *Small*, *9*(15), pp.2595-2601.

Zhao, W., Ali, M.M., Brook, M.A. and Li, Y., 2008. Rolling circle amplification: applications in nanotechnology and biodetection with functional nucleic acids. *Angewandte Chemie International Edition*, *47*(34), pp.6330-6337.

Zhao, W., Cui, C.H., Bose, S., Guo, D., Shen, C., Wong, W.P., Halvorsen, K., Farokhzad, O.C., Teo, G.S.L., Phillips, J.A. and Dorfman, D.M., 2012. Bioinspired multivalent DNA network for capture and release of cells. *Proceedings of the National Academy of Sciences*, *109*(48), pp.19626-19631.

Zhou, Y. and Xie, Q., 2016. Hyaluronic acid-coated magnetic nanoparticles-based selective collection and detection of leukemia cells with quartz crystal microbalance. *Sensors and Actuators B: Chemical*, *223*, pp.9-14.